Accumulation and Metabolism of Neutral Lipids in Obesity

By

JOHN DAVID DOUGLASS

A Dissertation submitted to the

Graduate School-New Brunswick

Rutgers, The State University of New Jersey

in partial fulfillment of the requirements

for the degree of

Doctor of Philosophy

Graduate Program in Nutritional Sciences

written under the direction of

Judith Storch

and approved by

_____

_____

_____

_____

_____

New Brunswick, New Jersey

[January, 2014]

ABSTRACT OF THE DISSERTATION
Accumulation and Metabolism of Neutral Lipids in Obesity
by **John David Douglass**
Dissertation Director:
Judith Storch

The ectopic deposition of fat in liver and muscle during obesity is well established, however surprisingly little is known about the intestine. We used *ob/ob* mice and wild type (C57BL6/J) mice fed a high-fat diet (HFD) for 3 weeks, to examine the effects on intestinal mucosal triacylglycerol (TG) accumulation and secretion. Obesity and high-fat feeding resulted in higher levels of mucosal TG and markedly decreased rates of chylomicron secretion, accompanied by alterations in intestinal genes related to anabolic and catabolic lipid metabolism pathways. Overall, the results demonstrate that during obesity and a HFD, the intestinal mucosa exhibits metabolic dysfunction.

There is indirect evidence that the lipolytic enzyme monoacylglycerol lipase (MGL) may be involved in the development of obesity. We therefore examined the role of MG metabolism in energy homeostasis using wild type and MGL-/- mice fed low-fat or high-fat diets for 12 weeks. Tissue MG species were profoundly increased, as expected. Notably, weight gain was blunted in all MGL-/- mice. MGL null mice were also leaner, and had increased fat oxidation on the low-fat diet. Circulating lipids levels were decreased in high fat-fed MGL-/- mice, as were the levels of several plasma peptides involved in energy homeostasis. Interestingly, MGL-/- mice had a blunted rate of intestinal TG secretion following an oral fat challenge. The leaner phenotype and improved metabolic serum profile in MGL-/- mice suggested that pharmacological inhibition may be a potential treatment for metabolic disease. To further examine this, C57BL6/J mice were fed low-fat and high-fat diets for 12 weeks, and then given daily oral administration of

vehicle or a novel reversible MGL inhibitor for 4 days or 27 days. No changes in food intake were found, nor were adiposity or glucose intolerance substantially altered by inhibitor treatment; this is likely due to the short-term effectiveness of the inhibitor, as the compound was barely detectable 7 hours following administration. Thus, the effects of transient MGL inhibition on energy metabolism are minimal, in contrast to chronic inhibition secondary to genetic ablation.

Acknowledgements

I would like to foremost thank my advisor Dr. Judy Storch, whose guidance and acute editing skills I have relied upon for these past five years. I also thank my dissertation committee, Dr. Malcolm Watford, Dr. Dawn Brasaemle, Dr. Greg Henderson, and Dr. Marge Connelly, for their feedback and oversight of my research. My beloved Storch lab members, Yin Xiu, Sarala, Leslie, and Angela, must be thanked for contributing their expertise and patience towards the research and my training as a scientist. I would also like to thank the Nutritional Sciences Department and the Nutritional Sciences Graduate Program for providing the necessary structure and resources that made this dissertation possible. My gratitude goes to the Rutgers Center for Lipid Research and its members, who are united under the common goal of furthering lipid research in service of human health. I also thank our collaborators at Janssen R&D who allowed us to pursue novel research ideas and provided key analytical support.

The seeds of higher education were planted while watching my father Dr. David Douglass tapping away on his own dissertation on a typewriter in our home basement. Inspiration for pursuing a career in science came from Dr. Dennis Winge and Dr. Lisa Joss-Moore. Finally, I owe a debt of gratitude to my dear wife Dr. Katherine Douglass, an exemplar for momentum in life, and whose ability to push through "analysis paralysis" and the tedious aspects of academia is nothing short of incredible.

Table of Contents

Page

List of Tables

List of Figures

x

List of Abbreviations

2-AG	2-arachidonoyl glycerol
2-AG-d8	Deuterated 2-arachidonoyl glycerol
2-MG	*sn*-2-monoacylglycerol
2-OG	2-oleoyl glycerol
2-PG	2-palmitoyl glycerol
2-SG	2-stearoyl glycerol
AA	Arachidonic acid
ABHD	α-β hydrolase
ACC1	Acetyl-CoA carboxylase 1
ACO	Acyl-coA oxidase
ACS	Acyl-CoA synthetase
ACSL	Long chain acyl CoA synthetase
AEA	Arachidonoyl ethanolamide
AEA-d8	Deuterated arachidonoylethanolamide
AgRP	Agouti-related protein
AMPK	AMP-activated protein kinase
ANOVA	Analysis of variance
AP	Apical
ATGL	Adipose triglyceride lipase
AUC	Area under curve
BAT	Brown adipose tissue
BL	Basolateral
Ca^{2+}	Calcium
CART	Cocaine and amphetamine regulated transcript
CB	Cannabinoid Receptor
CCK	Cholecystokinin
cDNA	Complementary deoxyribonucleic acid
CE	Cholesteryl ester
CEL	Carboxyl Ester Lipase
CLD	Cytoplasmic lipid droplet
CM	Chylomicron
CPT1	Carnitine Palmitoyltransferase 1
CRH	Corticotropin-releasing hormone
DG	Diacylglycerol

DGAT	Diacylglycerol acyltransferase
DHA	Docosahexapentanoic acid
DIO	Diet-induced obese
DNA	Deoxyribonucleic acid
EC	Endocannabinoid
EPA	Eicosapentanoic acid
ER	Endoplasmic Reticulum
FA	Fatty acid
FAAH	Fatty acyl amide hydrolase
FABP	Fatty acid binding protein
FABPpm	Plasma membrane fatty acid binding protein
Fa-CoA	Fatty acyl coenzyme A
FAS	Fatty acid synthase
FATP	Fatty acid transfer protein
FFA	Free fatty acid
G-3-P	Glycerol-3-phosphate
GI	Gastrointestinal
GLP1	Glucagon-like peptide 1
GPAT	Glycerol-3-phosphate acyltransferase
GPAT	Acyl-CoA:glycerol-3-phosphate acyltransferase
GPCR	G-protein coupled receptor
HF	High fat
HFD	High fat diet
HPβCD	(2-hydroxypropyl)-β-cyclodextrin
IDFP	Isopropyl dodecylfluorophosphonate
IFABP	Intestinal fatty acid-binding protein
iMGL	Intestine-specific overexpression of monacylglycerol lipase
IP	Intraperitoneal
IV	Intravenous
KO	Knockout
LCFA	Long chain fatty acid
LC-MS	liquid chromatography-coupled mass spectrometry
LD	Lipid Droplet
LF	Low fat
LFABP	Liver fatty acid-binding protein
LFD	Low fat diet

LPAT	Lysophosphatidate acyltransferase
MCFA	Medium-chain fatty acid
MCH	Melanin-concentrating hormone
MG	Monoacylglycerol
MGAT	Monoacylglycerol acyltransferase
MGL	Monoacylglycerol lipase
mpk	Milligrams per kilogram body weight
mRNA	Messenger ribonucleic acid
MTP	Microsomal Transfer Protein
NEFA	Non-esterified fatty acid
NPY	Neuropeptide Y
OEA	Oleoylethanolamide
PEA	Palmitoylethanolamide
PKC	Protein kinase C
PL	Phospholipid
PLA_1	Phospholipase A_1
PLC	Phospholipase C
PPAR	Peroxisome proliferator-activated receptor
PTL	Pancreatic triacylglycerol lipase
qRT-PCR	Quantitative real time polymerase chain reaction
Rim	Rimonabant
RNA	Ribonucleic acid
RT	Reverse Transcription
SCFA	Short-chain fatty acid
SEA	Stearoylethanolamide
SEM	Standard error mean
SI	Small intestine
SREBP	Sterol response element binding protein
$t_{1/2}$	Half-life
TG	Triacylglycerol
THC	Δ^9-tetrahydrocannabinol
TLC	Thin Layer Chromatography
TRPV	Transient receptor potential vanilloid receptor
UWL	Unstirred water layer
Veh	Vehicle
VLCFA	Very long chain fatty acid

VN	Vagus Nerve
WAT	White adipose tissue
WT	Wild type

Chapter 1

Introduction and Review of the Literature

1. **Introduction**

Lipids are a diverse group of compounds that are essential for life. While there is no consensus for their definition, lipids can be broadly defined as naturally occurring hydrophobic or amphipathic small molecules that participate in biological functions. There are many types of lipids, including fatty acids, acylglycerols, waxes, sterols, phospholipids, sphingolipids, and fat-soluble vitamins. Lipids support physiological processes in multiple ways. Lipids can be used for heat production and insulation against cold environments. They also allow organisms to store energy for later use as a fuel. Lipids are also fundamental cell membrane components, and are involved in many signaling functions within cells and between bodily tissues.

Metabolism is a term that describes the chemical processes of molecules in a living organism. The metabolism of lipids is highly regulated by a host of hormones and signaling molecules in order to maintain the crucial balance of lipids for energy production, membrane components, and signaling. Thus, aberrations in lipid metabolism can be highly problematic. This can be seen in the current obesity epidemic. This epidemic is driven, in part, by overconsumption of the highly caloric "Western style diet" causing storage of excess calories as fat. In turn, the resultant obesity can alter lipid metabolic pathways that reinforce fat deposition and exacerbate diseases such as atherosclerosis, type 2 diabetes, and obesity-related cancers.

Gaining new knowledge of human physiology, including how we acquire and utilize nutrients, has intrinsic value. When coupled with the necessity to better understand lipid metabolism in light of serious worldwide health challenges, it becomes imperative to study and investigate these pathways for the benefit of all.

The focus of this thesis is to investigate the metabolism of neutral lipids under conditions of high fat feeding and obesity, focusing on the small intestine, where little is known

about the consequences of obesity. Further studies seek to understand the contribution that acylglycerol catabolic enzymes have to overall energy homeostasis. We also test the efficacy of a novel inhibitor of the enzyme monoacylglycerol lipase in relationship to the treatment of obesity.

2. Intestinal Lipid Metabolism

2.1 The Small Intestine

The historic view of the intestine has been overly simplistic: a tube that extends from the pyloric sphincter of the stomach down to the anus; and a barrier that allows certain things into the body. We now understand much more about this vital organ. Certainly, the absorption and processing of nutrients is a chief function of the intestine. Yet, the intestine also acts as a sensory organ, and regulates energy balance by recognizing certain nutrients and activating pathways to influence central satiety mechanisms in the brain, as well as metabolic tissues in the periphery such as the pancreas and liver (1).

Structurally, the intestine can be divided into the small intestine, composed of the duodenum, jejunum, and ileum, and the large intestine, which includes the cecum, appendix, colon, rectum, and anus. The small intestine, and particularly the jejunum, is the site where most nutrient absorption takes place. There are distinct layers of cells in the small intestine. The mucosa is closest to the interior, and consists of the epithelium, lamina propria, and muscularis mucosa, followed by muscle layers and the enteric nervous system (2). The entire system is innervated by the vagus nerve (VN), which collects signals from the gut regarding nutritional status and transmits them to the hindbrain. Nutrients, enzymes, and fluids occupy the interior luminal space of the intestine. The lumen of the gut is also home for up to 500 different species

of bacteria, collectively called the microbiota, which vastly outnumber the eukaryotic cells in the human body by more than 10 times (3). These bacteria, the bulk of which reside in the large intestine, have a symbiotic relationship with their host, enabling the efficient processing of nutrients, and also likely interact with biological systems in many more ways than are currently known.

The epithelium of the small intestine contains a variety of cells. Enterocytes, the major absorptive cells for nutrients and composing 99% of all epithelial cells, as well as goblet cells, paneth cells, and enteroendocrine cells, form the lining of the intestinal wall (4). The epithelial cells are arranged in a two-dimensional structure of crypts and villi, which optimize the surface area exposed to nutrients. The crypt regions are sites for the self-renewal of epithelial cells and where endocrine cells reside. Maturing cells migrate from the crypt to the villus, where they participate in absorption and then are sloughed off into the lumen, with a turnover typically of around 1-2.5 days (2, 5).

Luminal contents cannot freely enter into the body. Epithelial cells form a barrier where nutrients and xenobiotics may only access the circulatory system through select routes. Gradient-driven diffusion occurs for certain molecules either directly into enterocytes, or bypassing them entirely through the tight junctions between the lateral membranes of epithelial cells and then into circulation (6). Most nutrients must be taken up into cells via protein-dependent processes, both active and facilitated, or via passive diffusion. This step is necessary, particularly for lipids, which must undergo metabolic changes and processing inside the enterocytes before they can be secreted into the circulation (7). Details regarding the digestion and metabolism of dietary lipids will be covered in the following sections.

2.2 Digestion of Dietary Lipids

The digestion and absorption of lipids is a remarkably efficient, multi-step process (Fig 1-1). More than 95% of fat in diets is absorbed, regardless of the amount of fat consumed (8). The lipid composition of a typical human diet is a mixture, with the bulk (more than 90%) in the form of triacylglycerol (TG), and the rest mainly phospholipids (PL), cholesterol, cholesterol esters (CE), and fat soluble vitamins (4). The first step in the digestion of TG is catalyzed by gastric lipase, which is secreted by chief cells in the stomach, and helps in the formation of lipid emulsions. Gastric lipase contributes roughly 17% to overall TG hydrolysis and works optimally in a low pH environment, so has little residual activity upon reaching the neutrally buffered small intestine (9, 10). Gastric lipase also has stereochemical specificity towards the *sn*-1(3) position of TG, generating 1,2-diacyglycerol (DG) and a free fatty acid (FFA) in the process (9, 11). Peristaltic movement in the stomach, along with the action of gastric lipase, results in crude lipid emulsions that then pass into the small intestine.

Pancreatic enzymes and bile salts are secreted into the duodenum, promoting the formation of micelles to aid in digestion. Pancreatic triacylglycerol lipase (PTL) is the major enzyme in luminal TG hydrolysis, and preferentially cleaves the *sn*-1(3) acyl chains of DG and TG, resulting in the formation of *sn*-2-monoacylglycerol (2-MG) and FFA (9). Free cholesterol, both naturally occurring and to a lesser extent formed by the lipolysis of CE by carboxyl ester lipase (CEL), and PL are also emulsified by bile salts and join the rest of lipid digestion products in a mixed micelle (7). The formation of mixed micelles by is critical for these hydrophobic molecules to move from the bulk fluid phase of the intestinal lumen and cross the unstirred water layer (UWL). Once past the UWL, they can then access the brush border surface, composed of thousands of surface area-enhancing microvilli, of the intestinal epithelial cells where absorption occurs (12).

2.3 Uptake and Transport of Dietary Fatty Acids and Monoacylglycerol

The majority of dietary fat uptake occurs via enterocyte cells located along the proximal and medial small intestine. The mixed micelles are not taken up wholly, so their constituents must enter the enterocytes as monomers. Surprisingly, the mechanisms of FA and 2-MG uptake are not entirely elucidated, but both passive diffusion and protein-mediated transport have been proposed (13). Due to their hydrophobic nature, FA and 2-MG may passively diffuse across the apical membrane into enterocytes, possibly driven by a concentration gradient created inside by the rapid re-esterification of TG hydrolysis products (14). Early studies performed in rat jejunum showed that short- and medium-chain FA (SCFA and MCFA, respectively) had linear uptake rates as a function of concentration, and lacked competitive inhibition, indicating a diffusion mechanism (15). More recently, it has been demonstrated that both long-chain FA (LCFA, chain length C13 to C22) and MG diffusion occurs at higher monomer concentrations in enterocyte-like Caco-2 cells (16).

There is also compelling evidence for protein-mediated transport of FA and 2-MG into enterocytes. Uptake of LCFA, but not SCFA, has a saturable kinetic profile in murine (17) and human intestinal cells (18, 19) at low monomer concentrations, indicating the presence of membrane carrier proteins. For MG, it has been shown that 2-oleoylglycerol (2-OG) uptake in intestinal cells is also saturable at lower concentrations, can be inhibited by trypsin digestion, and is competitively inhibited by FA, suggesting common protein-mediated transporters for both of these ligands (16, 20).

The plasma membrane proteins likely responsible for uptake of LCFA, and possibly 2-MG, are plasma membrane fatty acid binding protein (FABPpm), CD36, and fatty acid transfer protein 4 (FATP4) (21). FABPpm was first discovered in 1985, and later studies showed that treatment of rat mucosal cells with FABPpm antibody resulted in decreased influx of LCFA (17,

22). CD36 is highly expressed in the small intestine in proximal to distal fashion, and is upregulated by a LCFA-rich diet (23). Mice null for CD36 have reduced FA uptake in the proximal small intestine (24) and impaired chylomicron secretion (25). Expression of FATP4 in the intestine is high, in both mature enterocytes (26) and in Caco-2 cells (20). Anti-sense oligonucleotide knockdown of FATP4 reduced FA uptake by 50% in enterocytes (26). However, there is evidence that FATP4 is associated with the endoplasmic reticulum (ER), not the plasma membrane, and drives FA uptake by participating in the re-esterification process to aid the diffusion gradient, rather than directly binding and transferring FA across the membrane (14).

Upon entering the enterocyte at the apical membrane, it is necessary for the hydrophobic FA and 2-MG to have specialized proteins to transport them across the cytoplasm to the ER for processing. The two likely candidates for this are the intestinal and liver fatty acid binding proteins (IFABP and LFABP). These low-molecular weight soluble proteins are highly expressed in the proximal small intestine, particularly in the villus region where nutrient uptake occurs, and may have some non-overlapping functions. While IFABP appears to only bind LCFA, LFABP is capable of binding a wide variety of lipids, including FA, fatty acyl-CoA, MG, and lysophospholipids (27, 28). Kinetic studies also show different ligand transport mechanisms for these two proteins (29). Knockout studies of both FABP in mice show impaired intestinal lipid metabolism, and global changes in energy homeostasis, suggesting that both proteins are necessary for normal lipid metabolism and may also participate in lipid signaling functions (28, 30).

2.4 Intracellular Lipid Metabolism in Enterocytes

Once taken up into enterocytes, the products of dietary TG digestion have multiple metabolic fates. Most of these are anabolic processes, but some catabolism occurs in the

intestine as well. The activation of FA is a necessary first step, catalyzed primarily by long chain acyl-coA synthetases (ACSL), which result in formation of fatty acyl coenzyme A (Fa-CoA) species (31). Of the five different isoforms, only ACLS5, and to a much lesser extent ACSL3, are found in abundance in the small intestine (31). Some of the resultant Fa-CoA are then incorporated into PL or CE, or translocated into the mitochondria for β-oxidation. However, the vast majority of dietary FA and MG are rapidly re-esterified back into TG inside the ER, packaged with other lipids into apolipoprotein-studded chylomicrons, and then secreted across the basolateral (BL) membrane into the lymphatic system (13, 32). A portion of intestinal TG may also be shunted temporarily towards holding pools, i.e. lipid droplets, and released at a later point, which will also be discussed this section.

Synthesis of intestinal TG occurs quickly. Within 30 seconds, approximately 80% of intraintestinally administered FAs are incorporated into TG in rat mucosa (32). The two TG synthetic pathways responsible are known as the MG and glycerol-3-phosphate (G-3-P) pathways. The G-3-P pathway is relatively minor in intestine, but more important in other tissues such as liver and adipose (33), and involves the acylation of G-3-P to TG by specific acyltransferase (GPAT) proteins (33). The MG pathway is dominant in intestinal mucosa, particularly in the postprandial state when there is a large supply of available FA and MG (33, 34). In the first step of this pathway, MG and Fa-CoA form DG in a reaction catalyzed by MG acyltransferase (MGAT) proteins. In the second step, DG acyltransferase (DGAT) proteins facilitate the second esterification of DG and Fa-CoA to yield TG. While it is generally agreed that these reactions take place around the ER membrane, the locations and activities of isoforms of MGAT and DGAT have implications for the absorption and immediate fate of dietary TG.

There are three MGAT isoforms in humans and rodents; only MGAT2 and MGAT3 are expressed in small intestine (35–38), whereas MGAT1 is mainly found in other tissues such as

liver and adipose (39). Not surprisingly, the intestine has the highest level of MGAT activity of any bodily tissue (40). The MGAT process has been proposed to be the rate limiting step for intestinal fat absorption (36). This is supported by studies of MGAT2 null mice that have reduced fat absorption rates and also decreased TG storage in white adipose tissue (WAT) (41, 42). Both MGAT2 and MGAT3 are transmembrane proteins that localize to the ER, the site of TG synthesis (37, 38). Interestingly, MGAT3 also has significant DGAT activity, suggesting that it may catalyze both steps of TG re-esterification in the intestine (38).

Two DGAT isoforms are found in enterocytes, DGAT1 and DGAT2 (43, 44). Despite having similar activity, they do not share sequence homology (44) and seem to have different physiological functions. DGAT1 participates in more acyltransferase reactions, including catalyzing the acylation of MG and DG species, but DGAT2 only acts on DG substrates (45). Hepatic DGAT1 over-expression leads to increased very low density lipoprotein (VLDL) secretion, whereas DGAT2 over-expression leads to increased cytoplasmic TG storage, further indicating separate roles for the two enzymes (46). The knockouts also have divergent phenotypes. Despite efficient intestinal TG re-synthesis and chylomicron secretion (47), DGAT1-/- mice also have reduced TG stores in liver and WAT, increased energy expenditure, and are resistant to diet induced obesity (48). Mice lacking DGAT2 die soon after birth due to lipopenia and skin barrier defects (49), indicating that an intestine-specific knockout would be necessary to study the real function of these enzymes in mucosal TG synthesis. Nevertheless, the subcellular localization may shed some light on the apparently divergent roles of DGAT1 and DGAT2. DGAT activity occurs on both luminal and cytosolic sides of the ER membrane (50, 51), which may result in targeting of TG products towards cytoplasmic pools or chylomicron incorporation. Transfection of cos-7 cells showed that DGAT1 and DGAT2 co-localize with ER, but in another study DGAT1 was also found more widely distributed throughout the cell (38). DGAT2 also co-

localizes with mitochondria and lipid droplets (52). Overall, these studies indicate that TG

formed in the intestine from DGAT2 is targeted towards intracellular storage, while DGAT1

produces TG for secretion.

The existence of TG storage pools within enterocytes has been observed both indirectly

and directly. In humans, consumption of glucose resulted in the release of intestinal TG, even 5

hours after ingestion of fat (53). The glucose drink, but not water, also reduced jejunal TG

content, indicating neutral lipid storage in mucosa (53). However, it did not resolve whether this

was delayed release of pre-formed CM particles from dietary sources, or a separate pool of TG

stores. This matter was later addressed in studies using coherent anti-Stokes Raman

spectroscopy (CARS) to image neutral lipids, which demonstrated that mouse enterocytes have

TG-containing cytoplasmic lipid droplets (LD) that fluctuate in size based the amount and time

after dietary fat absorption (54). Interestingly, the induction of distinct LD-associated proteins

was also found to be different based on acute or chronic high fat challenges, suggesting the

existence of both long term and short term LD pools (55). It may be concluded from these

various studies that enterocytes store dietary TG in LD as a normal function of fat intake, and

are able to mobilize and secrete that TG in lipoproteins in the postprandial state.

While the intestine may be mostly considered an anabolic tissue in terms of lipid

metabolism, there is also catabolism of neutral lipids and the accompanying enzymes for these

processes. Hormone-sensitive lipase (HSL) is also present and has acylglycerol and cholesteryl

ester hydrolase activity, yet HSL deficient mice have reduced DG hydrolysis in some, but not all,

parts of the intestine (56). The CE hydrolase activity may be a dominant function of mucosal

HSL, as intestine-specific HSL ablation results in CE accumulation and accelerated cholesterol

absorption, but does not affect TG metabolism in the small intestine (57). The most likely

candidate in the catabolism of enterocyte TG may be adipose triglyceride lipase (ATGL), an

enzyme that associates with LD in cell types with large TG stores. Both global and intestine specific ATGL knockout mice (ATGL-KO and ATGLi-KO, respectively) have lipid accumulation in enterocytes (58, 59). Intriguingly, the absorption of dietary fat in ATGLi-KO mice was unaffected, yet BL-absorbed FA from circulation accumulated as TG in enterocytes and oxidation pathways were downregulated (59). These results suggest that intestinal ATGL is important for mobilizing FA from cytoplasmic LD pools of lipids absorbed from the bloodstream.

The presence of MG hydrolyzing activity in small intestine was first discovered in 1966 (60). The enzyme responsible for this activity, now known as MG lipase (MGL), was later partially purified in rat intestinal mucosa (61). Hydrolysis of MG was also demonstrated in human intestine-derived cells by adding [3H]-2-MG to either the apical or BL side of Caco-2 cells and recovering radioactive FA (62). These results were replicated *in vivo* using murine models, showing that systemically absorbed 2-MG in enterocytes was hydrolyzed, and the FA were preferentially incorporated into PL species or used for oxidation, rather than TG re-esterification (63). On the other hand, 40% of all 2-MG taken up into mucosa from the luminal side was used for TG synthesis within 2 minutes of administration, but 23% of the 2-MG was also hydrolyzed to FA (63). In subsequent studies, intestinal MGL protein and activity were found to be induced by high fat feeding, indicating a potential role for the enzyme in the assimilation of dietary fat (64). Surprisingly, over-expression of intestinal MGL in mice (iMGL) did not significantly alter dietary TG metabolism in enterocytes, but did result in whole body phenotypic changes involving appetite and energy homeostasis, opening the possibility that intestinal MG may also serve in signaling roles (65). The physiological function of MGL, both in intestine and elsewhere in the body, will be explored further in the following chapters and detailed experiments.

Figure 1-1
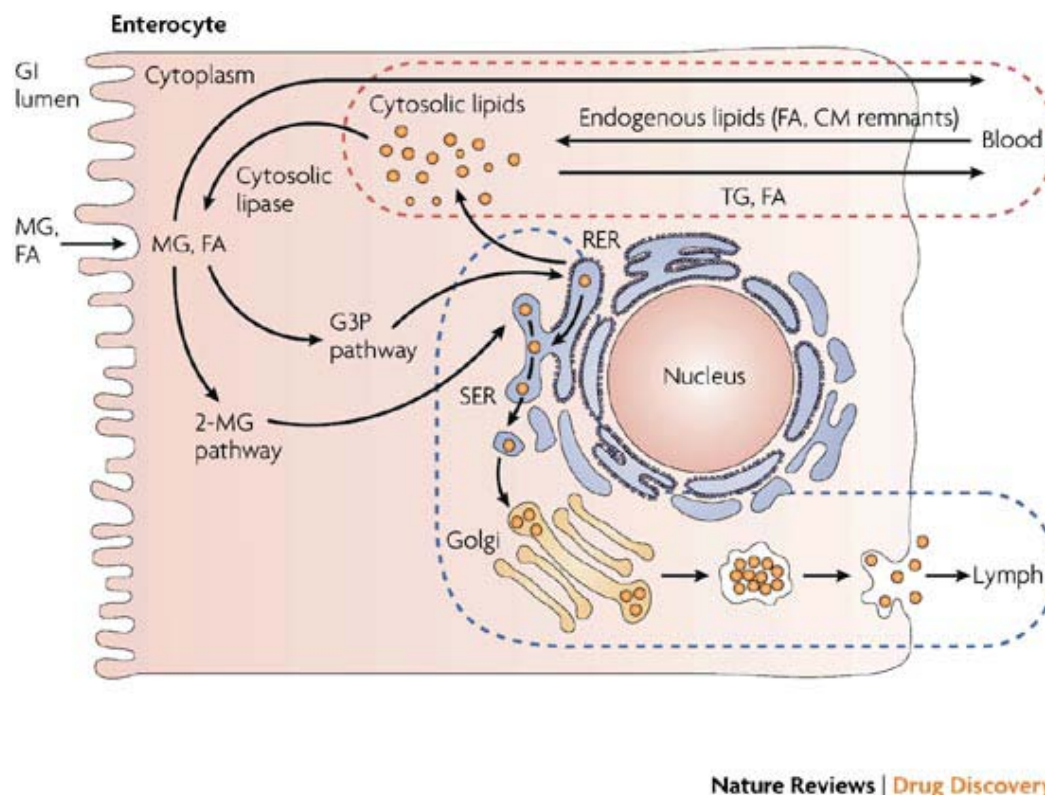
Figure 1-1. Intestinal lipid absorption. The main products of dietary TG digestion are taken up into enterocytes in the small intestine. The majority of 2-MG and FA are re-esterified back into TG in the endoplasmic reticulum (ER) and incorporated with apolipoproteins and other lipids into chylomicrons, which are then secreted into the lymphatic system. Some of the intestinal TG formed is stored in cytoplasmic lipid droplets for short periods, and then subsequently mobilized by various intracellular hydrolases. Lipids may also be absorbed from the bloodstream through the basolateral membrane and are preferentially used for phospholipid synthesis and oxidation. Illustration from Porter *et al.* 2007 (66). Adapted by permission from Macmillan Publishers Ltd: Nature Reviews Drug Discovery © 2007.

3. Monoacylglycerols

3.1 Formation and Biosynthesis of MG

MG can be found with the acyl chain bound to the glycerol backbone at the *sn*-2 or *sn*-1(3) position. Generally, most of the MG found in humans and rodents is *sn*-2-MG, due to the stereochemical properties of biosynthetic enzymes, and rate of isomerization of *sn*-2 to *sn*-1 being quite low at the physiological pH 7.4 (67). The hydrolysis of both extracellular and intracellular TG is one main source of 2-MG generation. In the gut lumen, PTL cleaves the sn-1(3) acyl chains of dietary TG to form 2-MG (9). Similarly, circulating lipoprotein particles containing TG are acted upon by lipoprotein lipase (LPL) or hepatic lipase (HL) to release 2-MG and FFA, which are then taken up into tissues (68). Within tissues that store TG, such as WAT and liver, the consecutive actions of ATGL and HSL result in 2-MG release (69, 70).

Another significant pathway for MG production is from membrane phospholipids. This is particularly important in the generation of 2-arachidonoyl glycerol (2-AG), a key signaling molecule in the endocannabinoid (EC) system. In this biosynthetic pathway, phospholipids are first hydrolyzed by phospholipase C-β (PLC- β) to form 1,2-DG (71), which is subsequently cleaved by DG lipase (DGL) to yield 2-MG (72). An alternative pathway involving phospholipase A_1 (PLA_1) and lyso-PLC may also produce 2-MG, but there is currently little evidence for its biological relevance (73).

3.2 Anabolism and Catabolism of MG

MG may be considered lipid intermediates because they are rapidly metabolized in most biological tissues. The anabolism of MG in the intestine has been previously discussed. In short, the high influx of MG derived from dietary fat is mostly used in enterocytes to produce TG for

CM synthesis, a process known as the MG pathway. This same pathway occurs in other TG storing tissues, such as adipose, but is relatively minor compared to the dominant G-3-P pathway, which has been reported to generate up to 20 times more glycerolipids in various fat depots (74, 75). A common product of both pathways is the generation of DG. While some of this DG continues towards the production of TG, it should be noted that *sn*-1,2-DG is also an intracellular ligand for protein kinase C (PKC) and other receptors, activating their downstream signaling pathways and modulating gene transcription (76). Therefore, the anabolism of MG may generate lipids for diverse purposes, from simple energy storage to signaling cascades with broad-reaching metabolic implications.

The catabolism of MG to yield a FFA and glycerol may be facilitated by one of several enzymes, and is contingent upon tissue specificity. The most well studied of these is MGL, which is considered to be the rate-limiting enzyme in MG hydrolysis in most tissues (Fig 1-2) (67, 77). HSL has also been found to have activity towards MG, as HSL inhibitor treatment reduced MG hydrolysis up to 35% in murine WAT (78). Structurally related to MGL, the serine hydrolase proteins ABHD6 and ABHD12 are two newly discovered integral membrane proteins capable of hydrolyzing MG, whose physiological functions are as yet not well understood. Using a combination of inhibitors in mouse brain samples, it was determined that MGL accounts for 85% for MG catabolism, while ABHD6 and ABHD12 make up for the combined 15% remainder (79). Distinct subcellular localization of each of these enzymes in neurons suggest that they may be individually involved in regulating different pools of MG (79, 80). Further, in pancreatic β-cells, ABHD6 has been shown to be the major MG hydrolase (81). While not yet fully explored, ABHD6 and ABHD12 may possibly be the prime regulators of MG levels in other peripheral tissues or cell types.

In a recent study by Thomas *et al.*, ABHD6 mRNA has been found to be ubiquitously expressed in various mouse tissues, with highest expression in the small intestine, liver and brown adipose tissue (82). Unlike MGL, ABHD6 was also found to have significant hydrolytic activity towards lysophospholipids. Anti-sense oligonucleotide knockdown of ABHD6 in peripheral tissues protected mice from development of metabolic syndrome, indicating a potential role for the enzyme as a mediator of metabolic disease (82).

Figure 1-2
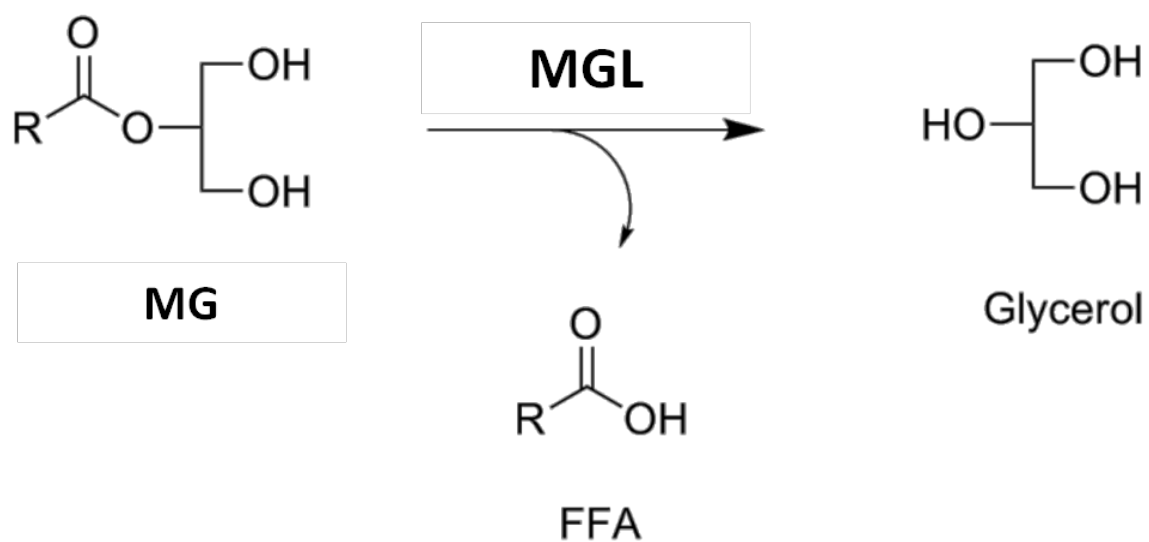
Figure 1-2. Hydrolysis of MG by MGL. The serine hydrolase MGL catalyzes the degradation of *sn*-1(3)-MG and *sn*-2-MG (pictured above) to yield a free fatty acid (FFA) and glycerol.

4.   Monoacylglycerol Lipase

4.1 Monoacylglycerol Lipase: From Gene to Regulation

Starting in 1966, MGL (*mgll*; EC 3.1.1.23) was first partially (83) and then later fully purified from rat epididymal fat (84). Nearly thirty years after, the MGL gene was cloned by digesting purified protein and then sequencing the peptide fragments to generate primers to screen a mouse adipocyte cDNA library (67). This resulted in identification of mouse MGL (mMGL) as a 303 amino acid, 33,218 Da protein, with a catalytic triad of three residues (67). It was later determined by the same group that the *mgll* gene was located on chromosome 6 in mice and 3q21 in humans, consisted of 7 coding exons, and protein expression size varied from 33 to 40 kDa across multiple tissues (85).

The three-dimensional structure of human MGL has been determined by X-ray crystallography to a resolution of 2.2 Angstroms (Fig 1-3) (86). Being a member of the α-β hydrolase fold family, it has the characteristic β-sheet surrounded by α-helices, and a highly conserved central domain that serves as a hydrophobic acyl chain binding pocket for MG and contains the catalytic triad Ser122-His269-Asp239. There is a small adjacent hydrophilic pocket that likely allows the glycerol to exit (86, 87). The non-polar cap domain is currently unexplored, but highlights the amphipathic nature of the MGL protein and its likely interaction with membranes (86).

The substrate specificity of MGL appears to be limited strictly to MG species. MGL is unable to hydrolyze TG, DG, CE, prostaglandin esters, or any lyso-phospholipids (84, 88, 89). Kupiecki originally demonstrated that MGL was optimally functional at pH 8.0 and had a preference for 2-MG (83), but later Tornqvist and Belfrage determined that *sn*-1(3)-MG or *sn*-2-MG were hydrolyzed at equal rates (84). MGL is capable of breaking down MG with both

saturated and unsaturated acyl chains of lengths from C8 to C28 (83, 90, 91). However, there is limited evidence that certain MG substrates are preferred, as 2-AG (C20:4) derivatives had a larger competitive inhibitory effect on 2-oleoylglycerol hydrolysis than did 2-palmitoylglycerol (C16:0) in brain samples (92).

The tissue and intracellular localization of MGL shows it to be a ubiquitously expressed protein. While originally discovered in rat adipose, the mRNA transcript was also found in liver, kidney, ovary, testis, heart, lung, adrenal glands, spleen and skeletal muscle (67). Expression of intestinal MGL was later shown by Ho *et al.* in Caco-2 cells and rodent intestinal mucosa (62). These studies were followed up by Duncan *et al.*, who found widespread MGL expression throughout the gut in mucosal, smooth muscle, and enteric nervous system cells, with the highest epithelial activity in the duodenum and decreased down to the distal colon (93). MGL is also highly expressed in the brain, particularly in pre-synaptic nerve terminals (94). Within cells, MGL was originally found associated with the lipid fraction in adipocytes (67, 84). However, further studies identified MGL in both membrane and cytosolic fractions in brain (95, 96) and intestine (93), supporting the amphipathic nature of the protein.

The transcriptional and post-translational regulation of MGL has been investigated but it not yet fully understood. Some evidence for regulation comes from expression size, as murine MGL exists as a 33, 35, or 40 kDa protein in various tissues (79, 85, 94). Possible explanations for this include different start codon sites, alternative splice variants, or post-translational regulation. Additionally, the peptide sequence has multiple putative phosphorylation sites by PKC, tyrosine kinase, and casein kinase 2 (64). Fatty acids may also play a role in regulation, as evidenced by the ability of the LCFA-activated peroxisome proliferator-activated receptor α (PPARα) to upregulate hepatic MGL expression (97). Further, highly elevated MGL protein and activity are found in aggressive tumor lines, although this may arise from random mutations

rather than regulation by other factors to promote the liberation of intracellular FFA (98).

Dietary fat may also be contributing to MGL regulation, as high fat feeding of mice induced MGL

protein and activity in intestine and liver. In the same study, the intestinal mRNA levels did not

correspond to its protein and activity during development in mice, suggesting some form of

post-transcriptional regulation (64). In the liver, by contrast, MGL transcript, protein, and

activity increased in parallel, suggesting transcriptional control (64). Overall, these studies imply

that the regulation of MGL by lipids and during development is complex and warrants further

investigation.

Figure 1-3
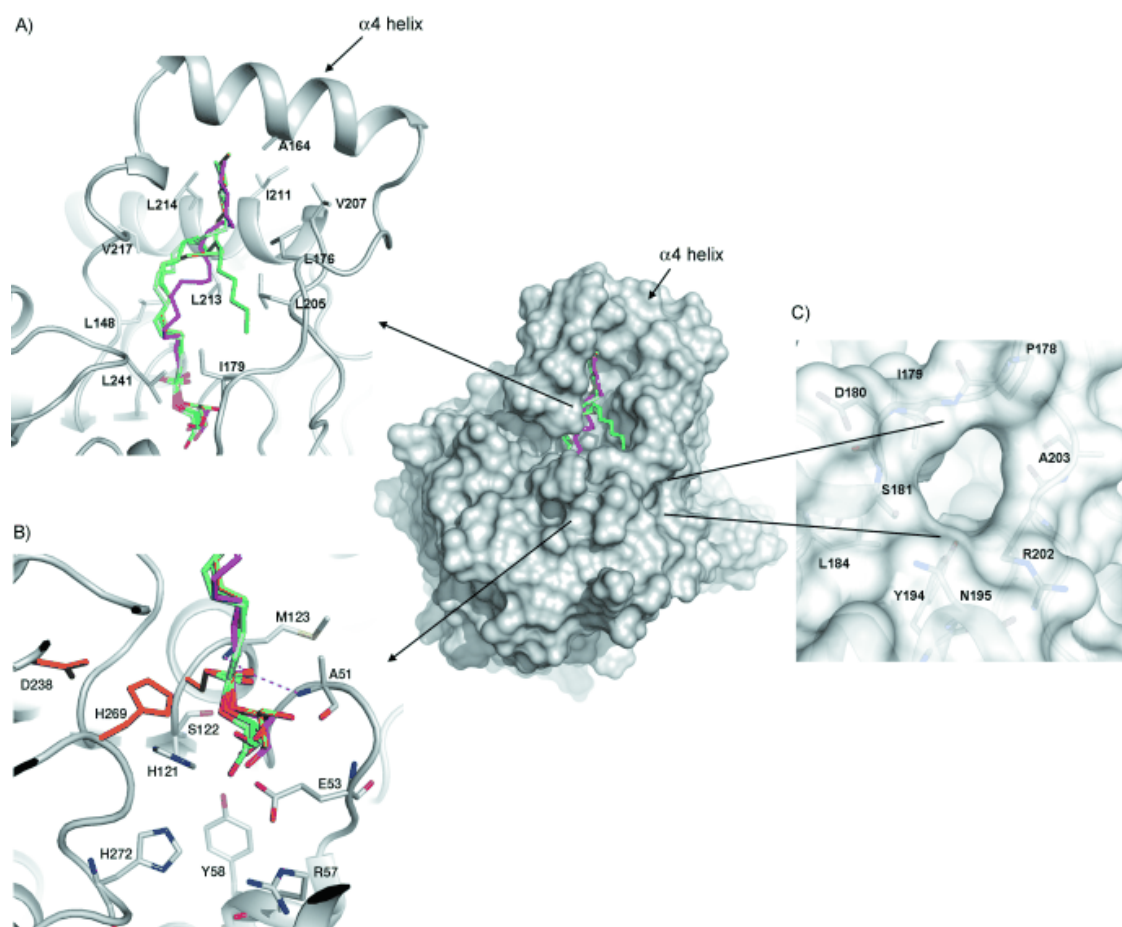
Figure 1-3. Three-dimensional structure of MGL. (A) Shown with 2-AG bound in the hydrophobic binding pocket. (B) The catalytic triad Ser122-His269-Asp239 is also inside the ligand binding pocket and directly interacts with the MG molecule. (C) The exit channel for the glycerol moiety. Figure from Labar *et al*. 2010 (86). Reprinted with permission from John Wiley and Sons © 2010 WILEY-VCH Verlag GmbH & Co. KGaA, Weinheim.

4.2 Monoacylglycerol Lipase: Physiological Roles

The traditional role of MGL has been the mobilization of lipid stores for energy or lipid synthesis. In tissues such as WAT, MGL is necessary to complete the hydrolysis of TG after ATGL and HSL (99, 100). Nevertheless, the quantitative contribution of MGL towards FA and glycerol release is not entirely clear. Immunoprecipitation of MGL in adipocyte lysates markedly reduces glycerol release *in vitro* (99). Yet ATGL and HSL are responsible for more than 95% of total TG hydrolysis in murine WAT, providing the bulk of FA mobilization (101). Further, the purported ability of HSL to hydrolyze MG and the compensatory HSL upregulation in the epididymal fat pads of MGL-KO mice (78) makes determining the *in vivo* contribution of MGL towards lipolysis complicated.

An additional role for MGL as a vital component of the EC system has been the subject of many recent investigations. In short, 2-AG is the most potent endogenous agonist of the cannabinoid receptors CB1 and CB2, which mediate a wide array of physiological adaptations to various stimuli in order to maintain homeostasis. Cessation of EC signaling occurs when 2-AG is degraded. To this effect, MGL has been found to be the primary regulator of 2-AG levels in the brain (95, 102, 103) and is highly expressed in regions with CB1 receptors (94). Due to the broad effects of the EC system on energy balance and lipid metabolism throughout the body, the importance of MGL function cannot be overstated.

Investigations of MG metabolism within intestinal mucosa have identified another potential function of MGL. Three weeks of 40% (kcal) high fat versus low fat (10%) feeding induced MGL expression and activity in mouse mucosa. This induction was not observed in mice after 24 hours of starvation, indicating that MGL may be part of the assimilation of postprandial fat influx in the enterocytes (64). Whether the lipolysis of MG is necessary for the mobilization of TG out of cytoplasmic LD within enterocytes remains to be determined. Nevertheless, the

existence of a MG hydrolyzing enzyme inside enterocytes, which primarily re-esterify MG for CM

synthesis (7), is intriguing and offers the possibility that MGL participates in other functions such

as signaling.

4.3 Monoacylglycerol Lipase: Transgenic Models

To further investigate the function of MGL in intestinal mucosa, Chon *et al.* developed a

transgenic mouse that, driven by the IFABP promoter, over-expressed MGL specifically in

intestinal mucosa (iMGL mouse) (65). Increased MGL expression and activity resulted in reduced

mucosal MG levels, including 2-AG (Fig 1-4A). While dietary lipids were absorbed and had

normal fates in the intestine of iMGL mice, HF-feeding (40% by kcal) resulted in increased

adiposity, which was secondary to hyperphagia and reduced energy expenditure (Fig 1-4 B-D).

There were also alterations in circulating leptin and brain EC system components. In total, the

results from Chon *et al.* suggest that local changes in intestinal MG metabolism by MGL have

broad effects on whole body energy homeostasis and appetite signaling (65).

The over-expression of MGL in mouse forebrain has also been recently described (104).

Forebrain 2-AG levels were decreased approximately 50%, without compensation by any other

EC components, and no differences in MG levels in peripheral tissues. The mice were lean,

hyperphagic, hypoactive, and resistant to HFD-induced obesity and its related effects. They also

had increased energy expenditure, which was associated with increased brown adipose tissue

(BAT) activity and sensitivity to β-adrenergic receptor-stimulated thermogenesis. These results

support an energy sparing role for central CB1 activation by 2-AG that involves multiple tissues

and likely different regions of the forebrain (104).

Figure 1-4
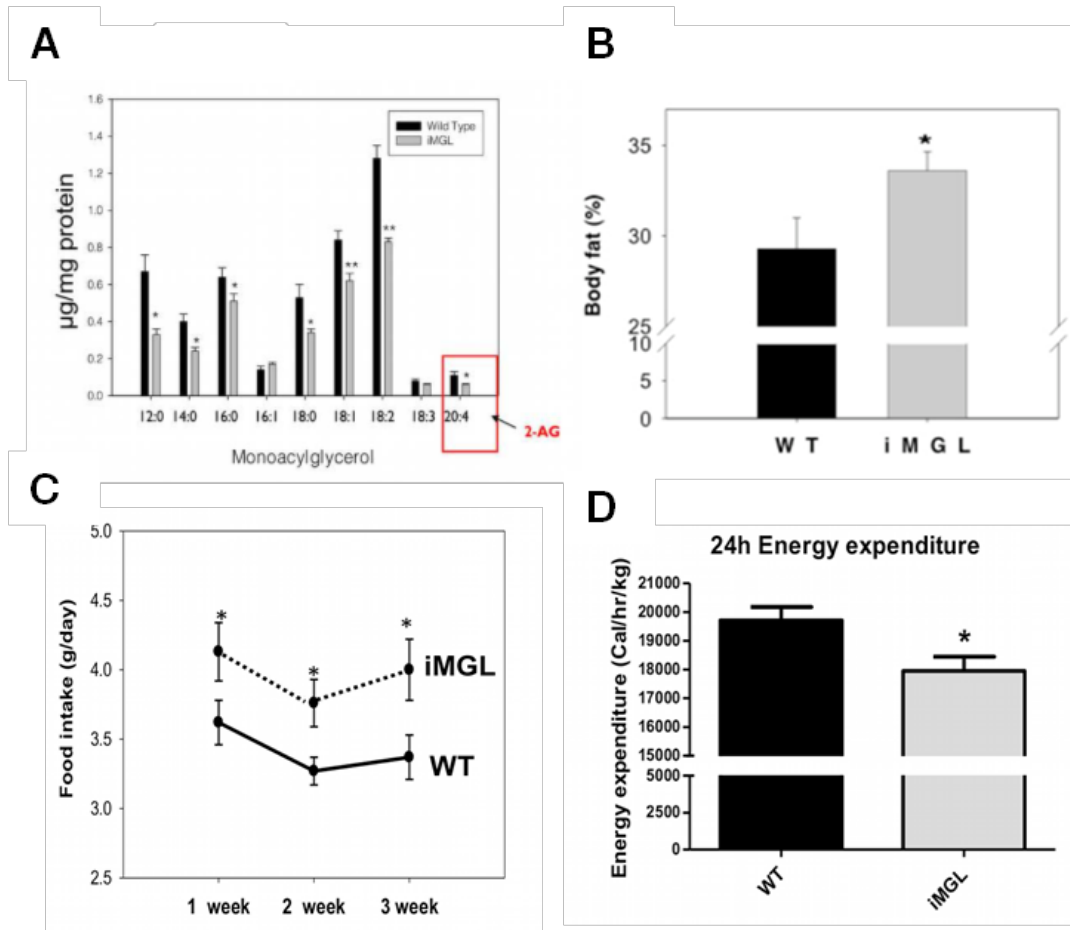
Figure 1-4. Over-expression of intestinal MGL in mice (iMGL) depletes mucosal MG levels and induces an obese, hyperphagic phenotype. (A) Decreased MG species in iMGL mouse small intestinal mucosa. *P < 0.05, **P < 0.01, n=5-8 per group (B) Increased body weight (A) and percent fat mass (B) in iMGL mice fed a 40% (kcal) HFD for 3 weeks. *P < 0.05, n=24-49 per group (C) Increased food intake in iMGL mice over 3 weeks of HFD feeding. *P < 0.05, n=15-20 per group (D) Decreased 24 h energy expenditure in iMGL mice. *P < 0.05, n=8 per group. Figure adapted From Chon *et al.* 2012 (65). Reprinted under Creative Commons Attributions license.

4.4 Monoacylglycerol Lipase: Knockout Models

Until very recently, there was little information on the physiological significance of MGL due to a lack of a knockout models. Currently there are a small number of studies, most of which focus on analgesic, neurological, or inflammatory aspects. The effects of MGL inactivation on MG metabolism, particularly in the brain, are profound. Mice with global MGL ablation have significantly reduced MG hydrolase activity and greater than 10-fold increases in brain 2-AG levels (102, 103). Normally, 2-AG stimulation of brain CB1 impacts core body temperature, locomotion, analgesia, and catalepsy (105), however, none of these have been found to be altered in MGL-/- mice. This may be attributed to tonic activation of CB1 receptors by 2-AG resulting in functional desensitization of the central EC system and reduced brain CB1 receptor density (102, 103). Broadly, this seems to affect neurological functions, as MGL-/- mice also have altered synaptic plasticity in the cerebellum (106), and even improved cognitive function in water maze and object recognition tests (107). There does not appear to be any compensation by other CB1 ligands, as brain levels of the other main EC, AEA, have not been shown to be changed in any of the knockout studies (78, 102, 103). While none of these studies directly assessed the implications of MGL ablation on energy metabolism, Chanda *et al.* found that both male and female knockout mice had a 16.5% decrease in body weight at 3 months of age that persisted over time (103). This phenotype was unaccounted for, but indicated that independent of its role in brain 2-AG regulation, MGL also may be involved in peripheral signaling or homeostatic pathways.

Recent investigations of MGL knockout mice have also highlighted a new aspect of the enzyme as a "coupler" of the endocannabinoid and eicosanoid inflammatory pathways, primarily through 2-AG catabolism. In a study where MGL-/- mice displayed protection against neuroinflammation, it was shown that prostaglandin biosynthesis was impaired due to greatly

reduced release of AA from 2-AG hydrolysis in the brain (108). These findings support a dual role

for MGL promoting inflammation through 2-AG metabolism. First, MGL degrades 2-AG, which

normally binds CB2 receptors to suppress pro-inflammatory pathways. Second, MGL activity

releases AA that is subsequently used as a precursor for a significant amounts of pro-

inflammatory eicosanoids (108). Indeed, it was recently shown that MGL-/- mice were also

protected from ischemia-induced hepatic injury by a mechanism involving increased CB2

activation by 2-AG and reduced prostaglandin production in the liver (109).

One study investigating the metabolic effects of MGL ablation was published by Taschler

et al. (78) while the experiments listed in Aim 2 were ongoing. In this study, there was

accumulation of MG species in multiple tissues, including a greater than 40-fold increase in brain

MG levels. EC system function was compromised, as MGL-/- mice were less-sensitive to the

hypometabolic effects of CB1 agonists. They reported no changes in food intake, body weight,

energy expenditure, or locomotor activity in MGL-/- mice. MGL ablation did affect lipolysis,

however, as there was decreased forskolin-stimulated release of FFA and glycerol, yet plasma

FFA levels were unchanged in both fed and fasted MGL-/- mice. When fed a very high fat diet

(74% kcal), MGL-/- mice had similar body composition to WT controls, but did have improved

glucose tolerance and lower serum insulin, TG, and glycerol levels (78).

4.5 Monoacylglycerol Lipase: Pharmacological Inhibition

The emerging importance of MGL as a key regulator within the EC system had led to the

development of many pharmacological inhibitors, with varying degrees of *in vitro* and *in vivo*

efficacy. Many of these inhibitors target one or more cysteine residues within the hydrophobic

binding pocket of MGL, while others modify the Ser-122 of the catalytic triad (77). The most

potent inhibitor is JZL184, which covalently modifies the nucleophilic serine and causes a

reduction in MG hydrolysis by more than 80% in most tissues (110).

Studies of the acute and chronic administration of JZL184 point to the complexity of the

effects of MGL inhibition. In acute, single dose experiments, JZL184 suppresses MG hydrolase

activity by more than 80% and elevates MG levels in multiple mouse tissues, causing

cannabimimetic behavioral effects such as analgesia, hypomotility, and hypothermia (110, 111).

When the same dose of JZL184 was administered repeatedly for 6 days, the analgesic effects

were lost over time due to desensitization of the EC system, similarly to the MGL null mice

(102). Yet repeated low-dose administration in mice preserved the cannabimimetic effects

(112), suggesting that the degree and timing of MGL inhibition is important in maintaining the

integrity of EC signaling. Moreover, there are more potentially beneficial effects to chronic MGL

inhibition. Eight weeks of JZL184 administration resulted in decreased β-amyloid production,

neuroinflammation, and neurodegeneration in mouse models of Alzheimer's disease, in a

mechanism that did not involve CB1 or CB2 receptors (113). Since none of the mentioned

studies investigated energy metabolism, it is unknown whether JZL184 alters food intake and

energy expenditure, or if there are time-dependent adaptations to pharmacological inhibition.

There is limited information on the effect of MGL pharmacological inhibition on energy

metabolism. Mice given an acute dose of the inhibitor isopropyl dodecylfluorophosphonate

(IDFP) had reduced clearance of circulating TG, hepatosteatosis, and insulin resistance (114,

115). These findings implicate MGL activity in the regulation of liver lipogenesis and glucose

homeostasis, likely through CB1-dependent pathways. However, IDFP is an inhibitor of both

MGL and fatty acid amide hydrolase (FAAH), the enzyme that regulates levels of the other main

EC arachidonoyl ethanolamide (AEA). There is evidence that AEA and 2-AG are not functionally

identical in the EC system. Their degradative enzymes, MGL and FAAH, are primarily localized in

pre-synaptic and post-synaptic regions, respectively (116). Furthermore, acute and chronic

pharmacological blockade of each enzyme independently results in distinctly different effects on

EC-mediated analgesia (102, 110, 111). These results indicate that studies involving inhibitors

that target both enzymes simultaneously are limited, particularly when isolating the individual

contribution of MGL to energy metabolism.

In short, the metabolic implication of specific pharmacological targeting of MGL is

understudied at best. Further research involving the acute and chronic inhibition of MGL may

yield valuable insight into the enzyme function and its use as a therapeutic.

5. The Endocannabinoid System

5.1 Overview of the EC System

The plant *Cannabis sativa* has been used for centuries for its anti-emetic, appetite-

inducing, and psychotropic effects. Only in 1964 was the active component, Δ^9-

tetrahydrocannabinol (THC), finally isolated from hashish (117). Since this discovery, many years

of research had led to a better understanding of the endogenous EC system in humans. At its

most basic level, the EC system is a homeostatic system whose purpose is to respond to stimuli

and regulate physiology. Cannabinoid binding sites are distributed throughout the body to allow

for a broad and diverse response to various physiological conditions. In the central nervous

system (CNS), the EC system regulates learning, pain, emotion, locomotor activity, appetite, and

energy balance. In the periphery, EC activity controls various aspects of macronutrient

metabolism, inflammation, gut motility, reproduction, cardiovascular function, and more (118).

5.2 Components and Mechanism of the System

The EC system is composed of receptors and ligands with their biosynthetic and degradative enzymes. In a basic EC mechanism detailed in neurons (Figure 1-5), depolarization induces an influx of intracellular Ca^{2+}, which results in the release of 2-AG and AEA from membrane phospholipids in the post-synaptic membrane (119). The ligands cross the synaptic cleft in a retrograde manner and bind CB receptors in the pre-synaptic membrane, inhibiting calcium influx and modulating the release of neurotransmitters (120). Signaling is terminated by the uptake of 2-AG and AEA into neurons through putative EC membrane transport proteins and their subsequent hydrolysis by MGL and FAAH, respectively (80). This signaling cascade also occurs throughout the body, albeit with different cell-specific responses to CB receptor activation (121).

The two isoforms of the CB receptors, CB1 and CB2, are both 7 transmembrane G-protein coupled receptors (GPCR) (122). CB1 was first identified and characterized in rat brain (123). While it was also found to be the most abundant GPCR in brain, CB1 is also expressed in peripheral tissues such as liver, adipose, muscle, pancreas, and throughout the small intestine (122). The other isoform, CB2, was first cloned in rat macrophages and is found primarily on immune cells (124).

At least 5 endogenous CB binding ligands have been identified so far (119), but AEA and 2-AG are thought to be the main mediators. In particular, 2-AG is considered the only full agonist of both CB1 and CB2 receptors (125), and is generally more abundant than AEA. Basal 2-AG levels in the brain and subcutaneous fat have been demonstrated to be approximately two orders of magnitude higher than AEA, yet the stimulus-induced flux of each EC has not yet been accurately determined (119, 126). There are other lipid amides, such as palmitoylethanolamide (PEA, N-palmitoylethanolamine), stearoylethanolamide (SEA), and oleoylethanolamide (OEA) that have been shown to potentiate EC stimulation in various tissues in a so-called "entourage

effect", but this may be mediated through other non-cannabinoid receptors such as transient receptor potential vanilloid receptor 1 (TRPV1) (119, 127).

Studies investigating the degradation of 2-AG and AEA by their hydrolyzing enzymes in the brain point to potentially different roles for each ligand. Whereas 2-AG is primarily degraded by MGL localized in pre-synaptic neurons, AEA degradation by FAAH occurs mostly in post-synaptic neurons (94, 116). Additionally, MGL and FAAH are heterogeneously expressed throughout the brain and in peripheral tissues (116), implying the dominance of one ligand over another in particular cell types. In the brain, a small proportion of 2-AG is also hydrolyzed by ABHD6 and ABHD12 (79). Due to the expression of ABHD6 being mostly limited to post-synaptic regions (79, 80), it is possible that the enzyme plays a regulatory function controlling 2-AG levels at its biosynthetic site.

Figure 1-5
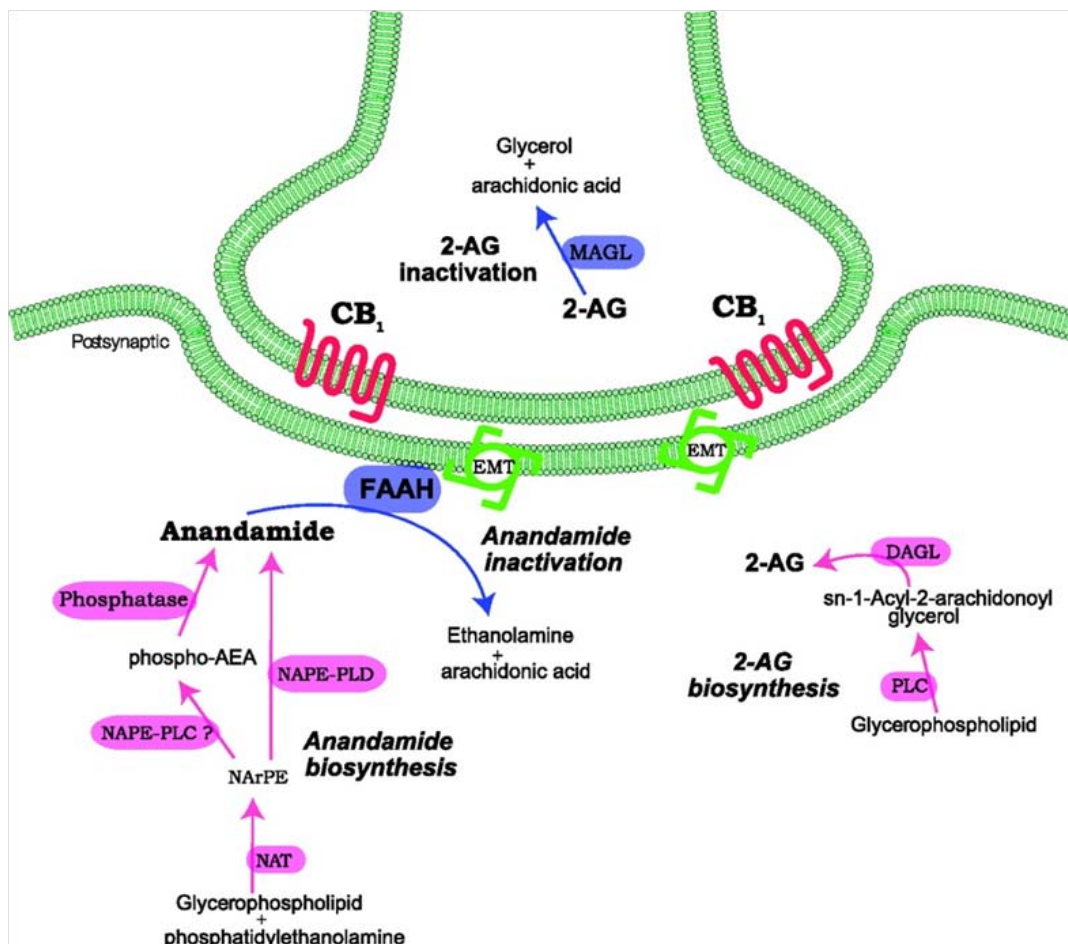
Figure 1-5. Overview of endocannabinoid system in neurons. The ligands 2-AG and anandamide (AEA) are produced from membrane phospholipids in the post-synaptic dendritic spines of neurons after various metabotropic factors and membrane depolarization induce the influx of intracellular Ca^{2+} levels. The EC are released from neurons and cross the synaptic cleft Stimulation of CB1 receptors on pre-synaptic membranes results in decreased Ca^{2+} influx and mainly the suppression of vesicular release of neurotransmitters. Cessation of signaling occurs when 2-AG and AEA are taken back up into neurons via putative endocannabinoid membrane transporters (EMT) and hydrolyzed by their degradative enzymes MGL and FAAH. Figure from Pacher *et al.* 2006 (119). Reprinted with permission from Pharmacological Reviews Online. U.S. government work not protected by U.S. copyright.

5.3 Role in Energy Homeostasis

The overall effect of acute EC activation is the simultaneous accumulation and decreased usage of energy, i.e. an "energy sparing" effect. This is part of a system wide mechanism that includes stimulation of food intake, increased fat storage in peripheral organs, and reduced energy expenditure through hypothermia and hypoactivity (128). Generally, the EC control of energy homeostasis can be divided into central and peripheral mechanisms that may occur both in tandem and independently of each other.

The central regulation of food intake by EC operates by both hedonic and homeostatic mechanisms. In the mesolimbic system, CB1 activation enhances dopamine release in regions such as the nucleus accumbens, thereby reinforcing motivation for intake of energy rich foods (129). In the hypothalamus, CB1 receptors induce the release of orexigenic peptides, such as orexin-1 (130), and downregulate anorectic mediators like corticotropin-releasing hormone (CRH) and melanin-concentrating hormone (MCH) (131, 132) to influence food intake. In support of this, injection of AEA or 2-AG into the brain of rats stimulates eating behavior (133, 134). Signals from the periphery are integrated in the brain to further regulate food intake. The orexigenic actions of the gastric-produced ghrelin seem to be mediated through the central EC system and can blocked by the CB1 antagonist Rimonabant (135, 136). Administration of leptin reduced production of 2-AG and AEA in the hypothalamus of mice (137), indicating a central mode of appetite regulation for this adipocyte-secreted pro-satiety hormone. Brain levels of EC appear to be an integral component of appetite regulation. Fasting induces hypothalamic and limbic forebrain 2-AG levels, which are normalized by feeding (134, 138). This system likely includes both the central control of food intake as well as activation of sympathetic outputs, as mice lacking forebrain-specific CB1 expression are resistant to diet-induced obesity, have reduced body fat, and increased BAT thermogenesis (139).

The peripheral control of energy balance by the EC system is extensive and involves multiple mechanisms. Treatment of mice with peripherally-restricted CB1 antagonists results in reductions in food intake, blunted body weight gain, and attenuated obesity and co-morbidities (140–142). Stimulation of CB1 receptors in WAT activates LPL and increases lipogenesis (131, 143), and also inhibits production of the anti-diabetic hormone adiponectin (144). Similarly in the liver, EC activation stimulates lipogenesis through sterol response element-binding protein 1c (SREBP-1c) and its downstream targets acetyl-CoA carboxylase 1 (ACC1) and fatty acid synthase (FAS), resulting in hepatosteatosis (145). Accordingly, hepatocyte-specific CB1-/- mice are resistant to diet-induced steatosis (146). In skeletal muscle, EC activity decreases oxygen consumption and has been linked to decreased insulin sensitivity (147, 148). Yet there is some controversy about the intracellular mechanisms downstream of CB1 activation. It has been shown that EC have opposite effects on the metabolic sensor AMP-activated kinase (AMPK) in different tissues, resulting in AMPK stimulation in the brain and heart and inhibition in liver and WAT (149). Reasons for these differential tissue effects of EC activation are unknown.

The EC system also appears to be very active in the gut in its contribution towards maintaining energy homeostasis, particularly in controlling food intake. Rodents that were fasted had 7-fold increases in intestinal AEA levels that were normalized upon feeding (150). It is possible, therefore, that EC produced in the gut are directly stimulating eating behaviors. This is also indirectly supported by findings that pharmacological CB1 antagonism abolishes the suckling response in newborn mouse pups, which can then be restored by supplementation of maternal milk with 2-AG (151). While both CB1 and CB2 are found throughout cells in the gastrointestinal system (152, 153), the CB1 receptors expressed on the vagal nerve afferents connecting the gastrointestinal system to the brainstem and medulla are good candidates for EC appetite signaling. Indeed, the satiety effects of the intestinally-released hormone

cholecystokinin (CCK) appear to be mediated by downregulation of CB1 on vagal afferents (154, 155). Moreover, the anorectic effects of peripherally administered CB1 antagonist/inverse agonist Rimonabant can be abolished by inactivating CCK-sensitive vagal nerves (150).

5.4 Dysregulation in Metabolic Disorders

Due to their pleiotropic effects on energy balance, EC have been implicated in the pathogenesis and progression of metabolic disease (156). The EC system is chronically overactivated in the periphery of obese humans (157). Obese subjects also have elevated circulating and adipose tissue levels of EC, including 2-AG (157, 158). Treatment with the CB1 antagonist/inverse agonist Rimonabant (SR141716A) reduced body fat and improved metabolic parameters in obese patients (159).

Whether EC activity is a cause or an effect of adiposity has not been definitively shown. However, there is evidence that dysregulation of the EC system drives obesity. Consumption of a diet rich in the EC precursor linoleic acid (C18:2, LA) by mice increases 2-AG and AEA production and ultimately results in obesity, which can be ameliorated by addition of the dietary n-3 PUFAs docosahexanoic acid (DHA) and eicosapentanoic acid (EPA) (160). Similarly, mice fed a high fat diet (60% fat kcal) for 3 weeks had increased hepatic AEA and CB1 expression prior to weight gain, suggesting that obesity-associated lipogenesis may by driven, in part, by the EC system. Additionally, weight loss of 5% in obese individuals did not normalize circulating EC levels or expression of EC system genes (161), indicating that EC dysregulation may be upstream of metabolic disorders.

Overall, there is a wealth of scientific evidence that the metabolism of neutral lipids, such as MG, is altered in obesity. Focusing on the gut as a vital organ for energy uptake and

homeostasis, we have already identified a potential new aspect that links intestinal MG

catabolism and whole body energy homeostasis. This opens the possibility that MGL inhibitors

may prove to be a valid treatment for obesity and the metabolic syndrome. Yet studies have

shown the effects of short- and long-term of modulation of MG levels to be complicated.

Nevertheless, the extent to which enzymes, such as MGL, are regulating energy homeostasis

under normal and pathological conditions warrants further investigation. This will be, in part,

the subject of the following studies.

6. Specific Aims of the Studies

1) **To investigate the effects of obesity and high fat feeding on intestinal mucosal triacylglycerol accumulation.**

   The accumulation of ectopic fat in liver and muscle during obesity is associated with

   metabolic dysfunction, yet little is known about the intestine in the obese state. We

   used *ob/ob* mice and 40% high fat (HF) fed wild type (C57BL6/J) mice to examine the

   effects on intestinal mucosal TG accumulation in both fed and fasted states.

2) **To investigate the metabolic effects of genetic MGL ablation in mice fed low fat and high fat diets.**

   Previous studies of MGL$^{-/-}$ mice have shown dramatically increased tissue levels of MG

   species and improved glucose tolerance after being a fed high-fat diet (HFD). The effect

   of MGL ablation on body weight has been variable among studies. Alternatively, we

   have shown that MGL overexpression in mouse intestine leads to hyperphagia and

   obesity, indicating a potential role for MGL as a regulator of lipid satiety signals in the

gut. In this aim, we evaluated wild type (C57BL6/J) and MGL$^{-/-}$ mice for 12 weeks on 10% low fat and 45% high fat semipurified diets, and examined effects on satiety and the development of obesity.

3) **To investigate the acute and chronic effects of pharmacologic MGL inhibition on feeding and energy homeostasis.**

The metabolic effects of MGL-specific inhibition have not been explored. Chronic treatment of mice with other MGL inhibitors indicates that endocannabinoid-mediated analgesic effects decrease over time due to CB1 receptor desensitization. We investigated the effects of pharmacological MGL inhibition in mice using a novel reversible inhibitor. In the acute study, we administered the MGL inhibitor to diet-induced obese (DIO) C57BL6/J mice for 4 days and measured the effects on body weight, food intake, and MG levels. In the chronic study, we administered the MGL inhibitor for 27 days and measured effects on metabolic parameters such as body composition, food intake, and glucose tolerance.

Chapter 2

Intestinal mucosal triacylglycerol accumulation secondary to decreased lipid secretion in obese and high fat-fed mice

Douglass, J.D., Malik, N., Chon, S.H., Wells, K., Zhou, Y.X., Choi, A.S., Joseph, L.B., and Storch, J.

ABSTRACT:

The ectopic deposition of fat in liver and muscle during obesity is well established, however surprisingly little is known about the intestine. We used the *ob/ob* mouse and C57BL6/J mice fed a high fat (HF) diet to examine the effects of obesity and the effects of HF feeding, respectively, on intestinal mucosal triacylglycerol (TG) accumulation. Male C57BL6/J (WT) mice were fed low fat (LF; 10% kcal as fat) or HF (45%) diets, and *ob/ob* mice were fed the LF diet, for 3 weeks. In this time frame, the WT-HF mice did not become obese, enabling independent examination of effects of the HF diet and effects of obesity. Analysis of intestinal lipid extracts from fed and fasted animals demonstrated that the mucosa, like other tissues, accumulates excess lipid. In the fed state, mucosal triacylglycerol (TG) levels were 3-fold and 5-fold higher in the WT-HF and *ob/ob* mice, respectively, relative to the WT-LF mice. In the fasted state, mucosa from *ob/ob* mice had 3-fold higher TG levels relative to WT-LF mucosa. Q-PCR analysis of mucosal mRNA from fed-state mice showed alterations in the expression of several genes related to both anabolic and catabolic lipid metabolism pathways in WT-HF and *ob/ob* mice relative to WT-LF controls. Fewer changes were found in mucosal samples from the fasted-state animals. Remarkably, oral fat tolerance tests showed a striking reduction in the plasma appearance of an oral fat load in the *ob/ob* and WT-HF mice compared to WT-LF. Overall, the results demonstrate that the intestinal mucosa accumulates excess TG during obesity. Changes in the expression of lipid metabolic and transport genes, as well as reduced secretion of dietary lipid from the mucosal cells into the circulation, may contribute to the TG accumulation in intestinal mucosa during obesity. Moreover, even in the absence of frank obesity, HF feeding leads to a large decrease in the rate of intestinal lipid secretion.

INTRODUCTION:

The increasing prevalence of metabolic syndrome presents a great challenge to world health. Contributing to the development of coronary heart disease and diabetes mellitus, metabolic syndrome is composed of multiple risk factors that include insulin resistance, dyslipidemia, and central obesity (162). Understanding the connection between dyslipidemia and obesity remains an important goal towards elucidating the pathological mechanisms. In particular, the ectopic deposition of fat seems to play a critical role in tissue dysfunction. Studies show that both obese children and adults exhibit fat deposition in liver and skeletal muscle (163–165). Intrahepatic triacylglycerol (TG) is a known marker for metabolic dysregulation in obese individuals (166). Further, intramyocellular TG can result in impaired insulin sensitivity, causing a direct effect on glucose and lipid metabolism (167). However, accumulation of lipid in other organs, and its potentially negative effects, has remained relatively unexplored. In particular, little is known about the effects of obesity on the small intestine.

During digestion and absorption dietary fat, composed mostly of TG, is broken down by lipases in the lumen of the digestive tract. The resultant monoacylglycerols and fatty acids (FA) are absorbed by enterocytes in the small intestinal mucosa, where they are reesterified back into TG in the endoplasmic reticulum (ER). The TG is incorporated into chylomicrons (CM), which are trafficked to the Golgi apparatus and secreted into the lymphatic system and eventually the general circulation (7). There is now a growing body of evidence that newly synthesized TG is not immediately shuttled out of enterocytes, but also stored in lipid droplets (LD). Human studies show that dietary lipids ingested in one meal are present in CM secreted following a second meal (168). Other human studies demonstrate that an oral fat load results in jejunal storage of the ingested lipid that can be released 4 hours later by glucose administration (53).

Intraduodenal lipid administration in rats shows that while postprandial TG synthesis is quite rapid, the lipid load can be increased until shuttling of TG from the ER to Golgi stops entirely and a cytoplasmic TG pool is formed that may be an overflow reservoir for later export (169). Finally, *in vivo* coherent anti-Stokes Raman scattering imaging of murine small intestine shows the existence of cytoplasmic LDs in enterocytes following an oral fat challenge (54). Interestingly, mice fed a high-fat diet had more and larger LDs in enterocytes compared to low-fat diet controls (54, 55).

We used two murine models to explore the effects of obesity and diet on the small intestine: *ob/ob* mice and high fat diet fed C57BL6/J mice. Owing to a single gene mutation that prevents the production of the adipokine leptin, the *ob/ob* mouse is a model for type 2 diabetes that exhibits hyperglycemia and marked obesity (170, 171). This is largely due to dysregulation of central appetite signaling which results in hyperphagia, as well as dysfunctions in FA and TG metabolism in peripheral tissues (172, 173). We also used C57BL6/J mice to examine the effects of HF feeding on mucosal TG. We hypothesized that in obese animals the intestinal mucosa, like liver and skeletal muscle, would accumulate lipids. In the present study, we report that obese mice accumulate mucosal TG in the fed and fasted state. This TG deposition is accompanied by changes in the mucosal expression of several lipogenic and lipid trafficking genes. Furthermore, both the ob/ob and the WT-HF mice display a marked reduction in TG secretion following an oral lipid load, relative to WT-LF mice. These results expand our understanding of obesity and reinforce the idea that tissue fat accumulation is often concurrent with metabolic dysfunction.

MATERIALS AND METHODS:

Animals, Diet, Surgical Procedures, and Tissue Collection

Thirty C57BL/6J (wild-type) male mice and thirteen *ob/ob* male mice were obtained from Jackson Laboratories (Bar Harbor, ME). All mice were 8 weeks old upon arrival and weighed 22-27 g (WT) or 47-54 g (*ob/ob*). The mice were housed three per cage and fed Purina 5015 rodent chow (60% carbohydrate, 12% fat, 28% protein by kcal) for a week before the start of the study. For the three-week feeding period, fifteen WT mice and thirteen *ob/ob* mice were fed a 10% kcal low-fat semipurified diet (D12325, Research Diets Inc., New Brunswick NJ) (Table 2-1). The remaining fifteen WT mice were fed a 40% kcal high-fat semipurified diet (D12327, Research Diets Inc., New Brunswick NJ) (Table 2-1). The WT-LF mice served as controls for dietary fat content (vs. WT-HF fed mice), and for genotype (vs. *ob/ob*-LF fed mice). These three groups were used for all analyses.

At the end of the three-week feeding period, body composition was analyzed by magnetic resonance imaging using an EchoMRI-100 (Echo Medical Systems, Houston TX). Food was removed from the mice cages 12 hours prior to sacrifice (fasted state) or the mice were given ad libitum food access (fed state). Unless otherwise noted, tissue collections were performed between 9 and 11 am. Before sacrifice, the mice were injected intraperitoneally with a ketamine-xylazine-ace promazine cocktail (54.5/5.45/0.8 mg/kg, respectively) to induce deep anesthesia, followed by exsanguination. The entire small intestine was excised, rinsed twice with saline (0.85% NaCl), and the mucosa harvested by scraping with a glass slide. The mucosa samples were immediately weighed in polypropylene tubes and frozen in dry-ice ethanol. The liver was excised, weighed, and frozen in dry-ice ethanol. The intestinal mucosa samples were immediately homogenized followed by subsequent lipid and RNA extractions on the same day of

Table 2-1

Diet	D12325		D12327	
	gm%	kcal%	gm%	kcal%
Protein	19	20	23	20
Carbohydrate	68	70	46.1	40
Fat	4	10	20.4	39.9
Total		100		100
kcal/gm	3.86		4.6	
Ingredient				
Casein	200	800	200	800
DL-Methionine	3	12	3	12
Sucrose	700	2800	396	1584
Cellulose	50	0	50	0
Soybean Oil	45	405	45	405
Coconut Oil			135	1215
Mineral Mix	35	0	35	0
Calcium Carbonate	5	0	5	0
Vitamin Mix	10	40	10	40
Choline Bitartrate	2	0	2	0
FD&C Blue Dye #1	0.05	0	0.05	0
FD&C Red Dye #40			0.05	0
Total	1050	4057	881.1	4056

Table 2-1 Diet composition

the experiment. The liver samples were stored at -80° C until later analysis. All animal procedures were approved by the Rutgers University Animal Use Protocol Review Committee and conformed to the National Institutes of Health *Guide for the Care and Use of Laboratory Animals.*

Lipid Extraction and TG analysis

Liver and mucosa samples were homogenized with 1X PBS pH 7.4 in 20X and 10X ml per gram of sample, respectively, on ice with a Dounce homogenizer and a Wheaton overhead stirrer at 5,000 rpm. Total tissue protein concentration was determined by Bradford assay (174). The homogenate was diluted to 1mg protein/ml in PBS and lipid extractions were performed on 1 ml of diluted sample by the Folch procedure (175). Lipid extracts and triolein standards were spotted on Silica Gel G TLC plates and separated by a non-polar solvent system (hexane-diethyl ether-acetic acid, 70:30:1; v/v). Lipids were visualized by iodine vapor and quantitation of TG determined using ImageJ (Bethesda, MD), as previously described (63).

Histological examination of mucosal lipid

Mice were maintained and fed as described in the previous section. All mice were given *ad libitum* access to food and water prior to necropsies (fed state), which were performed between 9 and 11 am. The mice were first anaesthetized as described above, followed by exsanguination. The small intestine was removed, rinsed with buffered PBS, trimmed, tied off, and filled with 4% paraformaldehyde in PBS for 2 hours at room temperature. The lumen was then rinsed with 2% sucrose in PBS, cut into 7mm pieces and embedded in 10mm Tissue-Tek Cryomolds (Sakura Finetek, Torrance, CA) filled with Tissue-Tek O.C.T. Compound (Sakura

Finetek, Torrance, CA). Molds containing OCT and tissue were snap frozen in liquid nitrogen and stored at -80ºC until use.

For Oil Red O analysis, 10 μm frozen sections were cut on a Microm HM505E cryotstat using Edge-Rite Low Profile Microtome Blades (Richard-Allan Scientific, Kalamazoo, MI) and mounted to Superfrost Plus Micro Slides (VWR, Radnor, PA). Sectioned tissue was stored at -20ºC. Tissue was removed from the -20°C and brought to room temperature for 15 minutes prior to Oil Red O staining. Oil Red O (Fisher Scientific, Pittsburgh, NJ) was prepared according to Humason (176). Immediately prior to use the stock solution was diluted with distilled deionized water (6:4, V/V) and filtered through a 0.2 μm filter. Tissue sections were post-fixed with 10% formalin (Fisher Scientific, Pittsburgh, PA) for 15 minutes, dipped in 60% isopropanol for 30 seconds, and stained with Oil Red O for 30 minutes. Tissue was destained with 60% isopropanol, rinsed under running tap for 2 minutes, and counterstained with hematoxylin (Invitrogen, Camarillo, CA). Oil Red O sections were preserved with glycerin (Fisher Scientific, Pittsburgh, NJ) under nail polish sealed cover glass (Fisher Scientific, Pittsburgh, PA). Random sections were analyzed and photographed using an Olympus BX51 microscope equipped with a DP71 digital camera.

RNA Extraction and quantitative RT-PCR Analysis

Total mRNA was extracted from intestinal mucosa using a modified method from Chomczynski and Sacchi (64) and analyzed as previously described (28). In brief, the tissues were homogenized in 4 M guanidinium thiocyanate with an Ultra-Turrax IKA-Werke (Wilmington, DE). Total RNA was isolated by phenol extraction, followed by precipitation and washing with ethanol. The RNA was further purified by removal of genomic DNA by DNase digest and RNeasy cleanup kit (Qiagen, Valencia, CA). The integrity of the RNA was assessed by gel electrophoresis

and visualization of the 18S and 23S rRNA subunits. Reverse transcription was performed on 2 μg of RNA using a high capacity cDNA kit (Promega, Madison, WI). Primer sequences were determined using the NCBI gene database and ordered from Sigma Aldrich (St Louis, MO) for the following primers shown in Table 2-2: β-actin, monoacylglycerol acyltransferase 2 (MGAT2), diacylglycerol acyltransferase 1 (DGAT1), diacylglycerol acyltransferase 2 (DGAT2), monoacylglycerol lipase (MGL), glycerophosphate acyltransferase 3 (erGPAT3), mitochondrial glycerophosphate acyltransferase (mtGPAT), CD36, microsomal triacylglycerol transfer protein (MTP), liver fatty acid binding protein (LFABP), intestinal fatty acid binding protein (IFABP), carnitine palmitoyltransferase 1 (CPT1), acyl-coA oxidase (ACO), fatty acid synthase (FASN), and acetyl-coA carboxylase 1 (ACC1). The efficiency (100 ± 5%) of each PCR primer set was first assessed by standard curve. Real time PCR (RT-PCR) was performed in triplicate using the ddCT method on the ABI 7300 PCR instrument (Applied Biosystems, Foster City, CA). Each reaction contained 80 ng of cDNA, 250 nM of each forward and reverse primer, and 12.5 μl of POWER SYBR Green Master Mix (Applied Biosystems, Foster City, CA) in a total volume of 25 μl. β-actin was used as the endogenous control for each standard and the relative quantitation of each gene was determined with respect to the average of the WT-LF mice.

Oral Fat Tolerance Test

Following the 3-week feeding study the mice were fasted for 16 hours overnight. All OFTT were conducted from 9AM-1PM. The mice were weighed and at t_0 were injected with 500 mg/kg body weight of Tyloxapol (Triton WR-1339) to block peripheral lipoprotein clearance. Thirty minutes following Tyloxapol injection, 300ul of olive oil (OO) was given by orogastric gavage. Blood samples were collected from the tail at time = 0 (t_0), 30, 60, 90, 150, 240 minutes.

Table 2-2

Gene	Primer Sequence (forward & reverse)
B-actin	5'-GGCTGTATTCCCCTCCATCG-3'
	5'-CCAGTTGGTAACAATGCCATGT-3'
MGAT2	5'-CGGAGGTGGACAACCTAACG-3'
	5'-TGAGGTATTCCGGCCTGTTAT-3'
DGAT1	5'-TGTTCAGCTCAGACAGTGGTT-3'
	5'-CCACCAGGATGCCATACTTGAT-3'
DGAT2	5'-TTCCTGGCATAAGGCCCTATT-3'
	5'-AGTCTATGGTGTCTCGGTTGAC-3'
MGL	5'-CAGAGAGGCCCACCTACTTTT-3'
	5'-ATGCGCCCCAAGGTCATATTT-3'
erGPAT3	5'-TATCCAAAGAGATGAGTCACCCA-3'
	5'-CACAATGGCTTCCAACCCCTT-3'
mtGPAT	5'-CTGCTTGCCTACCTGAAGACC-3'
	5'-GATACGGCGGTATAGGTGCTT-3'
CD36	5'-TCCCCCTACTAGAAGAAGTGGG-3'
	5'-TCCAACAGATTGGTTTCGTTCA-3'
MTP	5'-CTCTTGGCAGTGCTTTTTCTCT-3'
	5'-GAGCTTGTATAGCCGCTCATT-3'
LFABP	5'-GGGGGTGTCAGAAATCGTG-3'
	5'-CAGCTTGACGACTGCCTTG-3'
IFABP	5'-GTGGAAAGTAGACCGGAACGA-3'
	5'-CCATCCTGTGTGATTGTCAGTT-3'
CPT1	5'-AGCACACCAGGCAGTAGCTT-3'
	5'-AGGATGCCATTCTTGATTCG-3'
ACO	5'-ATATTTACGTCACGTTTACCCCGG-3'
	5'-GGCAGGTCATTCAAGTACGACAC-3'
FASN	5'-AGGTGGTGATAGCCGGTATGT-3'
	5'-TGGGTAATCCATAGAGCCCAG-3'
ACC1	5'-ATGGGCGGAATGGTCTCTTTC-3'
	5'-TGGGGACCTTGTCTTCATCAT-3'

Table 2-2 Primer sequences used for qRT-PCR analyses

The amount of TG present in blood plasma at each time point was determined using a Wako L-Type TG-H kit (Richmond, VA) and performed in duplicate in a microplate reader.

Statistical Methods

Unless otherwise noted, all group data are shown as average ± s.e.m. Statistical comparisons were determined using a two-sided *Student's* t-test or one-way ANOVA with Tukey's post-hoc comparison. Differences were considered significant at $p < 0.05$.

RESULTS:

High-fat fed and ob/ob mouse models

As expected at baseline the WT mice had a substantially lower body weight than their age-matched *ob/ob* counterparts (Fig 2-1A). Following the 3 week feeding period, the *ob/*ob maintained their weight. The WT-LF and WT-HF groups gained approximately 3 grams per mouse (Fig 2-1A). At the end of the three weeks, body composition was assessed by MRI and showed that the *ob/ob* mice had a significantly higher percentage of total body fat than both the WT-LF and WT-HF groups (Fig 2-1B). There was no significant difference in total body fat percentage between the WT-LF and WT-HF groups. The *ob/ob* group also displayed significantly more epididymal fat as a percentage of their body weight than either WT group (Fig 2-1C). While there was a trend of higher percent epididymal fat in the WT-HF compared to WT-LF mice, it did not reach statistical significance. The hedonic mouse strain C57BL6/J tends to develop obesity and hyperglycemia (177). That the WT-HF mice did not gain weight relative to the WT-LF group is in contrast to our previous studies using older mice (64), however, this allowed a comparison between the effects of HF feeding in the absence of obesity, to the effects of genetically mediated obesity.

TG content of intestinal mucosa and liver

Hepatic TG levels were 120 ± 29, 129 ± 35, and 3698 ± 323 ug/mg protein for the WT-LF, WT-HF, and *ob/ob* mice, respectively, in the fed state. We also quantified the amount of TG in the intestinal mucosa of fed and fasted mice (Fig 2-2). In fasted mice, the *ob/ob* group had - approximately 3-fold higher mucosal TG compared the WT-LF and WT-HF groups ($p < 0.01$). Thus, in the ob/ob genetic obesity model, intestinal mucosa has increased TG levels even in the

Figure 2-1
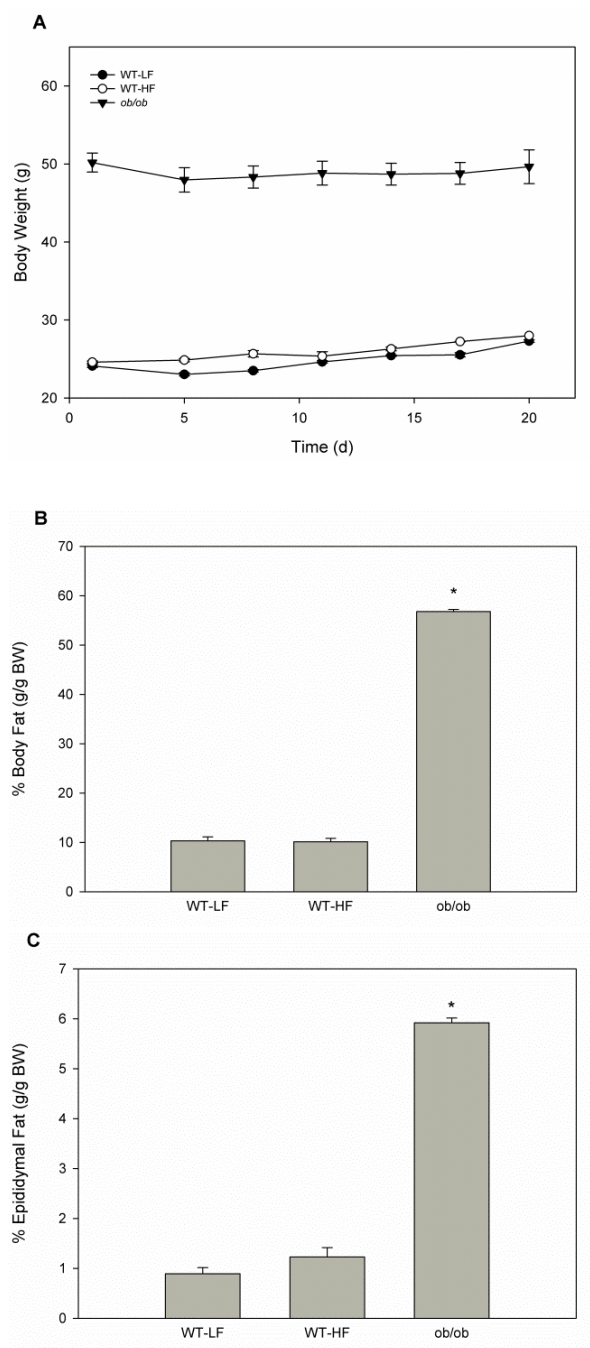
Figure 2-1. Weight and body fat of mouse models. (A) Average body weight of mice over the three-week feeding study. Error bars may not be visible within data point. (B) Percent body fat as determined by EchoMRI. (C) Percent of total body weight as epididymal fat determined by tissue weight. Data represent average ± s.e.m., p < 0.05 or lower versus WT-LF, n=5-6 for WT, n=3 for *ob/ob*.

Figure 2-2
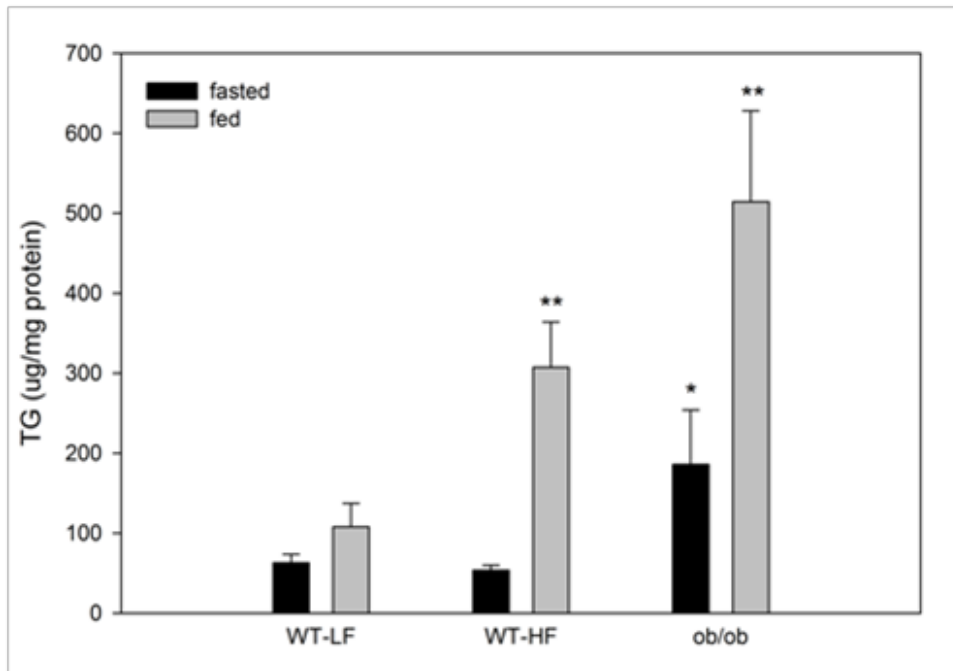
Figure 2-2. Intestinal mucosa TG content in fed and 12 h fasted mice. Average ± s.e.m., *p < 0.05, **p < 0.01 versus fed or fasted WT-LF, n=4-6 for WT, n=3-4 for *ob/ob*.

fasted state. In the fed state, mucosal TG levels in *ob/ob* were 5-fold greater than in the WT-LF mice (p < 0.01). In WT animals, a 3-fold increase in mucosal TG was found in the fed state in HF animals, however in the fasted state there were no differences in mucosal TG levels between HF- and LF-fed mice. Fecal fat levels were < 4% by weight in all groups (not shown).

Neutral lipid accumulation in duodenal sections from the proximal small intestine of fed mice was visualized using ORO staining. In keeping with the biochemical analysis, pronounced staining was observed in *ob/ob* mucosa, and greater staining was found in WT-HF compared to WT-LF mucosa (Fig 2-3A-C). We noticed during sectioning and histological preparation that the *ob/ob* mucosal samples were more fragile than either of the WT samples, as seen by decreased mucosal integrity (Figure 2-3C).

Lipid metabolic gene expression is altered in obese intestinal mucosa

To further understand the changes that may account for increased enterocyte TG storage, we quantified the relative expression of 14 lipid metabolic and transport genes in the intestinal mucosa of fed and fasted mice using RT-PCR. In fasted WT-HF mice DGAT2, MGL, MTP, and FASN expression were significantly greater than in fasted WT-LF controls (Fig 2-4A). In the fed state these same genes as well as erGPAT3, CD36, CPT1, ACO, and ACC1 were significantly increased in the WT-HF group, while MGAT2 transcript levels were significantly decreased. In both the fasted and fed states, mtGPAT, DGAT1, IFABP, and LFABP were not significantly different between the WT mice fed either a low-fat or high-fat diet.

In contrast to the WT-HF group, in fasted *ob/ob* mice, many of the genes analyzed were significantly down-regulated relative to the WT-LF controls (Fig 2-4B). However in the fed state, similar to what was observed in the WT-HF group, most of the genes analyzed were increased relative to WT-LF mice, including a robust upregulation of CPT1. These results indicate that both

Figure 2-3
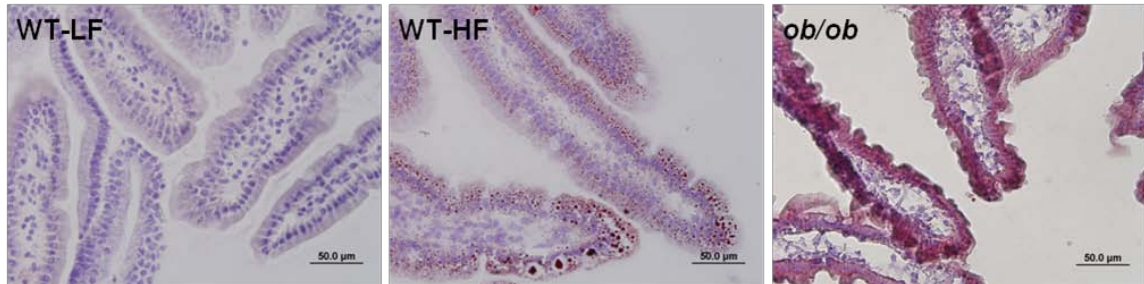
Figure 2-3. Lipid accumulation in fed state proximal intestinal mucosa. (Left) LF-fed WT mice (Middle) HF-fed WT mice (Right) LF-fed *ob/ob* mice. 40X magnification, 10 μm section, ORO and H&E stain, as described in Materials and Methods.

Figure 2-4
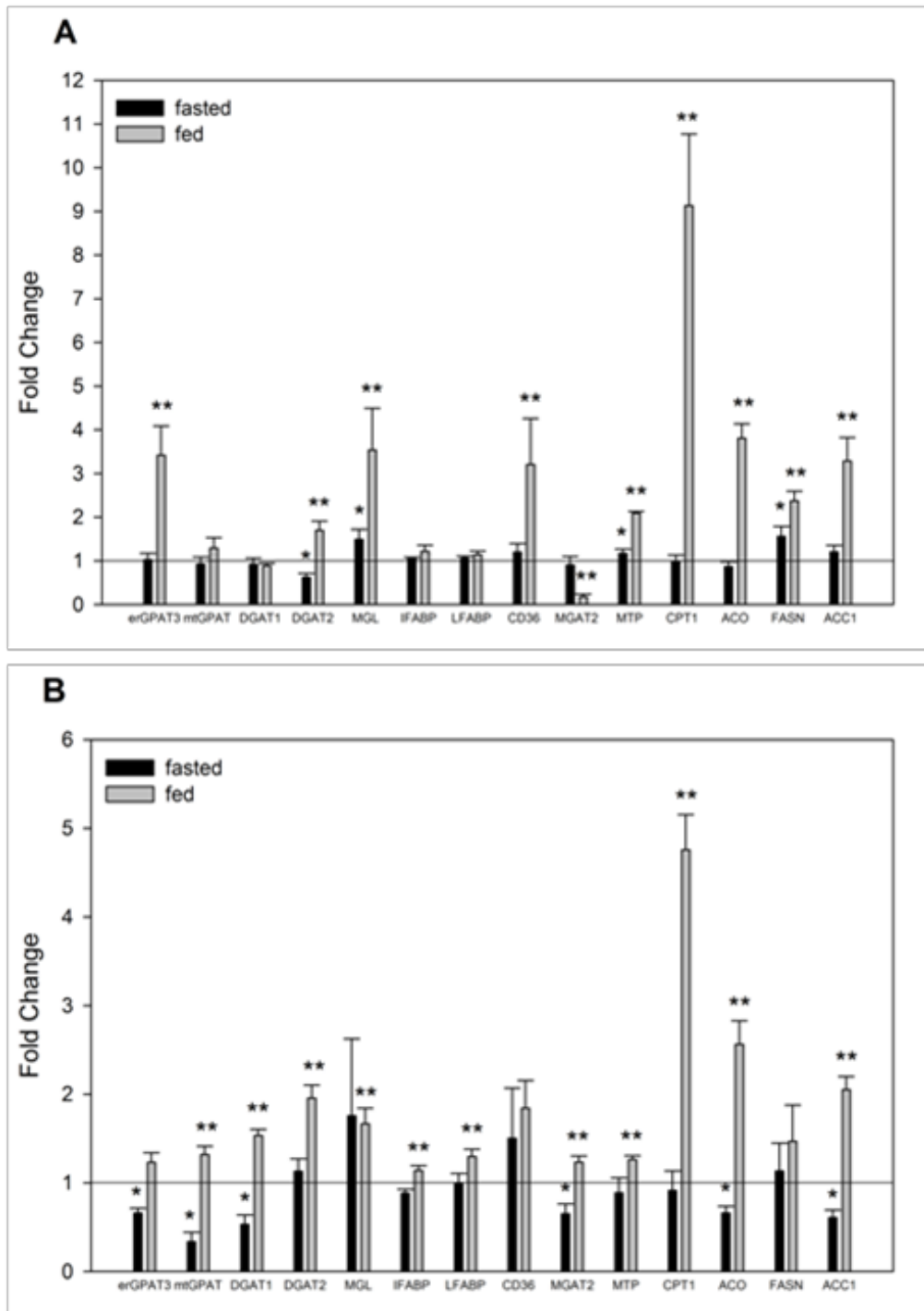
Figure 2-4. Relative quantitation of mRNA expression of lipid metabolic and transport genes.
(A) Fasted and fed WT-HF mice relative to fasted and fed WT-LF mice. (B) Fasted and fed *ob/ob* mice relative to fasted and fed WT-LF mice. Average $\pm$ s.e.m., *p<0.05 or lower versus fasted WT-LF, **p < 0.05 or lower versus fed WT-LF, n=3-6 per group.

the high fat diet and genotype influence the expression of genes in intestinal mucosa involved in TG synthesis, chylomicron secretion, and the uptake, oxidation, and *de novo* synthesis of fatty acids. It is therefore possible that gene expression differences in obese mice may, in part, contribute to the observed TG accumulation in *ob/ob* and WT-HF mouse intestine (Fig 2-2 and 2-3).

Decreased intestinal TG secretion in ob/ob and WT-HF mice

We challenged the three groups with an OFTT to determine their capacity to absorb a bolus of olive oil and release it into the bloodstream. Both the WT-HF and *ob/ob* mice had dramatic reductions in appearance of the oil load as serum TG over the 4-hour test. The differences between groups increased over time up to t_{240}, at which point serum TG levels for WT-LF, WT-HF, and *ob/ob* mice were 1180 ± 2, 359 ± 133, and 134 ± 17 mg/dl, respectively (Fig 2-5). The markedly slower rates of TG secretion in the WT-HF mice and the *ob/ob* mice suggest that obesity and high fat feeding are accompanied by intestinal dysfunction. The reduced rate of intestinal lipid secretion likely contributes to increased storage of dietary fat in enterocyte lipid droplets, resulting in increased mucosal TG accumulation (Fig 2-2 and 2-3).

Figure 2-5
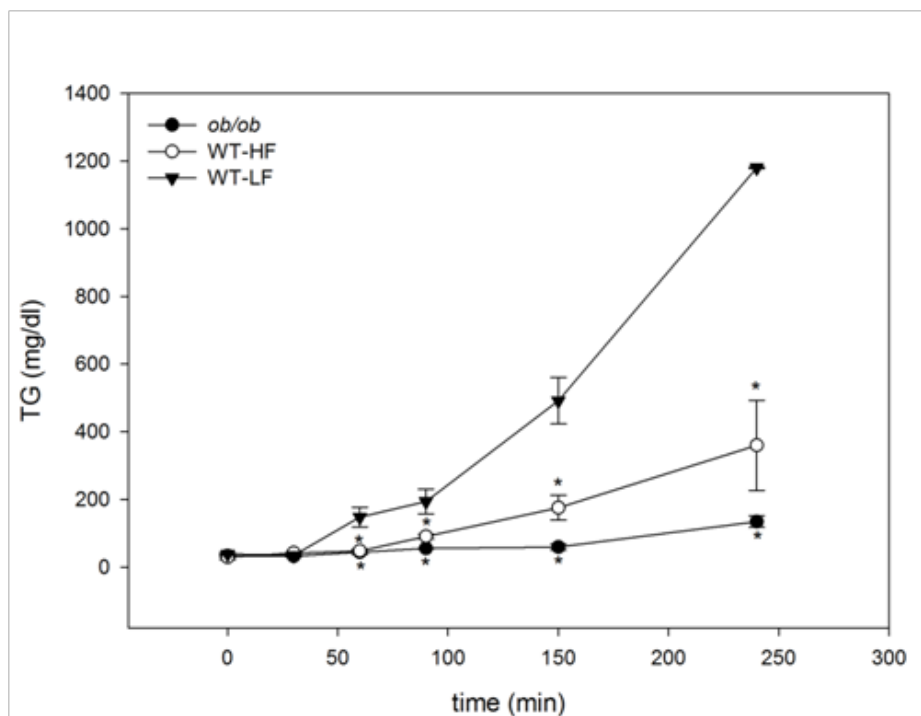
Figure 2-5. Oral fat tolerance tests. Fasted mice given the LPL-inhibitor Tyloxapol were gavaged with an olive oil bolus as described in Materials and Methods. Average ± s.e.m., n=4 per group, *p<0.05 or lower versus WT-LF.

DISCUSSION

In obesity, excess fat deposition occurs not only in adipocytes but also in liver and skeletal muscle. In the present study, we explored the effects of obesity and high fat feeding on the small intestine, and found that mucosal TG accumulation is accompanied by changes in lipid metabolic gene expression and markedly diminished secretion of dietary lipids.

As expected the *ob/ob* mice displayed significantly higher liver TG content. Ectopic fat deposition in the liver, or hepatosteatosis, is commonly associated with obesity and can progress into fibrosis and severely compromised liver function, eventually leading to cirrhosis and hepatocarcinoma (178, 179). The delayed lipoprotein secretion observed in the present study suggests a similar dysfunctional relationship to enterocyte lipid accumulation and tissue function. Inflammation is also likely to play a contributory role in the intestinal dysfunction, as it has been recently shown that obese rats fed a high-fat diet exhibit gut inflammation coupled with alterations in tight junctions and increased intestinal permeability (180).

In the fed state, the *ob/ob* mucosa contained 5-fold higher TG levels than WT mucosa. Notably, we found 3-fold higher TG levels in fasted *ob/ob* mice as well. A recent study by Zhu *et al.* (54) showed that in lean WT mice the enterocyte LDs present after an olive oil gavage of are almost entirely depleted 12 hours later. This is in agreement with the absence of TG accumulation in the 12 hour fasted WT-LF group. The results indicate that mucosal LDs in obese mice persist even after a long period of time following lipid ingestion. However, it remains to be determined if this is a result of obesity per se, or whether the absence of leptin has a specific effect in the small intestine to promote an energy sparing phenotype. Interestingly, Iqbal *et al.* (181) reported that leptin receptor B-deficient mice also had elevated intestinal mucosal TG levels. Other hormones may also play a role, particularly insulin, which has been reported to

produce effects in the small intestine. For example, it has been reported that adolescents with type I diabetes mellitus exhibit lipid accumulation within proximal jejunum mucosa (182). Insulin has also been shown to decrease chylomicron production in human jejunal explants (183), and rodent studies show many effects of insulin resistance on insulin signaling in enterocytes, including increased *de novo* lipogenesis and altered GLUT2 translocation (184, 185). Thus, the mucosal lipid accumulation shown here in *ob/ob* mice may, in part, be secondary to insulin resistance in this mouse model.

Increased postprandial TG biosynthesis and storage, as well as reduced CM secretion, are both potential contributors to the increased intestinal lipid content observed herein. TG biosynthesis in enterocytes can occur via MGAT2 and DGAT1/2 activity or the glycerol-3-phosphate pathway, with the former pathway thought to contribute more than 75% of TG resynthesis (33). We found increased mRNA abundance of most enzymes involved in both pathways in the fed *ob/ob* mice. Overexpression of DGAT2, but not DGAT1, in mouse liver promotes LD formation, suggesting a dominant role for DGAT2 in TG storage (46). DGAT1$^{-/-}$ mice display reduced CM secretion, supporting a preferential export of DGAT1-catalyzed TG. In the fed *ob/ob* mice, the DGAT2 expression increase was modestly greater than the increase in DGAT1 expression (1.96 $\pm$ 0.14 and 1.54 $\pm$ 0.07, respectively, p = 0.04), although both were significantly increased relative to fed WT-LF mice. Pharmacological inhibition of intestinal lipoprotein secretion in rats results in markedly increased intestinal lipid content, indicating a primary role for CM biogenesis and secretion in regulating intracellular lipid levels (8). MTP is important as an intracellular chaperone in lipoprotein biogenesis, and its function and activity may be altered in the obese intestine (186, 187). In the present study we found that MTP expression was unchanged in the *ob/ob* mice in the fasted state, despite the presence of

mucosal TG; expression in fed *ob/ob* mice was increased 1.3-fold, a change that appears to be insufficient for efficient export of a lipid load.

It is interesting that many of the mucosal genes analyzed were lower in fasted *ob/ob* mice compared to fasted WT-LF mice. While this would appear to oppose the obese phenotype of these mice, it is worth noting that that expression of adipogenic enzymes in adipose tissues of *ob/ob* mice is also reported to be significantly decreased, suggesting that absence of functional leptin signaling induces an energy sparing state in peripheral tissues (188).

De novo fatty acid synthesis could also be contributing to the observed mucosal TG accumulation. Although the contribution of endogenous synthesis to total intestinal TG is thought to be small, it has been shown that fatty acid synthesis is increased 2-fold in the small intestine of *ob/ob* mice relative to lean WT mice (189). We found increased ACC1 expression in fed *ob/ob* mice, and a trend toward increased FASN. It should be noted that our *ob/ob* mice consumed a high sucrose LFD, thereby providing an abundant supply of substrate for lipogenesis.

Markedly diminished secretion of a dietary lipid bolus was found not only in the ob/ob but also in the WT-HF group. Despite having a similar weight and body composition to the WT-LF mice, the WT-HF mice had a much lower rate of secretion, implying that enterocyte dysfunction may precede the accumulation of mucosal lipids. The HF diet may also be an independent contributor to the secretion defect. In human studies, HF diet interventions for as little as 3 days as well as for 2 weeks, have been shown to significantly decrease gastrointestinal transit time (190–192). Additionally, rodent studies show that increased gastric emptying as a result of chronic high-fat feeding may be attributed, in part, to impaired cholecystokinin (CCK) signaling (193). Thus, it is possible that the high-fat feeding in the present WT-HF group leads to an acute lipid load in the proximal small intestine secondary to increased gastric emptying. In turn, this

may underlie the increased postprandial lipid accumulation and upregulation of mucosal genes such as DGAT2 and CD36 in the intestinal mucosa of fed WT-HF mice. Adaptation to the high-fat diet by persistently increased gastric emptying rates may therefore contribute to the secretion dysfunction observed in the OFTT.

The reduced rate of intestinal TG secretion may also be secondary, at least in part, to changes in mucosal lipid metabolism. The increased expression of erGPAT3 coupled with the reduced expression of MGAT2 suggests the potential switch in anabolic metabolism from TG production to phospholipid biosynthesis, which may contribute to reduced TG available for secretion. In addition, the increased CPT1 and ACO mRNA in fed *ob/ob* and WT-HF samples, relative to WT-LF, suggest an increased level of lipid oxidation. Although the levels of mucosal FA oxidation are quite low (28, 63, 194), it is possible that an increase in FA oxidation could play a small role in reducing the secreted TG pool.

It is important to note that very little is known about the regulation of mucosal lipid metabolic gene expression. We showed previously that, unlike in the liver where transcriptional regulation of expression of MGAT and MGL were found, in the intestinal mucosa both of these genes appeared to be highly regulated by post-transcriptional mechanisms (64). Thus, in future studies we will determine the effects of obesity and HF feeding on the protein expression and activities of lipid metabolic and transport proteins, to gain further insight into the mechanisms by which the mucosa accumulates increased TG and develops reduced postprandial TG secretion.

The dramatically lower rates of lipid secretion in *ob/ob* and HF fed mice are surprising in light of multiple studies that show increased postprandial lipemia in obese subjects (195, 196). An important factor may be the contribution of the liver to plasma TG, as it has been shown that hepatic lipoprotein production accounts for a significant part of postprandial TG levels (195).

While we cannot rule out the influence of endogenous lipoprotein production by the liver, the OFTT protocol uses an intentionally large bolus of olive oil to focus on intestinal lipid secretion and minimize the hepatic contribution. In keeping with the present results, Ji and Friedman (197) found a significant inverse correlation between body weight increase and changes in plasma TG levels following an intragastric corn oil gavage in rats.

It is notable that diminished lipid secretion is also observed by Uchida *et al.* (198) in the current issue, in both diet-induced obese (DIO) and *ob/ob* mice. They found that plasma TG appearance following an acute intragastric fat challenge was reduced in the *ob/ob* and DIO mice relative to lean LFD-fed controls. This was accompanied by postprandial hypertriglyceridemia and a delayed TG peak in oral fat challenges without Tyloxapol, indicating a role for hepatic lipid secretion and lipoprotein clearance in determining circulating TG levels. Differences between our studies and theirs include the diet composition and length of feeding. Nevertheless, the intestinal lipid secretion results concur, demonstrating that reduced TG secretion is a persistent defect that can be observed after both 3 weeks of high fat feeding, in the absence of obesity, and after 6 weeks of high fat feeding, when DIO is present, as well as under varying dietary fat composition, suggesting that the amount rather than the type of fat in the diet is a primary determinant of intestinal lipid secretion rate.

In summary, we report for the first time that the intestinal mucosa accumulates excess TG during obesity. Both alterations in the expression of lipid metabolic and transport genes, as well as reduced secretion of dietary lipid, may contribute to the TG accumulation in intestinal mucosa during high fat feeding and obesity.

Chapter 3

Monoacylglycerol lipase ablation in mice alters energy homeostasis and diet induced obesity

ABSTRACT

Monoacylglycerol lipase (MGL) is a ubiquitously expressed enzyme that catalyzes the hydrolysis of monoacylglycerols (MG) to yield free fatty acids (FFA) and glycerol. MGL contributes to energy homeostasis through the mobilization of fat stores and also via the degradation of 2-arachidonoyl glycerol (2-AG), an important signaling molecule in the endocannabinoid system. To further examine the role of MG metabolism in energy homeostasis, MGL-/- mice were fed 10% (kcal) low-fat or 45% (kcal) semipurified high-fat diets for 12 weeks to examine effects on satiety and the development of diet-induced obesity. There were profound increases of MG species in the brain, liver, and gonadal fat of MGL-/- mice on both diets. The results showed that weight gain over the 12 weeks was blunted in both diet groups. MGL-/- mice were leaner at both baseline and after 12 weeks of LFD feeding, which was concurrent with increased fat oxidation. Nevertheless, energy expenditure and locomotor activity remained unchanged. Circulating lipids were decreased in HFD-fed MGL-/- mice, as were the levels of several plasma peptides involved in glucose homeostasis and energy balance. Moderate improvements in glycemic control were also found for both the LFD and HFD MGL-/- groups. Interestingly, HFD fed MGL-/- mice had a blunted rate of intestinal triacylglycerol secretion following an oral fat challenge. Overall, the results indicate that MGL ablation leads to systemic changes that produce a leaner phenotype in LF-fed mice, and an improved metabolic serum profile in HF-fed mice.

INTRODUCTION

Monoacylglycerols (MG) are intermediates within a large network of lipid molecules used for energy production, energy storage, membrane components, and signaling. Extracellular hydrolysis of dietary triacylglycerol (TG) in circulating lipoproteins yields free fatty acids (FFA) and *sn*-2-MG, which are then taken up by cells (7, 77). MG are also produced intracellularly from membrane phospholipids and the consecutive action of phospholipase C and diacylglycerol lipase, or from the hydrolysis of stored TG by adipose triacylglycerol lipase (ATGL) and hormone sensitive lipase (HSL) (71, 72, 77, 120). The ultimate fate of intracellular MG is hydrolysis to FFA and glycerol, or re-esterification by acyltransferases into diacylglycerol (DG) and TG (41, 48).

Monoacylglyerol lipase (MGL) is considered the rate determining enzyme in MG catabolism. MGL accounts for roughly 85% of MG hydrolysis in the brain, with the remainder catalyzed by the enzymes ABHD6 and ABHD12 (79, 110). MGL is expressed in many other tissues as well, including brain, liver, skeletal muscle, and intestine (65, 67, 84, 85). Within cells, MGL has been shown to localize to both the cytosol and membrane fractions, and hydrolyzes *sn*-1 and *sn*-2 MG of varying acyl chain lengths and degrees of unsaturation, with almost no activity towards other lipids such as TG and lyso-phospholipids (84, 90–92, 95, 96).

MGL contributes to energy balance through two important functions. First, by mobilizing cellular lipid stores in adipose and other tissues, MGL makes glycerol and FFA available for a variety of purposes including β-oxidation. Second, MGL is a key regulator of 2-arachidonoyl glycerol (2-AG) levels in the endocannabinoid (EC) system (103). 2-AG, along with arachidonoyl ethanolamide (AEA, or anandamide), are the most important endogenously produced ligands of the cannabinoid receptors CB1 and CB2 (118). The net effect of CB1 activation throughout the body, acutely, is energy accumulation. In the brain, this is mediated by hypothalamic

potentiation of orexigenic pathways to stimulate eating behaviors, and reinforced by the mesolimbic dopamine reward system (129, 132, 137, 199). Peripheral CB1 stimulation also enhances fat uptake in adipose tissue, increases *de novo* lipogenesis in liver, and decreases energy expenditure in muscle (131, 145, 156, 200). Notably, EC activity in the gut also appears to affect eating behaviors, as peripheral administration of CB1 agonists induce acute hyperphagia, an effect likely mediated by CB1 receptors on vagal afferents that innervate the GI tract (150, 155).

Studies of both *in vivo* pharmacological inhibition and genetic knockout of MGL have focused primarily on its role in the EC system. The potent MGL inhibitor JZL184 causes 8-fold increases in brain 2-AG levels and cannabimimetic behavioral effects in mice such as analgesia, hypomotility, and hypothermia (110, 111). Interestingly, however, in contrast to acute 2-AG elevation, prolonged administration of JZL184 results in desensitization of the central EC system, likely caused by tonic activation of CB1 by sustained elevated 2-AG levels (102, 106, 107). Studies in MGL-/- mice recapitulate the effect of chronically elevated 2-AG, demonstrated by CB1 agonist cross-tolerance and a lack of change in core body temperature, locomotion, or pain tolerance (102, 103). Some metabolic changes have been reported, including reduced lipolysis in the adipocytes of MGL-/- mice and improved insulin sensitivity after 12 weeks of very high fat feeding (78). MGL knockout mice have not been found to have increased body weight gain relative to WT mice, as might be expected from elevated 2-AG levels. In fact, one study of MGL-/- mice showed a reduction in body weight and another no change, relative to WT mice (78, 103).

In previous studies, we identified MGL transcript and protein expression in rat and mouse small intestinal mucosa, and subsequent studies in mice revealed that normally low levels of MGL expression and activity in adult mucosa could be increased through high fat

feeding, suggesting nutritional regulation and a potential role for MGL in dietary lipid assimilation (62, 64). To further explore this potential role of intestinal MGL, we generated a transgenic mouse that overexpressed MGL specifically in the intestinal mucosa (iMGL mice) (65). LC/MS analyses showed decreased mucosal MG levels, notably 2-AG, as well as decreased levels of AEA. While the iMGL mice showed normal intestinal FA and MG metabolism, they developed a remarkable obesity phenotype after only 3 weeks of 40% kcal HFD feeding, which was secondary to hyperphagia and decreased energy expenditure (65). The increased body weight and fat mass and the hyperphagia of iMGL mice was perhaps unexpected, given the known orexigenic effects of central CB receptor activation, yet in line with the reported absence of hyperphagia secondary to MGL ablation (15,31). We suggested, therefore, that gut 2-AG may possibly act as a satiety signal (65).

To further understand the role of MGL in energy homeostasis, in the present study we examined the effects of 12 weeks of semipurified low-fat and high-fat feeding in MGL null mice. The results show that although food intake of the MGL-/- mice appeared to be unchanged, there were systemic changes that led to a leaner phenotype in LF-fed mice and an improved metabolic serum profile in HF-fed mice. Therefore, it is possible that inhibiting MGL may be a useful strategy for treatment of metabolic disorders such as obesity and its co-morbidities.

MATERIALS AND METHODS

Generation of MGL knockout mice

MGL knockout mice were purchased from Lexicon Genetics, Inc. (Woodlands, TX). Briefly, MGL knock-out mice were generated from an OmniBank ES cell clone OST113734 (201), containing a gene trap cassette insertion in the second intron of MGL (accession number NM_011844). Mice were originally derived on a 129/SvEv background and were backcrossed to C57BL/6 for multiple generations. Quantitative TaqMan reverse transcription-PCR was performed to detect mouse MGL mRNA in RNA samples extracted from MGL+/+, MGL+/- and MGL-/- mice. Multiple mouse tissues were isolated and mRNA was extracted using RNAqeous Micro kit (Ambion). cDNA reverse transcription (RT) was performed on the isolated mRNA using a High Capacity cDNA RT kit (Applied Biosystems). Purified cDNA was quantified with Quant-iT OliGreen ssDNA reagent (Invitrogen) to ensure equal loading of cDNA per reaction. TaqMan gene expression oligos for MGL (Mm00449275_m1; made to order) were purchased from Applied Biosystems. Quantitative PCRs were performed in an ABI Prism 7000 sequence detection system (Applied Biosystems).

MGL activity assay

MGL +/+, MGL +/-, and MGL -/- mouse brains were isolated from Lexicon mice. One g of mouse brain was homogenized in 10 mL of buffer (20 mM PIPES, 150 mM NaCl and .001% Tween at pH 7.0) using a Polytron pestle homogenizer (speed 10.2, 3 times for 15 seconds) on ice. Protein concentrations were determined using the Bradford Assay (BioRad Laboratories, Hercules, CA), and samples were adjusted to 1 mg/ml. To a 1000 ml polypropylene block, 1.65 µg/ml brain homogenate, 4nM [^{3}H] 2-AG (American Radiolabeled Chemicals, St. Louis, MO) and

10 μM cold 2-AG (Sigma-Aldrich, St. Louis, MO) were added. The contents were shaken at 37°C

for 90 seconds at 750 RPM and incubated for 10 minutes more at 37°C. To each well, 5 mg/ml

activated acid-washed charcoal (previously prepared to 25 mg/mL in TE buffer) was added,

along with 10 mM Tris-HCl and 1 mM EDTA pH 7.4. This solution was further diluted to 5 mg/mL

in 0.5M HCl. The contents were shaken at 37°C for 90 seconds at 750 RPM. The contents were

further incubated at room temperature (RT) for 30 minutes and then centrifuged at 2000 x g for

10 min at RT. The supernatants were carefully removed without disturbing the charcoal and

combined with Scint 20 fluid (Perkin Elmer, Waltham, MA) into an Opti-96-well plate (Perkin

Elmer, Waltham, MA), which was shaken for 1 minute at 750 RPM and incubated for 1 hour at

RT. The plate was then read on a Top Count scintillation counter (Perkin Elmer, Waltham, MA) to

measure the amount of [^{3}H] glycerol in the supernatant cocktail (CPMs). The CPMs were

converted to pmol/min/mg protein according to the following equation:

$$= cpm \times \frac{dpm\ 100\%}{cpm\ 30\%} \times \frac{1uCi}{2.2x10^6\ dpm} \times \frac{mMol}{16\ uCi} \times \frac{1}{10\ min} \times \frac{1}{.0016mg}$$

or

$$= cpm \times 5.92 \frac{\frac{pmol}{min}}{mg\ protein}$$

Animals, Diet, Surgical Procedures, and Tissue Collection

Age matched C57BL/6J (wild-type) mice and MGL-/- C57BL/6J mice were acquired from

Ace Animals (SAGE Labs, Boyertown, PA) under agreement from Johnson & Johnson PRD (New

Brunswick, NJ). The same study procedure was repeated for both male and female groups. All

mice were 7 weeks old upon arrival and fed Purina 5015 rodent chow (60% carbohydrate, 12%

fat, 28% protein by kcal) for a week before the start of the study. The animal facility was

temperature controlled with a daily 12 h light/dark cycle and *ad libitum* access to food and

water. At 8 weeks of age, the mice were randomized to dietary group according to body weight and housed in individual cages. For the 12 week feeding period, half of the mice in each genotype was fed either a 10% kcal low-fat semipurified diet (D12450B, Research Diets Inc., New Brunswick, NJ) or a 45% kcal high-fat semipurified diet (D12451, Research Diets Inc., New Brunswick, NJ) (Table 3-1). Twice weekly food and body weight measurements were taken. For the necropsy, mice were fasted for 12 h prior, and injected intraperitoneally with a ketamine-xylazine-ace promazine cocktail (54.5/45/0.8 mg/kg, respectively) to induce deep anesthesia, followed by exsanguinations by the aortic artery for collection of blood. Whole blood samples in EDTA-coated tubes were immediately centrifuged and the plasma collected and stored at -70°C. The small intestine from pylorus to cecum was excised, rinsed twice with saline, and the mucosal cells were collected by scraping with a glass slide. Liver, brain, and adipose depots (gonadal, inguinal, retroperitoneal (perirenal), and intrascapular brown fat) were also collected. All tissues were weighed, snap frozen on dry ice-ethanol, and stored at -70°C. All animal procedures were approved by the Rutgers University Animal Use Protocol Review Committee and conformed to the National Institutes of Health *Guide for the Care and Use of Laboratory Animals.*

Table 3-1

Diet	LFD: D1450B		HFD: D12451	
	g %	kcal %	g %	kcal %
Protein	19.2	20	24	20
Carbohydrate	67.3	70	41	35
Fat	4.3	10	24	45
Total		100		100
kcal/gm	3.85		4.73	
Ingredient				
Casein, 80 Mesh	200	800	200	800
L-Cystine	3	12	3	12
Corn Starch	315	1260	72.8	291
Maltodextrin 10	35	140	100	400
Sucrose	350	1400	172.8	691
Cellulose, BW200	50	0	50	0
Soybean Oil	25	225	25	225
Lard	20	180	177.5	1598
Mineral Mix S10026	10	0	10	0
DiCalcium Phosphate	13	0	13	0
Calcium Carbonate	5.5	0	5.5	0
Potassium Citrate, 1 H2O	16.5	0	16.5	0
Vitamin Mix V10001	10	40	10	40
Choline Bitartrate	2	0	2	0
FD&C Yellow Dye #5	0.05	0	0	0
FD&C Red Dye #40	0	0	0.05	0
Total	1055.05	4057	858.15	4057

Table 3-1 Diet composition

Body Composition, Activity, and Indirect Calorimetry

At the beginning and at week 10 of the feeding study, fat mass (FM) and lean body mass (LBM) were analyzed in non-anaesthetized mice by magnetic resonance imaging using an EchoMRI-100 (Echo Medical Systems, Houston TX). After the 10 week MRI measurement, mice were then immediately acclimatized to individual Oxymax metabolic cages (Columbus Instruments, Columbus, OH) for 24 h prior to 24 h of data collection, during which they were given *ad libitum* access to water and their respective diets. Respiratory exchange ratio (RER) as VCO_2/VO_2 was used to determine substrate utilization, and energy expenditure (EE) was calculated using: EE (kcal/kg/hr) = $(3.815*VO_2 + 1.232* VCO_2)/$(kg LBM) (202). Locomotor and rearing activities were measured as the number of horizontal or vertical infrared beam breaks in a 24 period, respectively.

Tissue Lipid Extraction and Analyses

Brain, liver, gonadal fat, and mucosa samples were homogenized with 1X PBS pH 7.4 on ice with a Dounce homogenizer and a Wheaton overhead stirrer at 5,000 rpm. Total tissue protein concentration was determined by Bradford assay (174) and used to standardize volume of homogenate to extract lipid, as described (63). Mononanoin (C9:0) and C17:1 ethanolamide were added as internal standards to each sample of brain (12 mg protein), liver (10 mg), intestinal mucosa (10 mg), and gonadal fat (1 mg) homogenate. Lipid extractions were then performed using the Folch procedure (175) and sampled were dried down under nitrogen gas and reconstituted in chloroform.

Tissue monoacylglycerol and ethanolamide levels were determined by liquid chromatography (LC)-coupled mass spectrometry (MS). To be compatible with the reversed phase LC system, an aliquot of 100 µl of each lipid extract in chloroform was transferred into a

350 µl-glass insert on a 96 well plate. Solvent was removed under nitrogen gas, and the residue was reconstituted with 100 µl of tetrahydrofuran-isopropyl alcohol (20:80). The final solution (10 µl) was injected onto an LC/MS/MS system consisting of an Agilent 1100 Series Liquid Chromatographic system (Agilent Technologies, Palo Alto, CA) interfaced with a Waters *Quattro Premier* triple quadrupole mass spectrometer (Waters, Milford, MA) through a Z-spray electrospray ionization source. Separation of the analytes was performed on a Zorbax Eclipse XDB-C8 column (2.1 × 50 mm) eluted gradiently with 50-90% mobile phase B within 5 min, held 90%B for 3 min and returned to 30%B in 0.1 min. The mobile phase A was 5 mM ammonium formate and 0.1% formic acid in water and B was 5 mM ammonium formate and 0.1% formic acid in acetonitrile-water (95:5). The flow rate was set at 0.3 ml/min. The mass spectrometer was operated in the positive ion mode, and multiple reaction monitoring (MRM) was used for quantification. The mass transitions from precursor ion to product ion for detection of acylethanolamides were protonated molecular ion > protonated ethanolamine (*m/z* 62.0) at a collision energy of 15eV. The mass transitions for monoacyglycerols were protonated molecular ion > acylidyneoxonium at a collision energy of 20ev. Quantification of each analyte was achieved based on the relative peak area ratio of the analyte to the internal standard calibrated with the corresponding response factor. MassLynx software version 4.0 was used for system control and data processing.

Oral Fat Tolerance Test (OFTT)

After 12 weeks of 45% HFD feeding, mice were fasted for 16 h prior to the OFTT. At t_0 the mice were given an intraperitoneal (i.p.) injection with 500 mg/kg body weight of Tyloxapol (Triton WR-1339) to block peripheral lipoprotein clearance. Thirty minutes following Tyloxapol injection, 300 ul of olive oil was given by orogastric gavage. Blood samples were collected from

the tail at time = 0 (t_0), 60, 120, 180, 240 minutes and TG levels were assessed in 15 ul of whole

blood by Cardiochek lipid analyzer (Polymer Technology Systems Inc., Zionsville, IN).

RNA Extraction and Real Time PCR Analysis

Total mRNA was extracted from tissues using a modified method from Chomczynski and

Sacchi (203) and analyzed as previously described (204). In brief, frozen tissues were

homogenized in 4 M guanidinium thiocyanate with an Ultra-Turrax IKA-Werke (Wilmington, DE).

Total RNA was isolated by phenol extraction, followed by precipitation and washing with

ethanol. The RNA was further purified by removal of genomic DNA by DNase digest and RNeasy

cleanup kit (Qiagen, Valencia, CA). The integrity of the RNA was assessed by gel electrophoresis

and visualization of the 18S and 23S rRNA subunits. Reverse transcription was performed on 2

μg of RNA using a high capacity cDNA kit (Promega, Madison, WI). Primer sequences shown in

Table 3-2 were obtained from Sigma Aldrich (St Louis, MO). The efficiency (100 ± 5%) of each

PCR primer set was first assessed by standard curve. Real time PCR (RT-PCR) was performed in

triplicate using the ddCT method on an ABI 7300 PCR instrument (Applied Biosystems, Foster

City, CA). Each reaction contained 80 ng of cDNA, 250 nM of each forward and reverse primer,

and 12.5 μl of POWER SYBR Green Master Mix (Applied Biosystems, Foster City, CA) in a total

volume of 25 μl. β-actin was used as the endogenous control for each standard and the relative

quantitation of each gene was determined with respect to the average of the WT LFD mice.

Plasma Analyses

Plasma samples were obtained during the necropsy as described above. Triacylglycerol,

cholesterol, non-esterified fatty acid (NEFA) and adiponectin levels were measured by

colorimetric assay (WAKO Diagnostics, Richmond, VA). All other plasma peptide analytes were

Table 3-2

Gene	Function	Primer	Sequence
β-actin	Housekeeping	Forward	5'-GGCTGTATTCCCCTCCATCG-3'
		Reverse	5'-CCAGTTGGTAACAATGCCATGT-3'
MGAT2	TG synthesis	Forward	5'-TGGGAGCGCAGGTTACAGA-3'
		Reverse	5'-CAGGATGGCATACAGGACAGA-3'
GPAT3	TG synthesis	Forward	5'-TATCCAAAGAGATGAGTCACCCA-3'
		Reverse	5'-CACAATGGCTTCCAACCCCTT-3'
GPAT1	TG synthesis	Forward	5'-CTGCTTGCCTACCTGAAGACC-3'
		Reverse	5'-GATACGGCGGTATAGGTGCTT-3'
DGAT1	TG synthesis	Forward	5'-TCCGTCCAGGGTGGTAGTG-3'
		Reverse	5'-TGAACAAAGAATCTTGCAGACGA-3'
DGAT2	TG synthesis	Forward	5'-TTCCTGGCATAAGGCCCTATT-3'
		Reverse	5'- AGTCTATGGTGTCTCGGTTGAC-3'
MGL	MG hydrolysis	Forward	5'- CAGAGAGGCCCACCTACTTTT-3'
		Reverse	5'- ATGCGCCCCAAGGTCATATTT-3'
ACC1	Lipogenesis	Forward	5'-AGGTGGTGATAGCCGGTATGT-3'
		Reverse	5'-TGGGTAATCCATAGAGCCCAG-3'
FAS	Lipogenesis	Forward	5'-ATGGGCGGAATGGTCTCTTTC-3'
		Reverse	5'-TGGGGACCTTGTCTTCATCAT-3'
CB1	Cannabinoid receptor	Forward	5'- GGGCACCTTCACGGTTCTG-3'
		Reverse	5'- GTGGAAGTCAACAAAGCTGTAGA-3'
NPY	Orexigenic neuropeptide	Forward	5'-ATGCTAGGTAACAAGCGAATGG-3'
		Reverse	5'-TGTCGCAGAGCGGAGTAGTAT-3'
AgRP	Orexigenic neuropeptide	Forward	5'-ATGCTGACTGCAATGTTGCTG-3'
		Reverse	5'-CAGACTTAGACCTGGGAACTCT-3'
CART	Anorectic neuropeptide	Forward	5'-GCTCAAGAGTAAACGCATTCCG-3'
		Reverse	5'-ACAAGCACTTCAAGAGGAAAGAA-3'
POMC	Anorectic neuropeptide	Forward	5'-CTGGAGACGCCCGTGTTTC-3'
		Reverse	5'-TGGACTCGGCTCTGGACTG-3'

Table 3-2 Primer sequences used for RT-PCR analyses

determined by immunoassay using a MAGPIX instrument (Luminex Corp, Austin, TX) and a Milliplex multiplex panel for mouse metabolic hormones (Millipore, Billerica, MA).

Oral Glucose Tolerance Test (OGTT)

After 11 weeks of low fat or high fat feeding, the mice were fasted for 6 h prior to the OGTT, then given a bolus of 2 g/kg body weight D-(+)-glucose solution by oral gavage. Blood glucose was measured using a glucometer at t=0, 30, 60, and 120 min after collecting blood from tail nicks (Accuchek, Roche Diagnostics).

Statistical Analyses

A total of 50 mice for n=6-7 females and n=6 males per group were used in this study. Females and males were compared both independently and together using the WT LFD group averages to normalize data for each sex. All group data are shown as average ± SEM. Statistical comparisons were determined between genotypes on the same diet, using a two-sided *Student's* t-test or one-way ANOVA with Tukey's post-hoc comparison. Differences were considered significant for $p < 0.05$. Area under the curve (AUC) for the OGTT was calculated using the trapezoid rule.

RESULTS

Genetic ablation of MGL in mice

We first assessed the ablation of the MGL gene and its resultant loss of function. Brain transcript levels of MGL were significantly reduced in heterozygous (MGL+/-) mice and undetectable in MGL-/- mice (Fig 3-1A). Activity of MGL was determined in whole brain homogenates, demonstrating that catabolism of 2-AG is reduced by 30% in MGL+/- mice, and by 83% in MGL-/- mice compared to WT counterparts (Fig 3-1B). These results confirm the absence of MGL expression in the homozygous MGL knockout mice, and its effect on MG hydrolytic activity in brain (102).

Tissue MG and acylethanolamide levels in MGL-/- mice

We examined effects of MGL ablation on MG and acylethanolamide species in various tissues by LC-MS. For these and all subsequent analyses, results were generally similar for male and female test groups. There were profound increases of MG species in the brain, liver, and epididymal fat of both LFD and HFD fed MGL-/- mice (Fig 3-2A-C). Notably, brain 2-AG levels were increased up to 131-fold in MGL-/- mice (Fig 3-2A). In contrast to brain, liver, and adipose tissue, there were only modest elevations in several MG species in intestinal mucosa. This may be attributed to the low constitutive expression of mucosa MGL (34), the depletion of dietary fat after the 12 h fasting period prior to necropsy, or perhaps the rapid esterification of excess MG. Acylethanolamide levels, including AEA, were not substantially altered in intestinal mucosa or adipose tissue (Fig 3-3C-D). However, some brain and liver acylethanolamides were increased, particularly in the HFD-fed MGL-/- mice (Fig 3-3A-B).

Figure 3-1
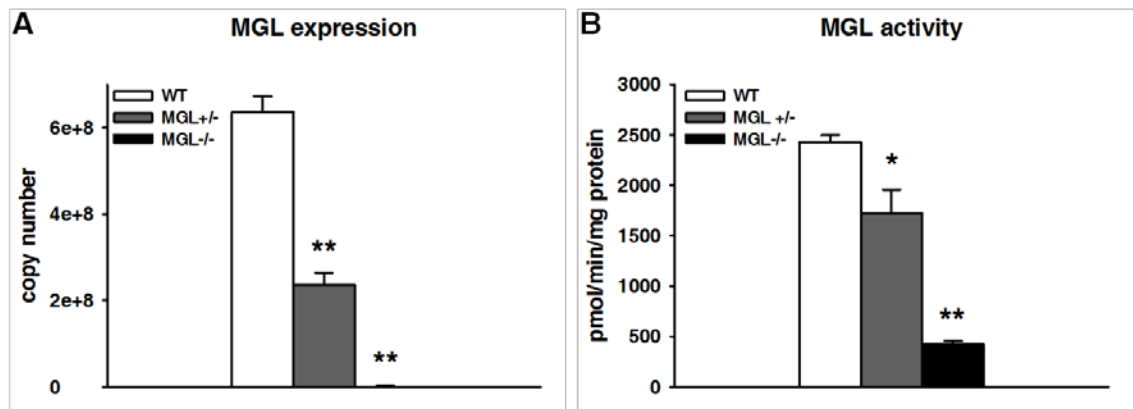
Figure 3-1. Ablation of MGL gene and function in MGL-/- mice. (A) Quantitative PCR of MGL transcript in brain; (B) MGL activity determined by [^{3}H]2-AG hydrolysis to AA and [^{3}H]glycerol in whole brain homogenates. Data are expressed as average ± SEM (n = 4-6). * $p < 0.01$, ** $p < 0.001$ compared MGL+/+ (WT)

Figure 3-2
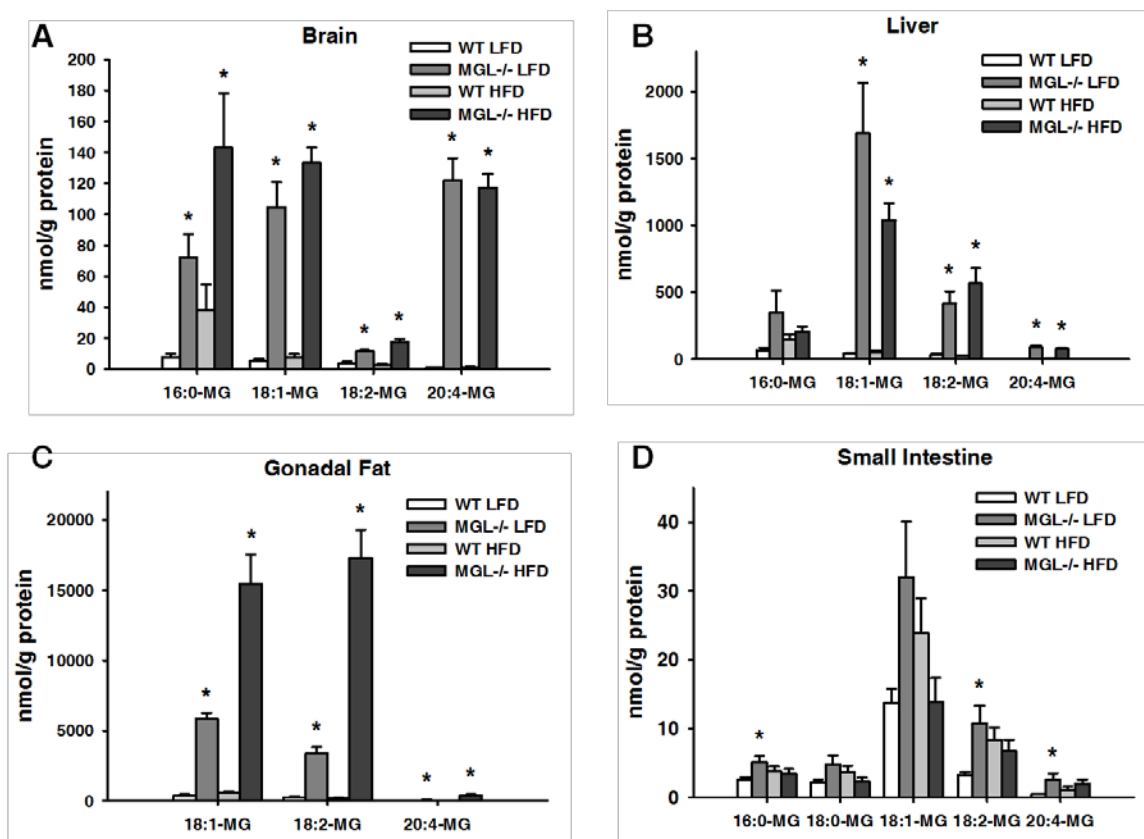
Figure 3-2. Tissue content of MG species as determined by HPLC-MS analysis. (A) Brain (B) Liver (C) Gonadal fat (D) Small intestine mucosa. Data are expressed as average ± SEM (n = 6). * $p < 0.05$ compared to control group of the same diet.

Figure 3-3

Figure 3-3. Tissue content of acylethanolamide (EA) species as determined by HPLC-MS analysis. (A) Brain (B) Liver (C) Gonadal fat (D) Small intestine mucosa. Data are expressed as average ± SEM (n = 6). * $p < 0.05$ compared to control group of the same diet.

Alterations in body mass and composition with MGL ablation

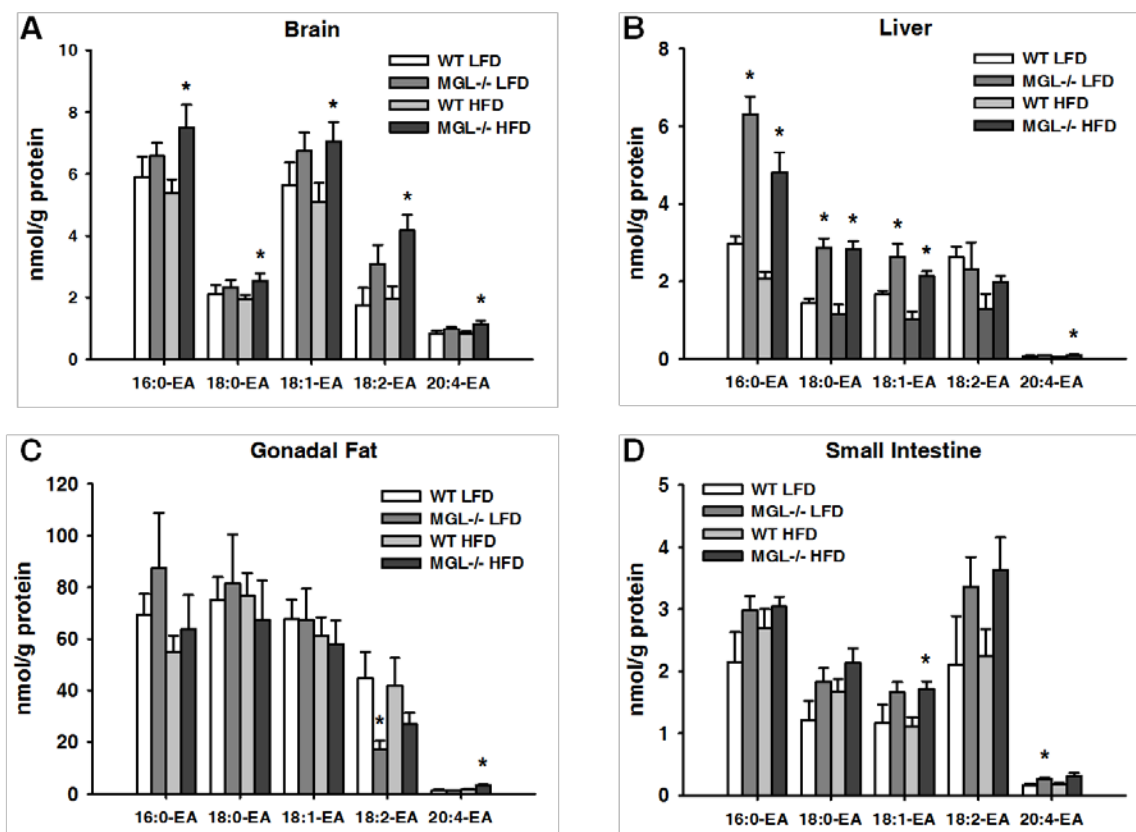There were no differences in body weight for either group of mice at the beginning the experiment. Over 12 weeks of feeding, however, we observed lower body weights in both LFD and HFD fed MGL-/- mice compared to their WT counterparts (Fig 3-4). Using univariate repeated measures ANOVA, a significant effect of MGL ablation on total body weight for the female LFD fed group was found (Fig 3-4B). Body weight gain over time was also significantly blunted in the male MGL-/- LFD fed mice (p < 0.001), with a similar trend for the HFD fed mice (p = 0.06) (Fig 3-4A-B). When results for both males and females on either diet were normalized to WT LFD controls, the effects of the MGL knockout were highly significant (p < 0.001). Interestingly, we found that the MGL-/- mice were leaner at both baseline and after 12 weeks of LFD feeding, with 33% and 30% less body fat than WT mice, respectively (Fig 3-5A). These finding were supported by lower gonadal and retroperitoneal fat pad weights in the same mice (Fig 3-5C-D). While a trend toward decreased fat mass was also seen in HF-fed mice, particularly the females, the results did not reach statistical significance (Figure 3-5A, C, and D).

Food intake, lipid absorption, and energy utilization in MGL-/- mice

During the 12 week dietary intervention, there were no apparent changes in food intake (Fig 3-6A), nor were there changes in dietary lipid absorption, as determined by fecal fat content (Fig 3-6B). We also placed the mice in metabolic chambers for indirect calorimetry and activity measurements during the first and last weeks of the feeding period. RER values at baseline and after 10 weeks of LFD feeding in MGL-/- mice were lower over a 24 h period, indicating increased fat oxidation, but there were no differences in the HFD fed mice (Fig 3-6C-D). The decrease in RER may explain, in part, the reduced fat mass observed in LFD fed MGL-/- mice. During the first week of HFD feeding, the MGL-/- mice had lower energy expenditure over the

Figure 3-4
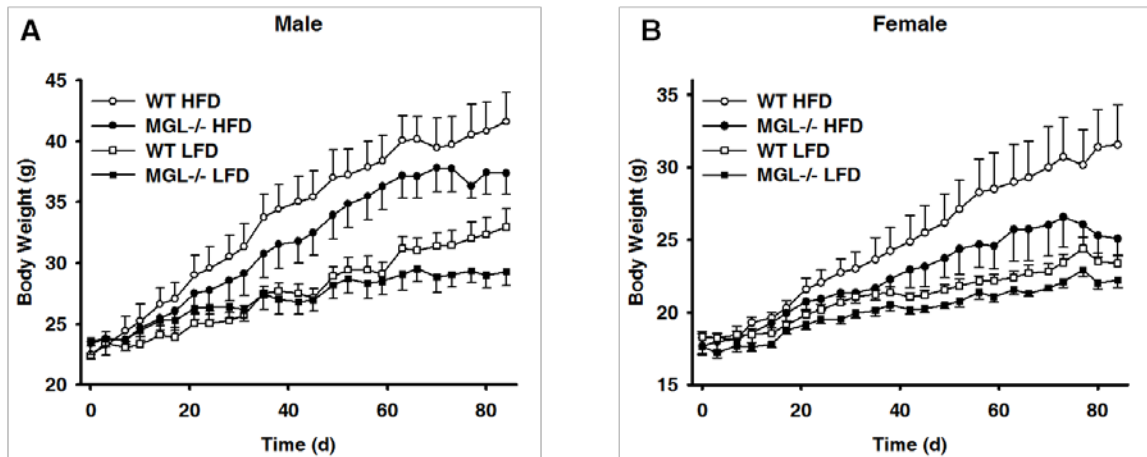
Figure 3-4. Body weights during 12 weeks of LFD or HFD feeding. (A) male and (B) female mice. Data are expressed as average ± SEM (n = 6). Repeated measures ANOVA was used to determine statistical differences in body weight gain over time for each group individually, and then for both sexes combined.

Figure 3-5
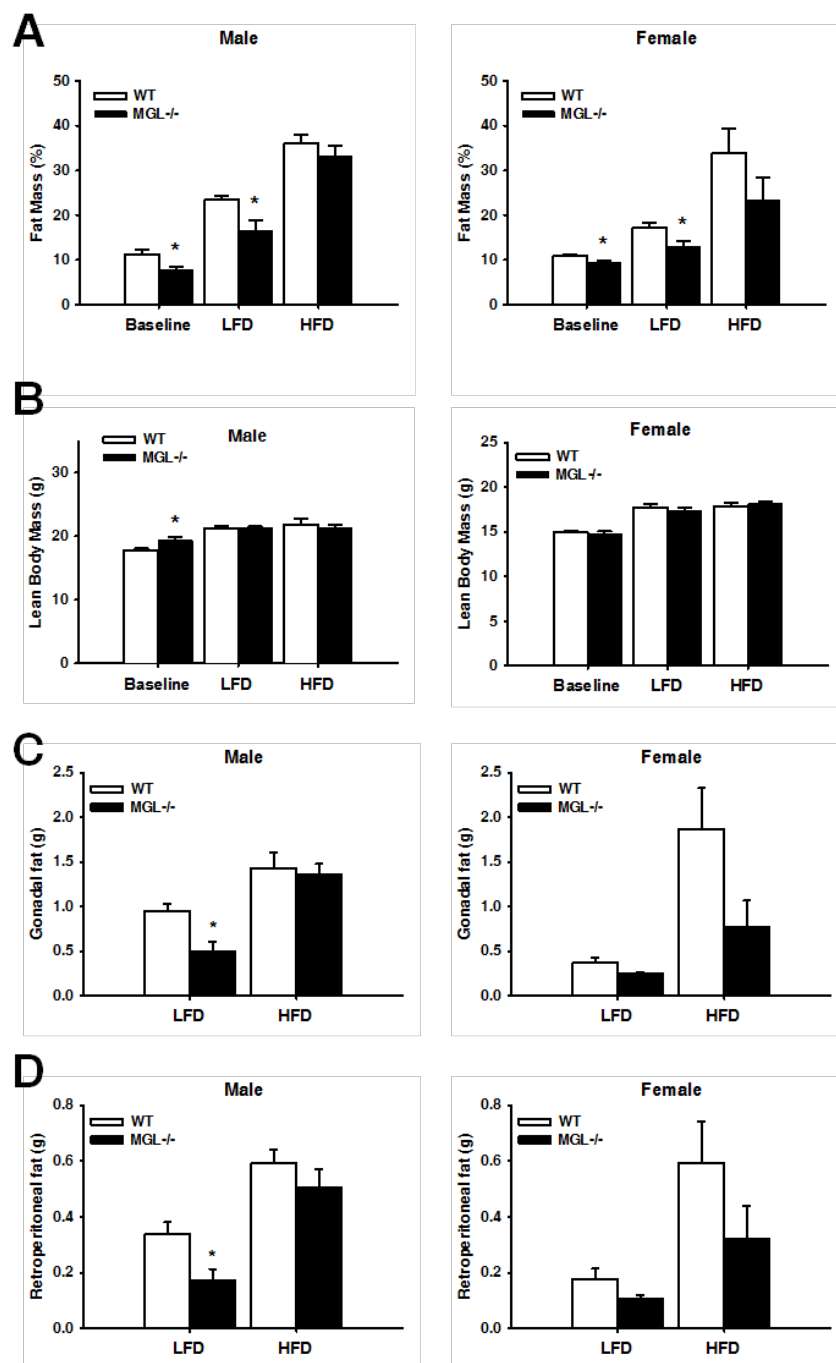
Figure 3-5. Body composition and tissue weights in MGL-/- mice. (A) Fat mass percentage for male and female mice at the beginning (baseline) and after 10 weeks of diet; (B) Lean body mass at the beginning (baseline) and end of study; (C) Gonadal and (D) retroperitoneal (perirenal) fat pad weights at necropsy. Data are expressed as average ± SEM (n = 6). * $p < 0.05$ compared to control group of the same diet.

Figure 3-6
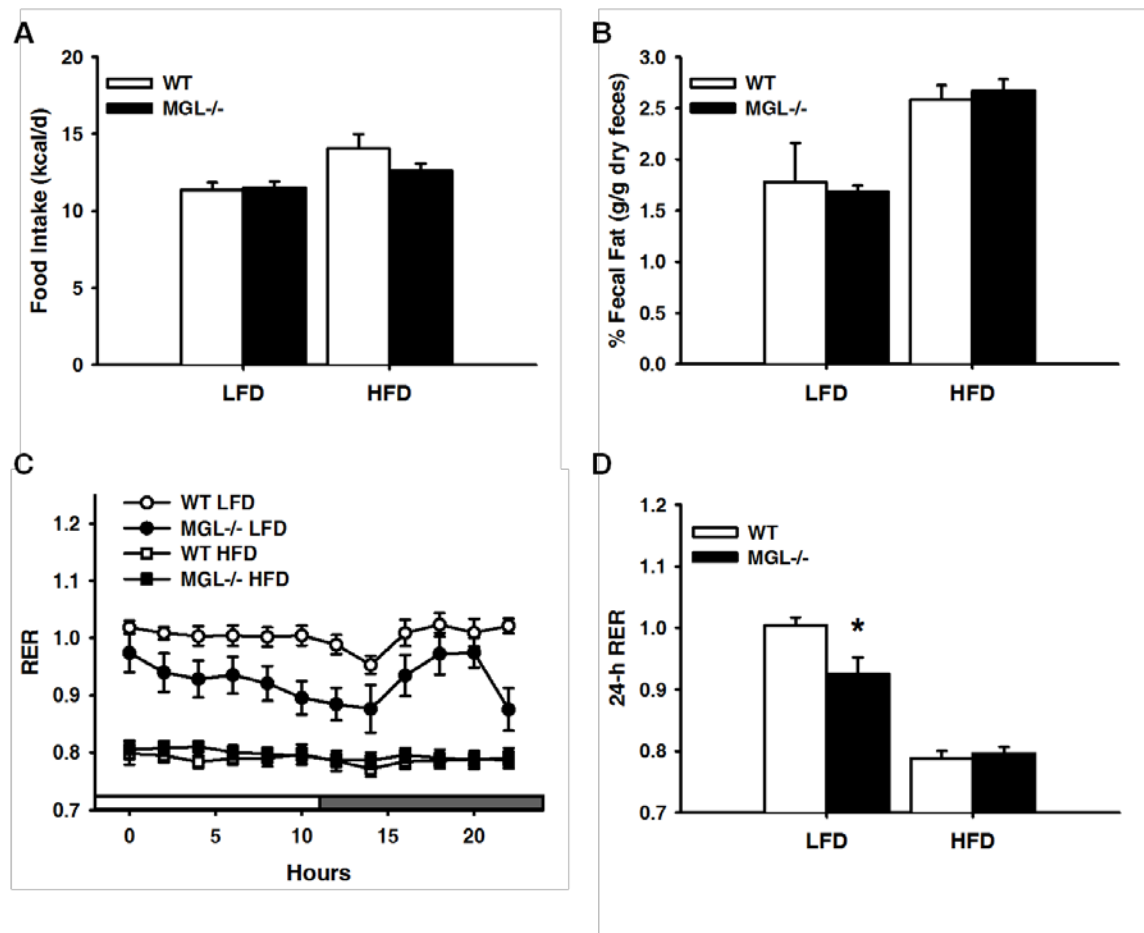
Figure 3-6. Energy consumption and utilization for male mice. (A) Average daily caloric intake; (B) Fecal fat; (C) Endpoint (10 weeks of feeding) RER values over 24-h period. Data were binned into 2-h averages with light/dark cycle shown on bottom; (D) Endpoint 24-h average of RER values for HFD mice. Data are expressed as average ± SEM (n = 6). * $p < 0.05$ compared to control group of the same diet.

24 h data collection period (not shown), but there was no difference between any of the dietary groups at the end of the study. Additionally, locomotor activity and rearing remained unchanged for both diet groups (not shown).

Blunted intestinal TG secretion in MGL-/- mice

We assessed intestinal lipid absorption by OFTT in male mice fed the 45% HFD for 12 weeks. There was a strong trend (p = 0.06) for lower blood TG levels in fasted MGL-/- mice (i.e. t_o). After mice were given an injection of the LPL inhibitor Tyloxapol and administered an orogastric bolus of olive oil as described in Methods, MGL-/- mice had markedly lower (p < 0.01) levels of TG in circulation (Fig 3-7).

Glycemic control in MGL-/- mice

Blockade of EC system signaling via CB1 receptor knockout or chemical inhibition results in improved glucose tolerance in DIO mice (205, 206). To assess whether glucose disposal is altered in MGL null mice, we performed a 2 h oral glucose tolerance test (OGTT) in week 11 of the feeding study. Moderate improvements in glycemic control were observed, with trends for lower blood glucose levels for both LFD and HFD fed MGL-/- groups (Fig 3-8A-B).

Circulating lipids and peptides

Reduced serum TG and glycerol levels were found in a previous study of very HF-fed MGL-/- mice (78). In the present study, trends for reduced plasma TG, cholesterol, and NEFA levels were found in both dietary groups of male MGL-/- mice (Fig 3-9A-C). Indeed, when normalized for both sexes, the HF-fed MGL-/- mice had significantly lower TG, cholesterol, and NEFA levels (p < 0.05 or below).

Figure 3-7
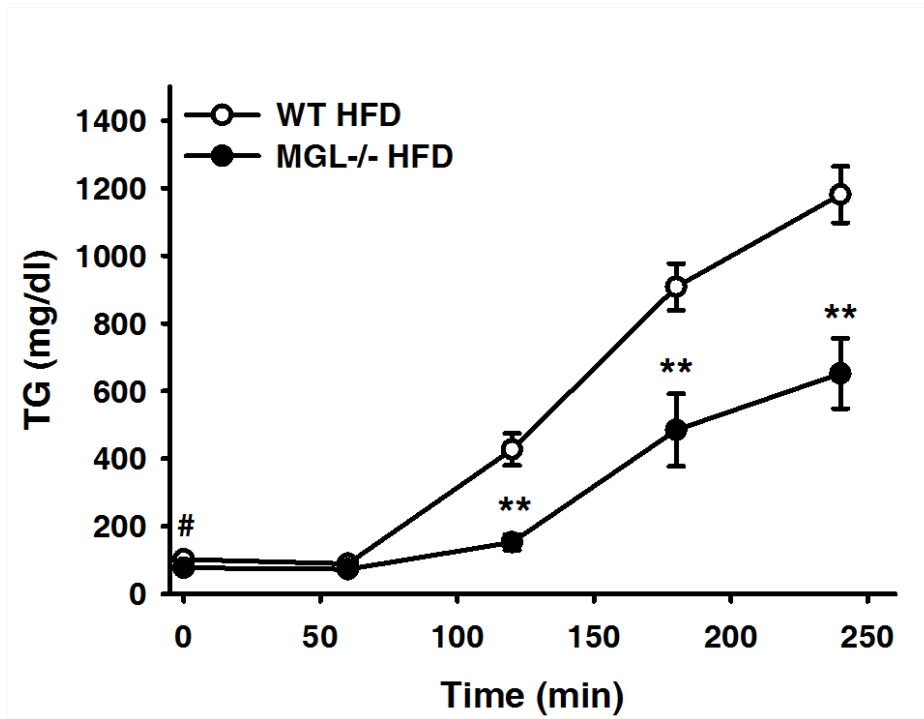
Figure 3-7. Reduced appearance of TG from an oral fat bolus in the blood of 12 week HFD-fed male MGL-/- mice. All mice were fasted 16 h prior to OFTT, given an i.p. injection of the LPL inhibitor Tyloxapol at 0 min, and an oral gavage with 300 ul olive oil at t = 30 min. Data are expressed as average ± SEM (n = 7-8). [#] p = 0.06, ** p < 0.001 compared to WT.

Figure 3-8
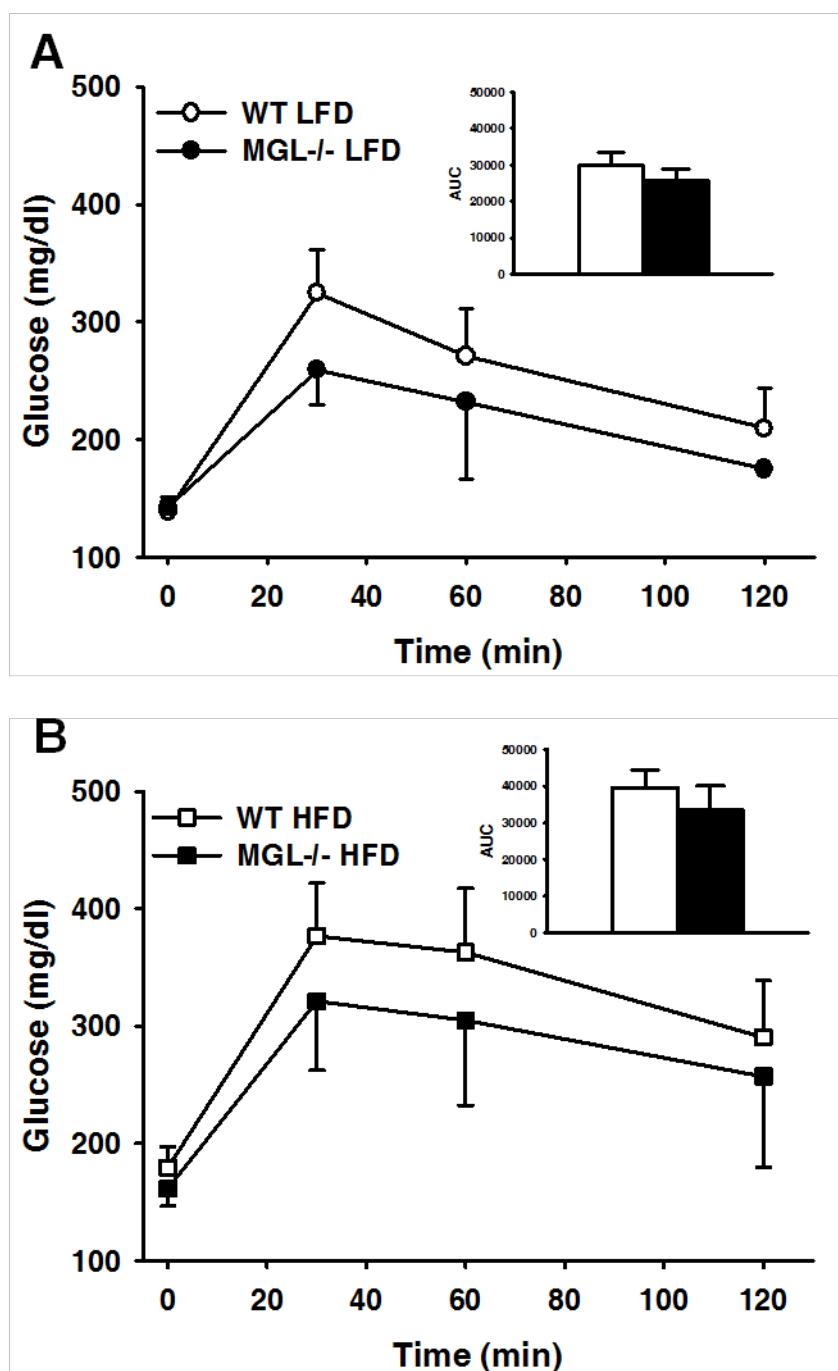
Figure 3-8. Oral glucose tolerance test. (A) LFD and (B) HFD fed male mice at endpoint (11 weeks of diet feeding). Inset graphs are AUC. Data are expressed as average ± SEM (n = 6).

Figure 3-9
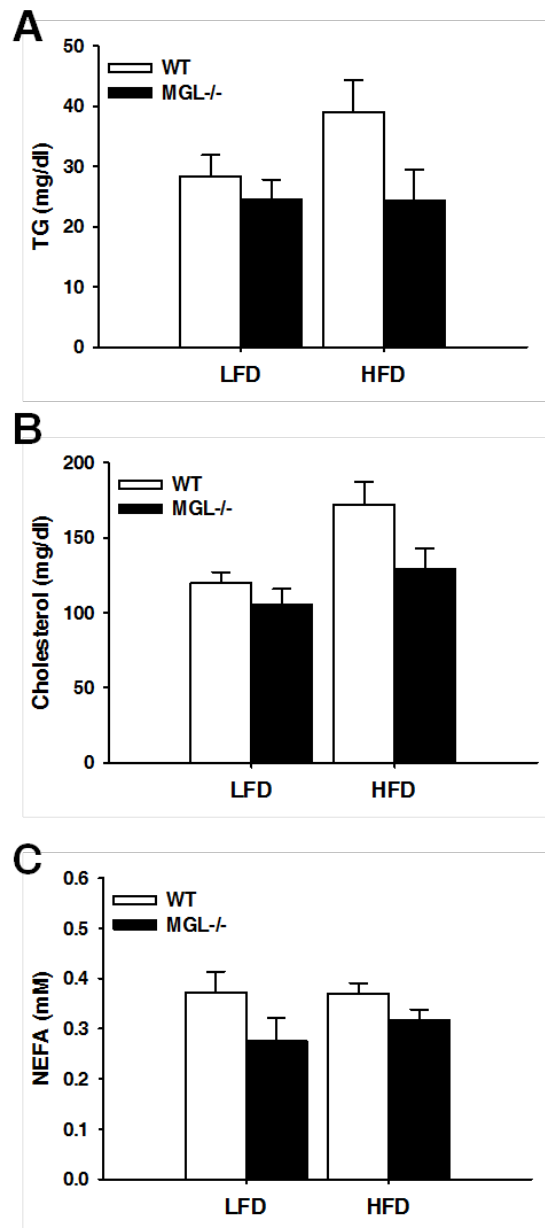
Figure 3-9. Plasma lipids in 12 h fasted male mice after 12 weeks of LF or HF feeding. (A) TG; (B) Total cholesterol; (C) NEFA. All lipids shown were significantly decreased ($p < 0.05$) in the HFD-fed MGL-/- mice when male and female groups were normalized and combined. Data are expressed as average ± SEM (n = 6).

Plasma analyses using a multiplexed ELISA assay showed a significantly improved metabolic

profile of HFD MGL-/- compared to WT mice. Peptides involved in glucose disposal such as

insulin and c-peptide were significantly lower, as were the adipocyte-derived hormones leptin

and resistin (Table 3-3). There were also trends for reductions in the pro-inflammatory cytokine

MCP-1. This improved plasma metabolic profile in the MGL-/- mice indicates that MGL ablation

may confer some protection against pathologies associated with long-term HFD feeding.

Gene expression in brain, liver, and small intestinal mucosa

We determined the effects of MG ablation and the consequent elevated levels of

intracellular MG on the expression of genes encoding for lipid metabolic enzymes and

cannabinoid receptors. Brain CB1 receptor expression in MGL-/- mice has been reported to be

downregulated (102) or unchanged (103); we did not find any significant differences in brain

CB1 mRNA abundance (Fig 3-10A). Expression of the hypothalamic orexigenic peptides NPY and

AgRP was also unchanged in the brain (Fig 3-10A). Additionally, while EC activation has been

found to stimulate hepatic *de novo* lipogenesis via SREBP1c (200), we did not find any

differences in the expression of its downstream targets FAS and ACC1 (Fig 3-10B).

Since the majority of intestinal MG derived from dietary sources is used for TG

biosynthesis (33), we measured the expression of lipid metabolic enzymes involved in these

processes. Increases in MGAT2, DGAT2, and particularly DGAT1 (Fig 3-10C), suggest an

upregulation of the dominant pathway for TG re-esterification in the small intestine (7).

Intestinal transcript levels of GPAT1 and GPAT3 were lower in MGL-/- mice (Fig 3-10C),

indicating decreased synthesis of TG through the glycerol-3-phosphate pathway, which normally

contributes approximately 20% of overall TG re-esterification in the enterocyte (7).

Table 3-3

	WT LFD	MGL-/- LFD	WT HFD	MGL-/- HFD
Analyte (pg/ml)				
Insulin	333±103	249±21	724±196	255±56*
Glucagon	47±5	69±8*	45±9	43±9
C-peptide	634±166	298±55	883±164	382±85*
PP	18±3	38±10	17±4	23±6
Leptin (ng/ml)	12±2	4±2*	27±4	18±3
Adiponectin (ng/ml)	15±1	14±1	13±1	15±1
Resistin (ng/ml)	14±2	10±1*	25±3	14±2*
GIP	161±28	126±40	145±46	102±16
PYY	105±8	103±9	112±22	79±13
MCP-1	87±20	44±12	103±14	89±22
TNFα	23±7	19±2	20±5	32±3
IL-6	48±15	44±15	85±61	52±20

Table 3-3. Plasma peptide levels in male mice as analyzed by multiplex immunoassay. Data are expressed as average ± SEM (n = 5-6). * $p < 0.05$ compared to WT mice on the same diet.
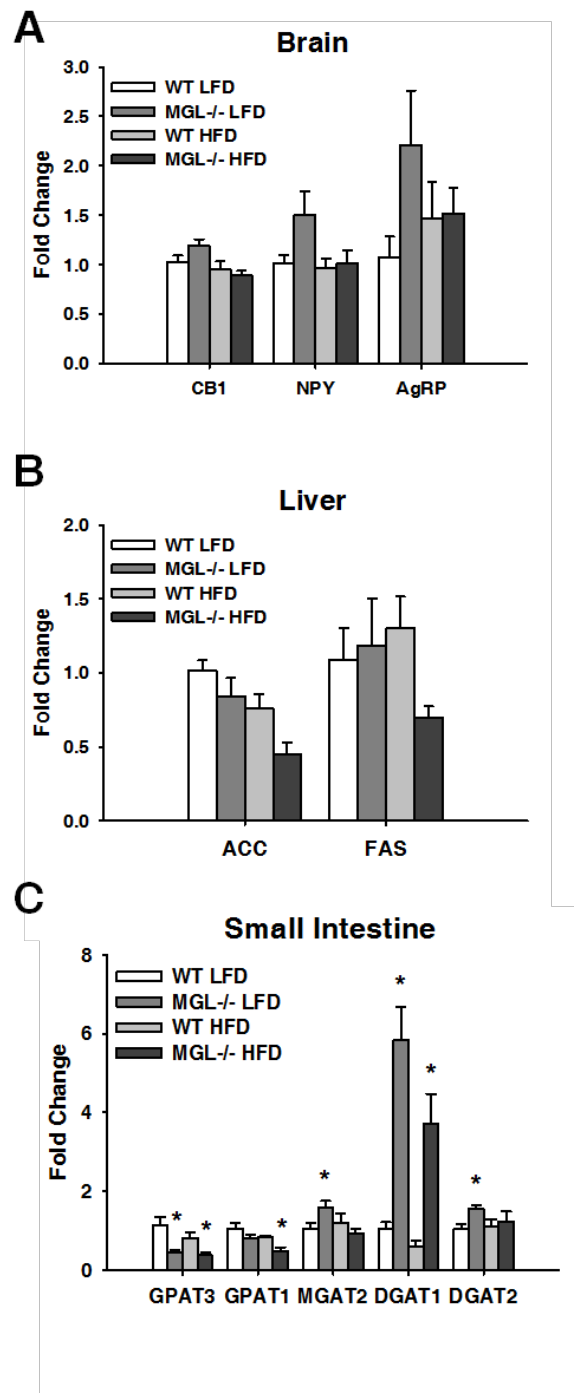
Figure 3-10

Figure 3-10. Gene expression measured by RT-PCR and analyzed by ddCT method. (A) Brain (B) Liver and (C) Small intestine mucosa. All transcript levels are presented relative to the WT LFD group. Data are expressed as average ± SEM (n = 5-6). * $p < 0.05$ compared to control group of the same diet.

DISCUSSION

The results showed that MGL ablation results in lower body weight gain, and that the

MGL-/- mice had lower body fat content. The leaner LFD-fed mice also had increased fat

oxidation that was not apparent in the HFD fed mice. This is possibly because reductions in

lipolysis have a more pronounced effect when fat is limited, and is in keeping with the lack of

effect of MGL ablation on mice fed an extreme high fat diet (78), and the lower body weights

reported for animals that were fed a chow diet (103). MGL-/- mice fed both LFD and HFD also

showed lower levels of serum lipids, and an overall trend for lower levels of circulating

metabolic peptides, particularly insulin, c-peptide, leptin, and resistin. It is likely that these

reductions are secondary to the decreased fat mass, which is positively correlated with serum

lipids and peptides involved signaling of energy homeostasis (162). There was little evidence for

either central or peripheral EC activation by the increased tissue levels of 2-AG, consistent with

desensitization caused by chronic EC elevation, and suggesting that much of the metabolic

effects may arise from other aspects associated with decreased MG catabolism.

The reduced body fat in the MGL-/- mice does not appear to be secondary to changes in

food intake or energy expenditure, nor have changes in thermogenesis been reported in other

studies (103). However, loss of MG hydrolysis may affect fat stores in other ways. First,

desensitization of the EC system may result in functional antagonism, producing effects on fat

mass similar to those seen when CB1 is targeted pharmacologically or by genetic deletion (206,

207). This would include the inability to activate CB1 pathways, which would normally inhibit

intracellular lipolysis in adipose and FA oxidation in muscle and other tissues (208). Second, the

metabolism of excess 2-AG by cyclooxygenase-2 (COX-2) produces prostaglandin glycerol esters

(209). It has been proposed that these resultant prostanoids inhibit adipogenesis (210). Thus, an

abundance of 2-AG prostanglandin metabolites may be limiting the formation of new adipocytes and thereby causing the diminished fat mass seen in our MGL-/- when fed lower fat diets. On the other hand, hypertrophy of existing adipocytes by HF feeding may mask differences in fat mass of MGL-/- mice, as found here and with very high fat feeding (78).

The large increases in MG levels in brain, adipose, and liver was expected based on other studies of MGL null mice (78, 102, 103). For brain, the high 2-AG levels are likely reflective of the 83% reduction in MG hydrolysis we observed. The remainder of activity may be ascribed to ABHD6 and ABHD12, which had previously been thought to contribute 15% of total brain MG catabolism (79), and is very similar to our residual activity. It is possible that ABHD6 and ABHD12 may be regulating MG content in certain tissues and cell types. However, mRNA levels of both enzymes were previously found to be unchanged in MGL-/- mice in brain, liver, and adipose tissue (78), indicating a lack of compensatory upregulation. Our results provide further support that MGL is the dominant MG-hydrolyzing enzyme in these major tissues. While other studies of MGL-/- mice reported no changes in brain AEA levels (102, 103), we found modest increases in AEA and other acylethanolamides in liver and brain for both diet groups. Nevertheless, brain FAAH activity in the MGL-/- mice was essentially unchanged (data not shown), and therefore cannot account for the increased acylethanolamides.

In the intestinal mucosa, a far more modest effect of MGL ablation on tissue MG levels was observed (Fig 2D), which may be attributed to a number of factors. First, intestinal MGL expression is low compared to other tissues such as adipose (65), where the lipolytic release of TG pools is a more prominent function. Perhaps more importantly, the resynthesis of TG using dietary MG and FFA as substrates is the dominant pathway in the small intestine (33), and serves the vital role of rapidly delivering dietary lipids to the rest of the body. Thus the 12 h fast prior to necropsy in the animals is likely sufficient time for any excess MG to be re-esterified,

packaged into chylomicrons, and exported into the circulation. Additionally, the observed

increase in intestinal MGAT and DGAT enzyme expression (Fig 8C) may be a transcriptional

response to an overabundance of MG in the postprandial state, and therefore compensate for

excess MG in the MGL-/- mice by increasing its incorporation into TG. This is further supported

by a concomitant decrease in GPAT expression (Fig 8C), which become less necessary to

generate glycerolipid precursors when MG is already present for TG synthesis. Indeed, studies

have demonstrated the inhibition of the glycerol-3-phosphate pathway in intestinal mucosa by

the addition of excess 2-MG (211).

The reduced appearance of TG in the bloodstream following oral fat challenge in the

MGL-/- mice was quite striking and somewhat unexpected. In another study using transgenic

mice overexpressing MGL in intestinal mucosa, we found no difference in mucosal TG re-

esterification (65), indicating that altered intestinal MGL activity may not affect that particular

aspect of dietary fat absorption. The present results are similar to those for MGAT2 deficient

mice, that, despite having quantitatively normal intestinal fat absorption, also have markedly

reduced intestinal TG secretion rates in oral fat tolerance tests (41, 42). The MGAT2 null mice

are also resistant to DIO and have increased energy expenditure through upregulation of FA

oxidation (41, 42, 212). It is unknown whether the delayed entry of fat into circulation in the

MGL-/- and MGAT2-/- mice proceeds through similar mechanisms, perhaps via transiently

increased cellular MG levels. Yet, these two mouse models share a common inability to process

MG normally in the small intestine and other tissues. This raises the possibility that the

pathways are indeed similar and further underscores the importance of intestinal MG

metabolism in dietary lipid assimilation.

Although, as noted, relatively little has been reported about effects of MGL gene

ablation on body weight gain and associated metabolic processes, the results to date are

conflicting. In a study by Chanda *et al*., both male and female adult MGL-/- mice showed a 16.5%

reduction in body weight that persisted over time (103). This decreased body weight is similar to

the those seen in CB1-/- mice and in antagonist treated mice (137). In contrast, Taschler *et al*.

did not observe changes in the weight or body composition of MGL-/- mice fed either an 11%

(kcal) chow diet or a 74% (kcal) very high fat diets for 12 weeks (78). Underlying reasons for this

discrepancy between phenotype in the two studies remain unclear. Both used gene targeting

methods to generate the knockout mice, albeit with different targeting vectors, and both have

similar genetic backgrounds, C57Bl6 (78) and C57Bl6/NTac (103). Differences in diet

composition, and particularly fat sources, between the studies could potentially contribute to

phenotypic differences however this information was not available. In the present study we

used controlled semipurified diets of defined composition which differed in the percent of

energy as fat. Moreover, the higher fat diet was set at 45% of total calories to more closely

reflect physiological levels of fat intake. The reduced body mass gain that we found in our MGL-

/- mice was consistent with results from Chanda *et al.* (103). It is worth noting that the degree of

reduction in body mass was not as pronounced on the 45% fat diet as it was on the 10% fat diet.

Together with the absence of an effect in Taschler *et al.* (78), at least on the 74% fat diet, this

could reflect desensitization of CB1 receptors by continuous marked elevations of 2-AG levels.

Indeed there is strong evidence for the desensitization of central CB1 receptors by chronically

elevated 2-AG (78, 102, 103). This may also explain the lack of change in food intake, as well as

other cannabimimetic effects on activity, for the MGL-/- mice in the present study. Acute

administration of 2-AG into the nucleus accumbens stimulates feeding behavior in rats (134).

However, chronic MGL inhibition, and the associated effects of 2-AG elevation on food intake

and energy balance, have not be reported to our knowledge. Intermittent elevation of 2-AG may

be a potential method for avoiding EC desensitization. Interestingly, it has been shown that CB1

mediated analgesia is sustained by repeated low-dose administration of the MGL inhibitor JZL-184 (112).

The trend for decreased glucose excursions secondary to an oral glucose challenge in the MGL-/- mice supports the studies of Taschler *et al,.* who found that MGL ablation in mice mitigated HFD-induced insulin resistance (78). Whether this points to a pathogenic role of MGL in the liberation of FFA associated with inflammation and obesity-related illnesses remains to be seen. Certainly, the decreased levels of resistin shown in the present study provide further evidence that MGL ablation confers some protection against the development of insulin resistance. In the murine model, resistin is an adipocyte-derived cytokine that has been suggested to be an important link between obesity and type 2 diabetes mellitus (213). Increasing circulating resistin in mice through transgenic over-expression (214) or recombinant treatment (215) causes insulin resistance, whereas genetic deletion preserves insulin sensitivity in obese mice (216). Additionally, given the broad acyl chain substrate specificity of MGL (91), we cannot rule out that elevations of MG species other than 2-AG may be aiding in glucose disposal through newly discovered pathways. Notably, 2-oleoylglycerol has recently been shown to bind GPR119 receptors in enteroendocrine and pancreatic β-cells, stimulating the release of glucagon-like peptide 1 and insulin, respectively (217, 218).

A potentially beneficial consequence of MGL inhibition or knockout is the sequestering of arachidonic acid (AA) in the form of 2-AG. Brain AA levels were found to be significantly reduced alongside elevations in 2-AG in MGL-/- mice (102), similar to those found in the present study. Because the majority of AA used in prostaglandin production is thought to be derived from 2-AG catabolism (108), beneficial effects on diseases from cancer to hepatic ischemia have been ascribed to MGL ablation or pharmacological inhibition (98, 109, 219). In fact, MGL inhibition appears to limit progression of neurodegenerative disorders such as Alzheimer's

disease, both by decreasing prostaglandin production and by the anti-inflammatory response of CB2 stimulation by 2-AG (113). Considering the interrelationships between inflammation and metabolic function (220), it is therefore possible that alterations in these signaling pathways underlie the healthier phenotype we see in our MGL null mice, including trends for reductions in cytokines such as MCP-1.

In summary, we show that knockout of MGL in mice results in high tissue levels of MG. For intestine, there was evidence of upregulation of the already predominant pathway of intestinal TG synthesis via MGAT and DGAT. MGL-/- mice on both LF and HF diets had reduced weight gain over the 12 weeks of feeding, and when dietary fat was limiting, MGL-/- mice were significantly leaner and displayed increased fat oxidation. Serum lipid levels were decreased, as were many signaling peptides involved in maintaining energy homeostasis. MGL-/- mice on a HFD also had greatly reduced rate of intestinal TG secretion. These results suggest that large reductions in MGL hydrolysis have the potential to affect whole body energy homeostasis, as well as be protective against some of the deleterious downstream effects of HFD-induced obesity.

Chapter 4

Short-term reversible pharmacological inhibition of monoacylglycerol lipase in mice does not alter food intake or diet induced obesity

ABSTRACT

Monoacylglycerol lipase (MGL) regulates MG levels in various tissues throughout the body. There are currently no studies on the short- and long-term metabolic effects of MGL-specific inhibition in lean or obese mice. To further examine the role of MG metabolism in energy homeostasis, C57BL/6J mice were fed low (10% kcal) and high fat (45%) diets for 12 weeks, and given daily oral administration of vehicle or 1,3,10, and 30 mg/kg MGL inhibitor for 4 days (acute) or 27 days (chronic) while continuing on their respective diets. There were no observed acute or chronic changes in food intake. Nor were other aspects of obesity, such as increased adiposity or glucose intolerance, substantially altered by inhibitor treatment. From these results, we conclude that the effects of transient MGL inhibition, up to 28 days, on aspects of energy metabolism are minimal.

INTRODUCTION

Monoacylglycerol lipase (MGL) is the rate limiting enzyme in the hydrolysis of MG in many tissues. This activity contributes to energy balance by mobilizing cellular lipid stores in adipose and other tissues, and also through the regulation of 2-arachidonoyl glycerol (2-AG) levels in the endocannabinoid (EC) system (103).

We have previously demonstrated that intestinal MGL over-expression in mice depletes mucosal MG levels and induces a hyperphagic, obese phenotype (65). These results suggest that MGL activity in the intestine contributes to the stimulation of food intake and progression of diet induced obesity. In another previously detailed study, we also assessed the metabolic implications of MGL ablation in mice fed low fat and high fat diets. We found that genetic knockout results in decreased body weight, lower fat mass, and an overall leaner phenotype including reduced circulating lipids and metabolic peptides. These results indicate that inhibition of MGL may be beneficial in treating metabolic disorders such as obesity.

The pharmacological inhibition of MGL has been used to examine effects on the EC system. In brief, a single high dose treatment of mice with the irreversible inhibitor JZL184 resulted in an 8-fold elevation of brain 2-AG levels and produced CB1-dependent behavioral effects such as hypothermia, hypomotility and analgesia (110, 111). It may be concluded from these results that, on a short-term basis, MGL inhibition activates the EC system. In contrast to acute inhibition, administration of JZL184 up to 6 days at the same high dose results in progressively diminished analgesia and functional desensitization of the EC system (102). These effects appear to be mediated by tonic activation of CB1 by sustained high 2-AG levels (102, 106, 107). Interestingly, repeated low dose administration of JZL184 for 6 days in mice sustains the analgesic effects of 2-AG activation (112), suggesting that the overall degree and length of time

during which MG levels are elevated are highly important in maintaining EC system functionality.

The acute and chronic effects of MGL inhibition on energy metabolism are virtually unexplored. One study has reported that dual MGL/FAAH inhibition by an acute dose of isopropyl dodecylfluorophosphonate (IDFP) in mice resulted in reduced clearance of circulating TG, hepatosteatosis, and insulin resistance (114, 115). In this case, however, evidence that MGL and FAAH regulate different aspects of the EC system precludes the determination of the true *in vivo* effects of MGL-specific inhibition on energy homeostasis. Still, the previously mentioned results of acute MGL inhibition by JZL184 (110, 111) would predict that elevating 2-AG would stimulate the orexigenic effects mediated by CB1 in the hypothalamus and mesolimbic system. This has been demonstrated, in part, by direct brain infusion of 2-AG resulting in hyperphagia (134). Additionally, acutely elevated 2-AG in the periphery from MGL inhibition would be predicted to stimulate hepatic lipogenesis, enhance fat uptake in adipose, and result in increased deposition of body fat as in other examples of peripheral CB1 activation (131, 145, 156, 200). However, it may also be hypothesized that sustained elevation in 2-AG, and other MG species, as shown in the genetic ablation and chronic MGL inhibitor treatment, diminishes the energy-sparing effect of acute EC activation and ultimately proves to be beneficial towards reducing food intake and promoting peripheral energy utilization.

In the present study, we investigated the dose-dependent effects of acute (4 day) and chronic (27 day) inhibition of MGL on food intake and energy homeostasis. The results showed that daily oral administration of a novel reversible MGL inhibitor to lean and obese mice did not produce effects on caloric intake. Body weight and composition was also unchanged in any of the treatment groups, regardless of dose. We also did not observe any change in serum lipid levels or response to oral glucose challenge. Overall, we conclude that transient

pharmacological blockade of MGL by a reversible inhibitor has minimal effect on feeding behavior and energy homeostasis.

MATERIALS AND METHODS

Animals, Diet, and Necropsy

Four week old, male C57BL/6J mice were acquired from Jackson Laboratories (Bar Harbor, ME) and maintained at the Rutgers animal facility. Starting upon arrival, the mice were housed 3-4 per cage during the 12 week period, in which they were fed either a 10% kcal low-fat semipurified diet (D12450B, Research Diets Inc., New Brunswick, NJ) or a 45% kcal high-fat semipurified diet (D12451, Research Diets Inc., New Brunswick, NJ). The 16 week old mice from each diet were then randomized by body weights into groups, and were singly housed for the 4-day and 27-day inhibitor administration. During this time, the mice continued to have *ad libitum* access to the same diet they had been on during the 12 week feeding period, which was refreshed daily to ensure palatability. On the day of necropsy, mice were fasted for 3 h (6:30 to 9:30 AM). Necropsy was performed as previously described (Aim 2). It was necessary to split the mice from both the acute and chronic studies into 4 cohorts, each composed of equal numbers of dosage groups. All animal procedures were approved by the Rutgers University Animal Use Protocol Review Committee and conformed to the National Institutes of Health *Guide for the Care and Use of Laboratory Animals*.

Pharmacological Compounds and Administration

The MGL inhibitor JNJ-MGLi was generously provided in agreement with Johnson and Johnson PRD (New Brunswick, NJ). This lipophilic compound reversibly binds to MGL, and was previously determined to have an *in vitro* IC_{50} = 16 nM, K_d = 5 nM, and an *in vivo* EC_{50} = 1.2 uM for a stimulation of 2-AG elevation in rat brain. Rats given JNJ-MGLi post-orally at 10 mg/kg body weight had a maximal blood concentration of 4.3 uM at 1.8 h after administration, and a half life

$t_{1/2}$ = 2.8 h. The compound was also shown to be acutely toxic, resulting in death in 0.5-2 h at a dose of 300 mg/kg (M. Connelly, personal communication).

Compound suspensions of the MGL inhibitor were prepared prior to the beginning of each experiment at the following concentrations: 0.1, 0.3, 1, and 3 mg/ml in vehicle (20% (g/ml) (2-hydroxypropyl)-β-cyclodextrin (HPβCD) and 0.1% Tween 80). Rimonabant (SR141716, an inverse agonist of CB1 receptors) suspension was prepared by first dissolving the compound in 100% ethanol, adding Tween-80, drying the solution under nitrogen gas to evaporate the ethanol, then dissolving in a 20% HPβCD solution and sonicating in a water bath for 30 minutes.

All compound or vehicle administration was done by oral gavage. The mice received sham doses of water at 5 PM for 3 days prior to beginning of each experiment to reduce stress. Each group received daily doses of vehicle, Rimonabant (10 ml/kg in vehicle as a positive control), or MGL inhibitor (1, 3, 10, and 30 mg/kg body weight (mpk) JNJ-MGLi in vehicle). For 4 or 27 days, mice were administered 10 ml/kg body weight of their respective doses via oral gavage at 5 PM each day (Tables 4-1 & 4-2). Body weights were recorded daily and used to calculate the dosing volume.

Table 4-1

Group	Treatment		Animal # Total = 48
	Compound	**Dose volume**	
Group 1, A1-8	A. 20% HPβCD, 0.1% Tween 80 (Veh) (HFD)	10 ml/kg	#1-8
Group 2, B1-8	B. JNJ-MGLi - 1 mpk in Veh (HFD)	10 ml/kg	#9-16
Group 3, C1-8	C. JNJ-MGLi - 3 mpk in Veh (HFD)	10 ml/kg	#17-24
Group 4, D1-8	D. JNJ-MGLi - 10 mpk in Veh (HFD)	10 ml/kg	#25-32
Group 5, E1-8	E. JNJ-MGLi - 30 mpk in Veh (HFD)	10 ml/kg	#33-40
Group 6, F1-8	F. JNJ-MGLi - 30 mpk in Veh (LFD)	10 ml/kg	#41-48

Table 4-1 Acute MGL inhibitor dosing protocol

Table 4-2

Group	Treatment		Animal # Total = 64
	Compound	Dose volume	
Group 1, A1-8	A. 20% HPβCD, 0.1% Tween 80 (Veh) (LFD)	10 ml/kg	#1-8
Group 2, B1-8	B. Veh (HFD)	10 ml/kg	#9-16
Group 3, C1-8	C. Rimonabant- 10 mpk in Veh (HFD)	10 ml/kg	#17-24
Group 4, D1-8	D. JNJ-MGLi - 1 mpk in Veh (HFD)	10 ml/kg	#25-32
Group 5, E1-8	E. JNJ-MGLi - 3 mpk in Veh (HFD)	10 ml/kg	#33-40
Group 6, F1-8	F. JNJ-MGLi - 10 mpk in Veh (HFD)	10 ml/kg	#41-48
Group 7, G1-8	G. JNJ-MGLi - 30 mpk in Veh (HFD)	10 ml/kg	#49-56
Group 8, H1-8	H. JNJ-MGLi - 30 mpk in Veh (LFD)	10 ml/kg	#57-64

Table 4-2 Chronic MGL inhibitor dosing protocol

Body Composition

For the chronic study, fat mass (FM) and lean body mass (LBM) were analyzed at 3:00 PM on days 1 and 26 in non-anaesthetized mice by magnetic resonance imaging using an EchoMRI-100 (Echo Medical Systems, Houston TX).

Lipid Extraction and Analyses

Lipids from brain (10 mg protein), liver (10 mg), gonadal fat (1 mg), and mucosa (10 mg) samples were extracted as previously described (Aim 2). For plasma samples, 150 ul of plasma was diluted to 300 ul with 1X PBS pH 7.4 and extracted by Folch protocol (175). Prior to all lipid extractions, deuterated 2-AG (2-AG-d8, 100 pmol, from 10 uM stock in chloroform) and deuterated AEA (AEA-d8, 10 pmol, from 1 uM stock in methanol) were added as internal standards to each sample homogenate. Tissue and plasma monoacylglycerol and acylethanolamide levels were determined by liquid chromatography (LC)-coupled mass spectrometry (MS) as previously described (Aim 2). During analyses, AEA-d8 was used as the reference standard for both acylethanolamide and MG species due an insufficient signal from the 2-AG-d8 internal standard.

Food Intake

Food intake was measured for the acute study using the BioDAQ system (Research Diets, New Brunswick, NJ). This system allows for simultaneous real-time monitoring of food consumption, as well as monitoring of ambient temperature and humidity. Mice were acclimatized to individual BioDAQ cages for 10 days prior to drug administration and data collection period. The diet was refreshed daily to ensure palatability. For the chronic study, food intake was measured daily for the first week and then twice weekly afterwards by manual weighing of diet pellets in each cage.

Plasma Analyses

On the day before necropsy, blood samples were collected from all mice at 1.5 h and 7 h after inhibitor administration. Dried blood spot (DBS) were used to measure compound levels and assess pharmacokinetics. In this procedure, 30 µl of blood taken from the tail vein was placed on a Whatman FTA DMPK card (GE Healthcare, NJ) and allowed to dry. The compound was later eluted and quantified by LC-MS.

Triacylglycerol and glucose were measured in whole blood samples by Cardiochek (Polymer Technology Systems, Inc., Zionsville, IN) and glucometer (Accuchek, Roche Diagnostics), respectively.

Oral Glucose Tolerance Test (OGTT)

On day 24 of the chronic study, the mice were fasted for 6 h prior to the OGTT, then given a bolus of 2 g/kg body weight D-(+)-glucose solution by oral gavage. Blood glucose was measured using a glucometer at t = 0, 30, 60, and 120 min after collecting blood from tail nicks (Accuchek, Roche Diagnostics). Area under curve (AUC) was calculated using the trapezoid rule.

Statistical Analyses

A total of 48 mice (acute) and 64 mice (chronic) (n=8 per group in both studies) were used in this study. Group data were expressed as average ± s.e.m. Statistical differences were calculated for each treatment and compared using one-way analysis of variance (ANOVA) with Tukey's post-hoc comparison and $p < 0.05$ considered significant. Within group comparisons for initial and final values were also determined using a two-sided *Student's* t-test and $p < 0.05$ considered significant.

RESULTS

Pharmacokinetics of MGL inhibitor administration

We first assessed the pharmacokinetics of oral compound administration in mice on day 4 and day 27 of the acute and chronic studies, respectively. There was a dose-dependent response in blood levels of the MGL inhibitor JNJ-MGLi observed at 1.5 h after administration in the acute study (Fig 4-1A). Low-fat fed mice receiving the highest inhibitor dose (30 mpk) had a trend for increased inhibitor blood levels compared to HFD fed mice given the same dose. At 7 h after administration, very little circulating levels of compound were found in both the acute (Fig 4-1A) and chronic studies (Fig 4-1B). The half-life ($t_{1/2}$) for blood concentrations of the MGL inhibitor given at 30 mg/kg was approximately 3.6 h.

Tissue MG and acylethanolamide levels

We then examined effects of MGL inhibition on MG and acylethanolamide species in various tissues by HPLC-MS/MS. Lipid extractions were performed on tissues on day 5 and 28 of the acute and chronic studies, approximately 16 h after the final inhibitor dose. There were no statistically significant differences in MG levels in the small intestine (Fig 4-2A-B), or in 2-AG levels in the brain and liver (Fig 4-2C-F) between any of the groups. These results suggest that the *in vivo* MGL inhibition by the compound was, if at all, transient and did not produce sustained effects on MG levels observable 16 h after administration. Overall, acylethanolamide levels were unchanged in any of groups in small intestine, brain, and liver lipid extracts (Fig 4-3 A-F).

Figure 4-1
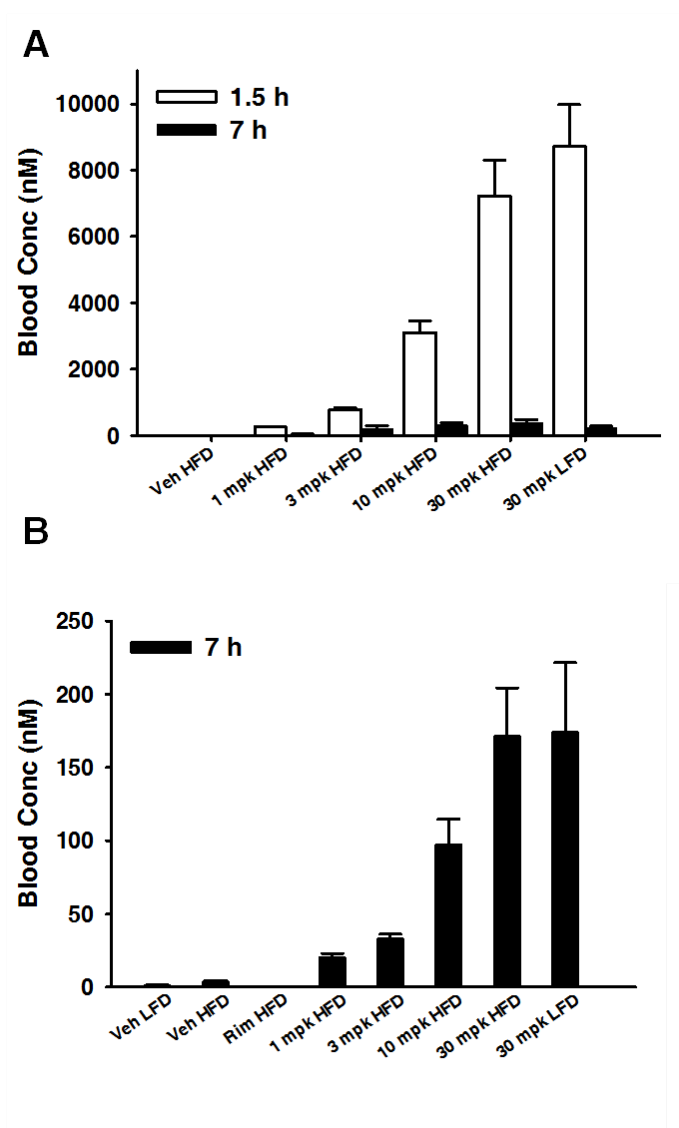
Figure 4-1. Blood levels of MGL inhibitor JNJ-MGLi taken 1.5 and 7 h after oral administration.

(A) Acute study (B) Chronic study (7 h only). Data are expressed as average ± SEM (n = 8).

Figure 4-2
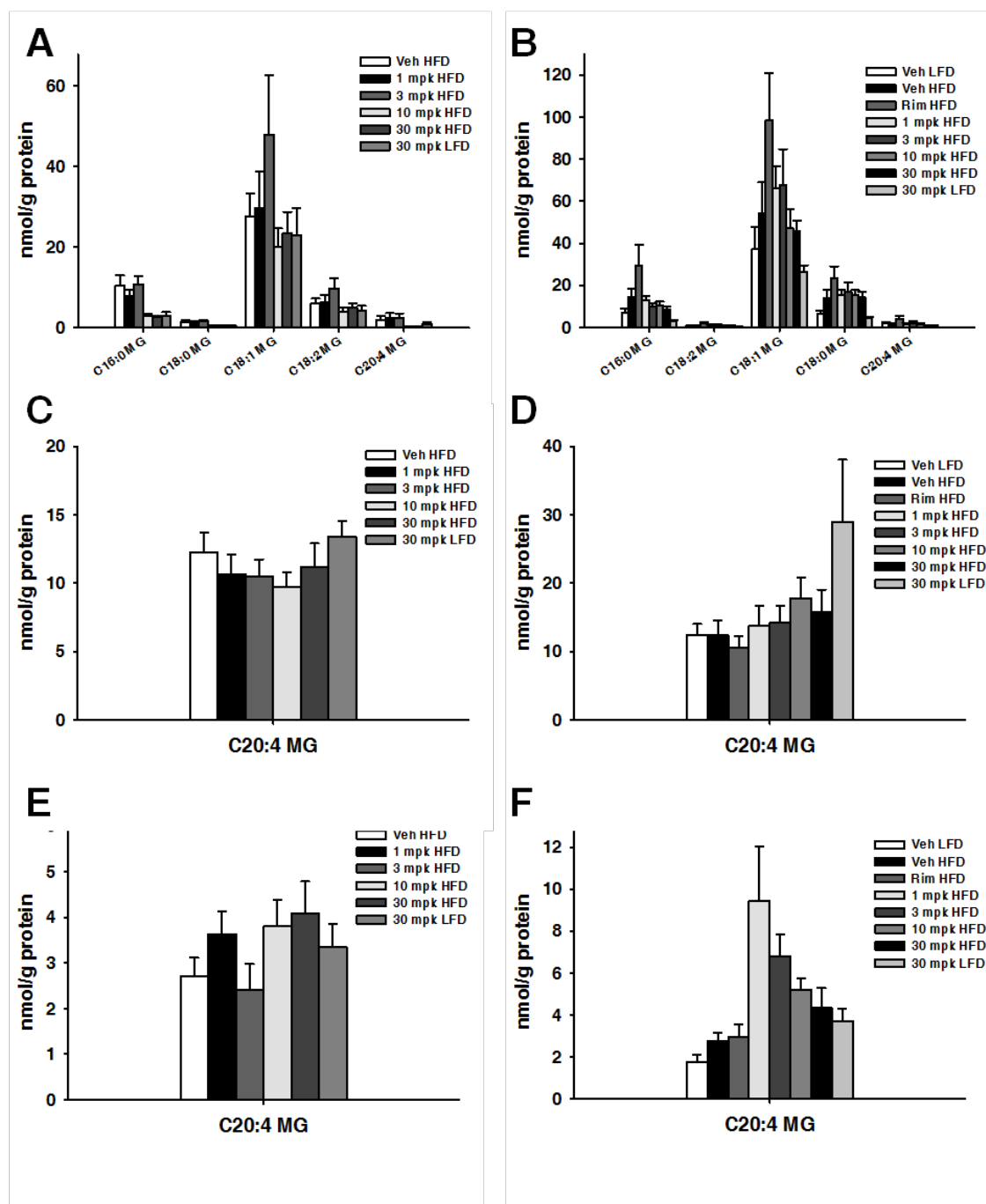
Figure 4-2. Tissue monoacylglycerol (MG) levels after 4 and 27 days of compound administration. Sample lipid extracts were taken during necropsy after a 16 h fast following dosing. Lipid levels expressed as nmol per g of total cellular protein in each extraction. (A) Small intestine acute (B) Small intestine chronic (C) Whole brain acute (D) Whole brain chronic (E) Liver acute (F) Liver chronic. Data are expressed as average ± SEM (n = 7-8).

Figure 4-3

Figure 4-3. Tissue acylethanolamide (EA) levels after 4 and 27 days of compound administration. Sample lipid extracts were taken during necropsy after a 16 h fast following dosing. Lipid levels expressed as nmol per g of total cellular protein in each extraction. (A) Small intestine acute (B) Small intestine chronic (C) Whole brain acute (D) Whole brain chronic (E) Liver acute (F) Liver chronic. Data are expressed as average ± SEM (n = 7-8).

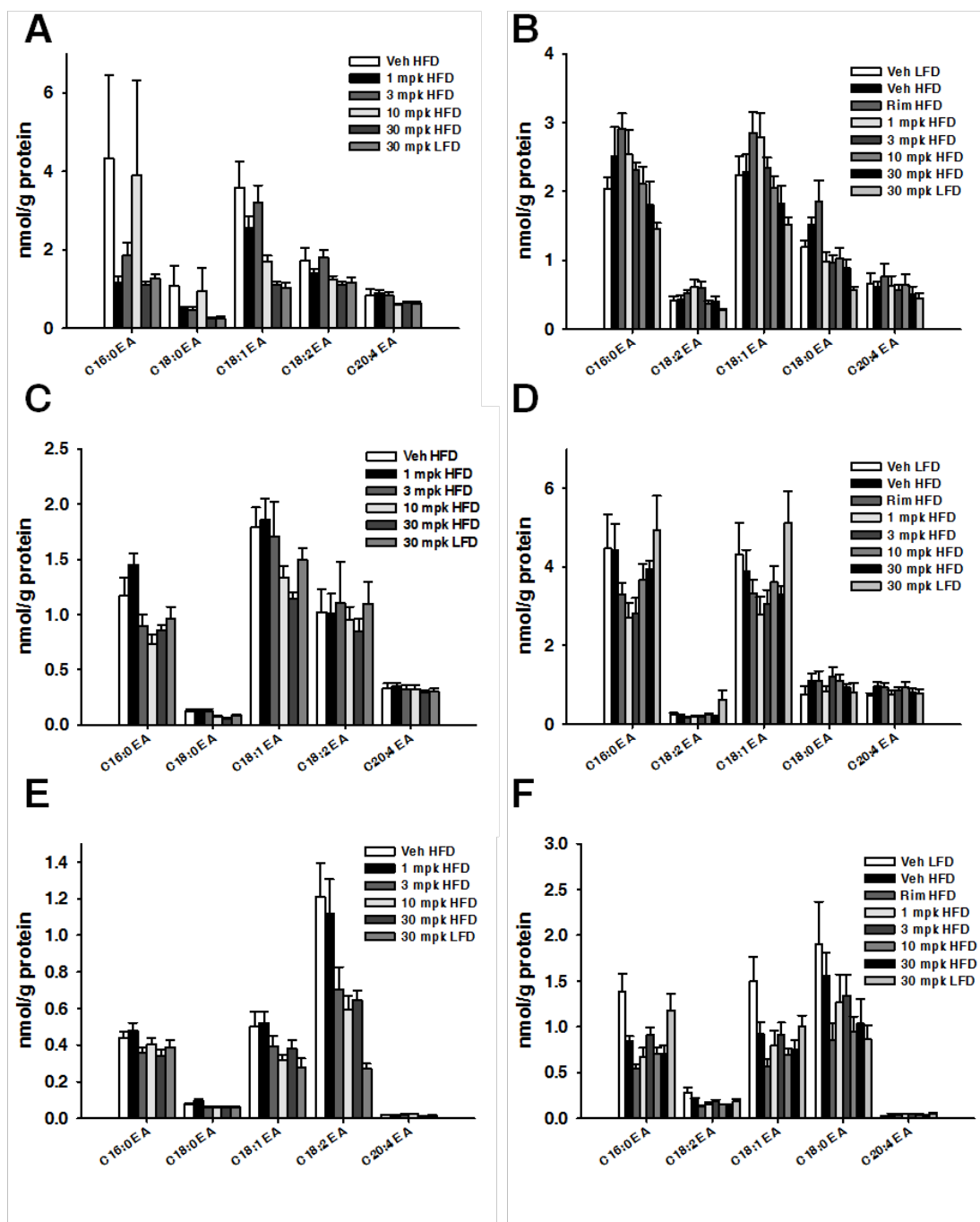**Body mass and composition**

In the acute study, body weight was unchanged by treatment over the 5 days of monitoring (Fig 4-4A-B). Similarly, there was no effect on body weight over 28 days of inhibitor administration (Fig 4-4C-D). Moreover, lean mice fed the LF-diet did not differ in body weight when given the maximum MGL inhibitor dose. Mice receiving the positive control, Rimonabant, had a profound loss of body weight, particularly in the first 10 days, that was sustained over the rest of the study (Fig 4-4C-D). Overall, mice in both studies lost body weight over the course of the experiment, regardless of diet or treatment group, likely due to effects of daily oral gavage (Fig 4-4 B&D).

Body composition was assessed by MRI on day 1 and day 26 of the chronic inhibitor treatment. The 12 weeks of 45% HFD feeding resulted in increased body fat ($p < 0.05$) compared to LFD feeding, generating obese mice. All groups displayed a non-significant loss of body fat over the course of the study that was larger for HF-fed groups (~ 4 % change) than LF-fed groups (~ 1% change) (Fig 4-5). Nevertheless, there were no inhibitor-related effects on fat or lean mass. Body fat, as a percentage of total body mass, was significantly reduced ($p = 0.009$) after Rimonabant treatment only (Fig 4-5).

Food intake

To test whether MGL inhibition affects eating behaviors, total caloric intake was monitored in real time throughout the acute study, and initially daily and then biweekly for the chronic study. For both time courses of inhibitor treatments and in both diet groups, there were no apparent effects on total food intake. In the acute study, there was no effect of inhibitor treatment on total caloric intake (Fig 4-6 A-B), nor were there immediate effects on dark and light cycle food intake on each of the treatment days (Fig 4-7A-D). In the chronic study, inhibitor

Figure 4-4
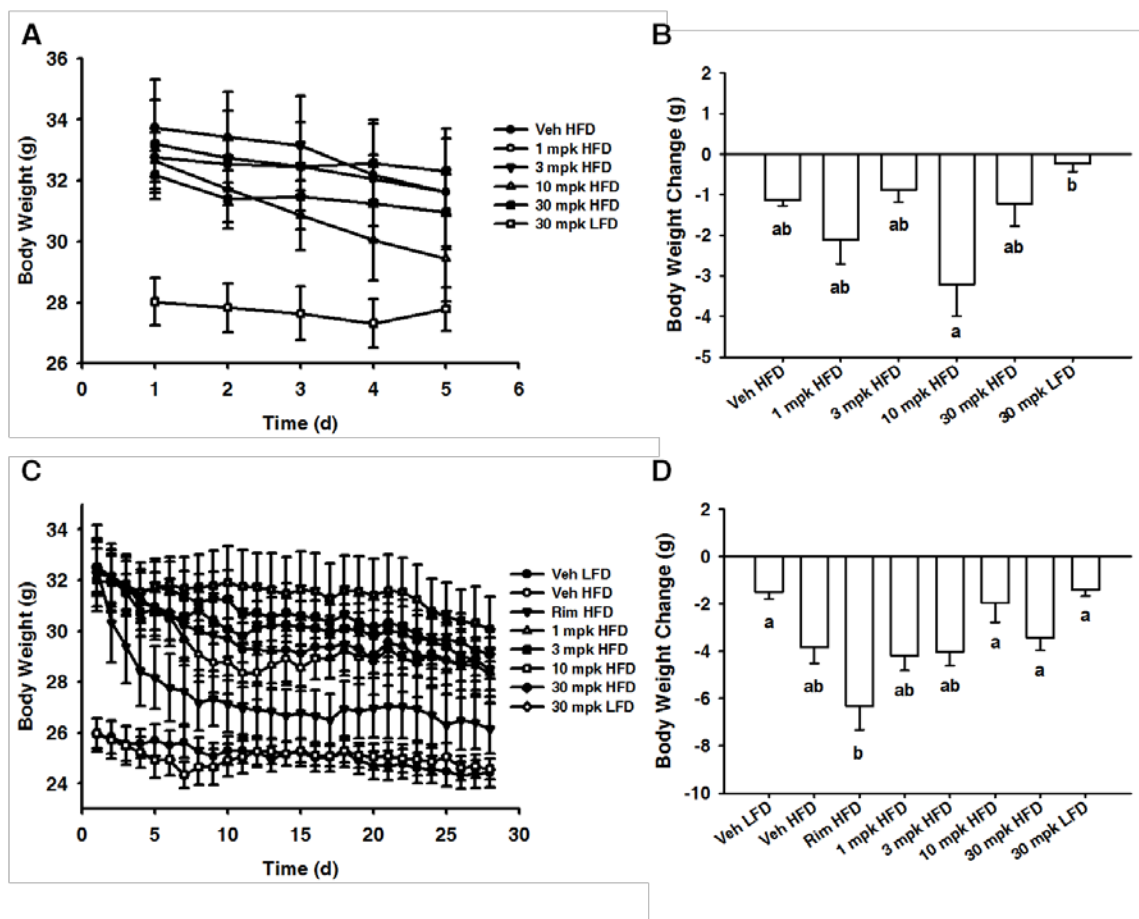
Figure 4-4. Body weights during the 4 day (acute) and 27 day (chronic) compound administration. (A) Acute study body weight over 5 days of compound administration (B) Acute study overall body weight change. (C) Chronic study body weight over 28 days of compound administration. (D) Chronic study overall body weight change. Data are expressed as average ± SEM (n = 7-8). Differences between groups were determined by one way ANOVA with Tukey's post hoc test. Groups that do not share a similar letter are considered statistically different for p < 0.05.

Figure 4-5
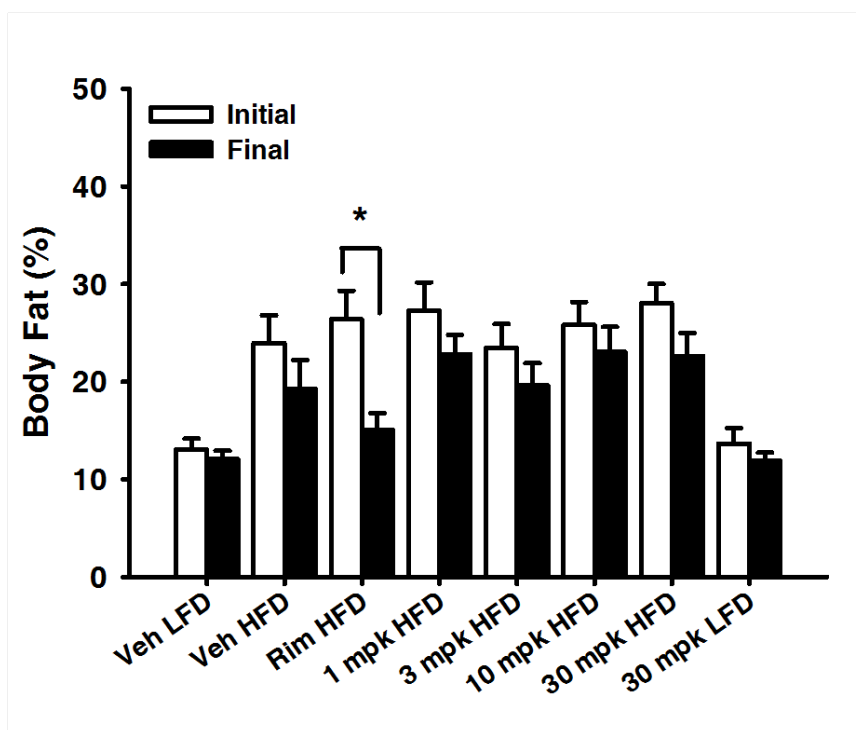
Figure 4-5. Body fat for the chronic study. Body fat (as a percentage of total body weight) was measured on day 1 before compound administration (initial), and on day 26 (final). Data are expressed as average ± SEM (n = 7-8). Initial and final differences within each treatment determined by Student's t-test, with * p < 0.05.

Figure 4-6
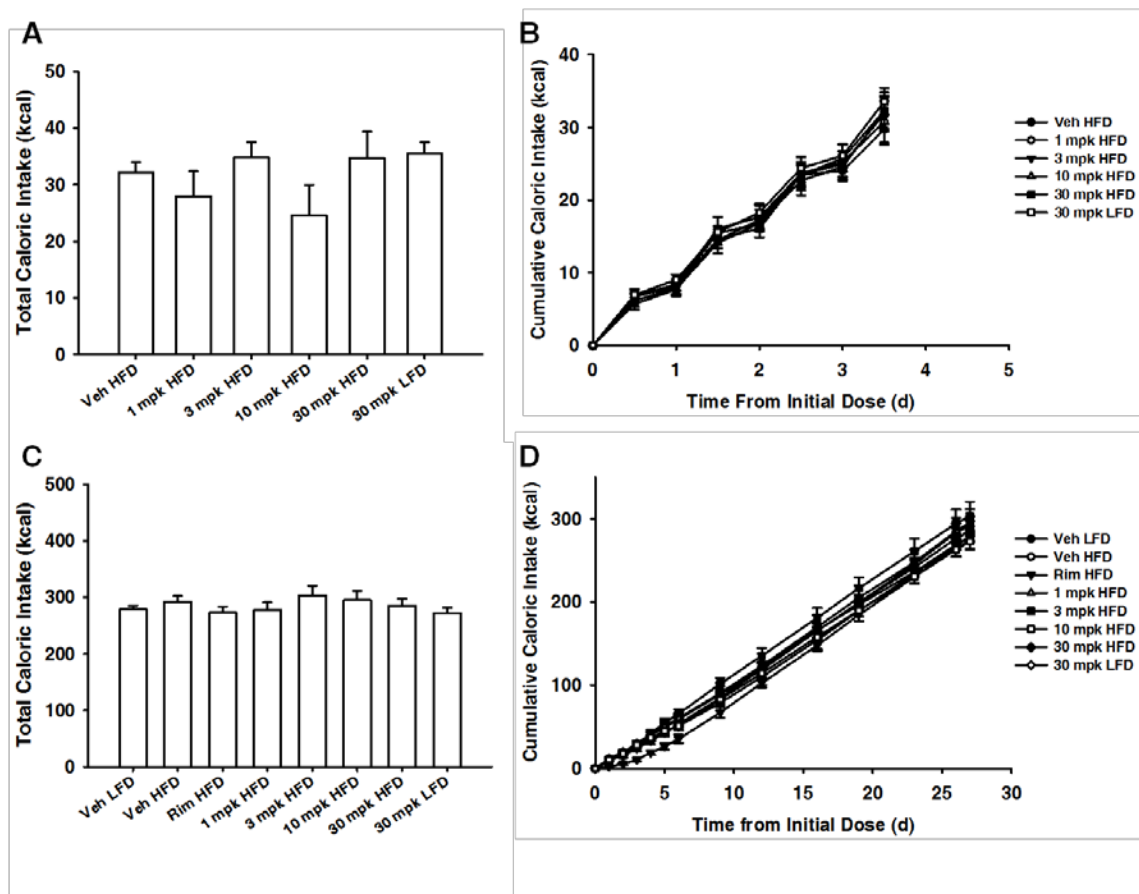
Figure 4-6. Food intake during the 5-day (acute) and 28 day (chronic) compound administration. (A) Acute study total caloric consumption (B) Acute study cumulative caloric intake starting from the initial dose at 5 pm. (C) Chronic study total caloric consumption. (D) Chronic study cumulative caloric intake starting from the initial dose at 5 pm Inset shows Veh HFD and Rimonabant HFD groups only. Data are expressed as average ± SEM (n = 6-8). There were no statistical differences between inhibitor treatment groups.

Figure 4-7
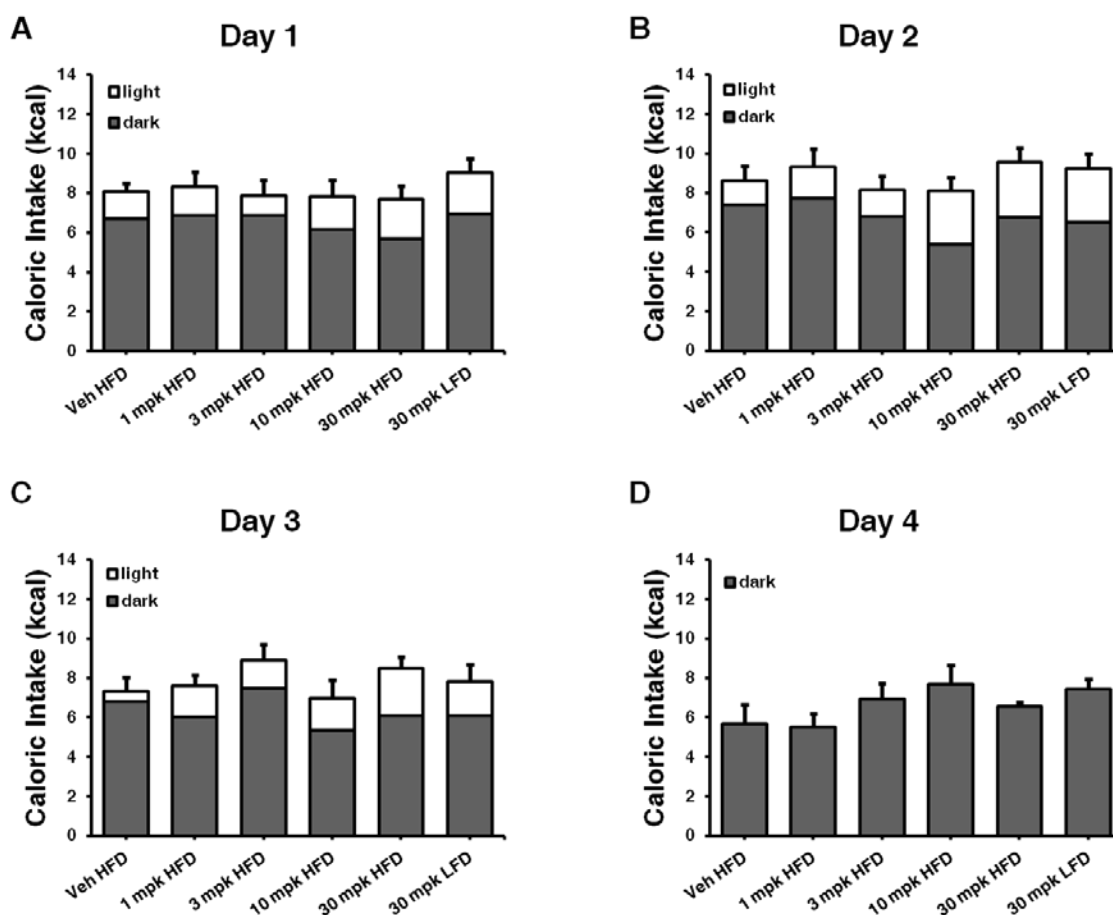
Figure 4-7. Food intake in each day of acute compound administration. Stacked bars indicate dark and light phase caloric consumption. (A) Day 1, beginning on the dark cycle immediately following animal dosing (B) Day 2 (C) Day 3 (D) Day 4. Data are expressed as average for each phase ± SEM for total light and dark combined (n = 6-8). There were no statistical differences between groups.

treatment did not alter caloric intake (Fig 4-6C-D). Rimonabant administration caused an immediate reduction in food intake in the first 4 days after administration, after which the mice consumed more calories to slightly overcompensate and resulted in a similar total caloric intake as the other groups (Fig 4-6C-D).

Glucose Tolerance

Glycemic control was assessed in the chronically-treated mice by OGTT on day 24. Inhibitor treatment did not significantly affect glucose excursions in the experimental groups (Fig 4-8A-B). Surprisingly, total glucose AUC did also not differ between the LF-fed and HF-fed mice (Fig 4-8B), possibly due to an overall negative energy balance and the small loss of body fat in all experimental groups.

Figure 4-8
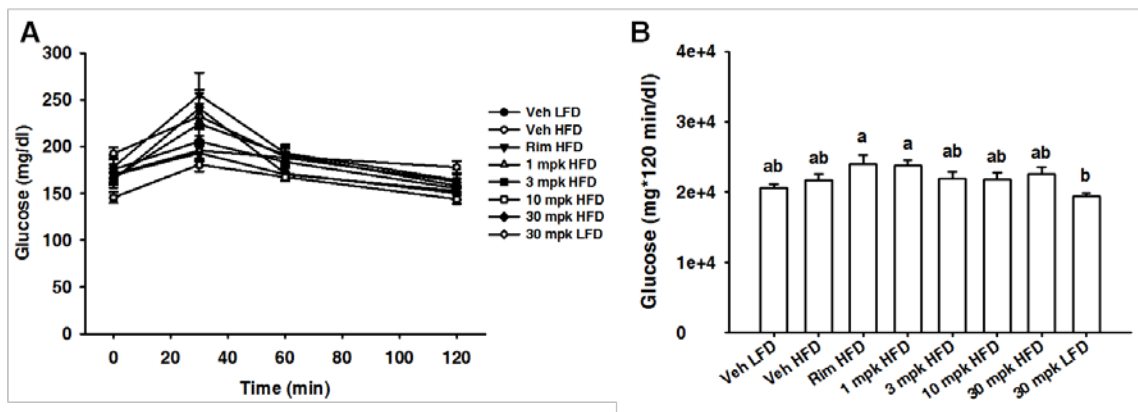
Figure 4-8. Oral glucose tolerance test on day 24 in the chronic study. Mice were fasted 6 h and given an oral bolus of 2 g/kg body weight D-(+)-glucose solution. Glucose was measured in whole blood from tail nicks at 0, 30, 60, and 120 minutes post glucose administration. (A) OGTT time course (B) Glucose area under curve (AUC) for 120 min. Data are expressed as average ± SEM (n = 7-8). Differences between groups were determined by one way ANOVA with Tukey's post hoc test. Groups that do not share a similar letter are considered statistically different for p < 0.05.

DISCUSSION

Here we show that pharmacological inhibition of MGL using a novel reversible inhibitor does not produce dose-dependent effects on food intake or the development of diet-induced obesity. Body weight and body composition were not altered by increasing concentrations of this inhibitor, nor was the length of administration a factor.

We confirmed a dose-dependent presence of the MGL inhibitor in the bloodstream of mice 1.5 h after administration. This indicates that the compound was in circulation for, at least, the early part of the dark cycle, when mice are most active and feeding. At 7 h, inhibitor levels were greatly reduced in all dosage groups. The absence of inhibitor in the bloodstream did not allow us to conclusively understand the fate of the compound, i.e. whether it is metabolized and excreted in the 7 h after administration, or simply distributed throughout bodily tissues. However, due to the hydrophobic nature of the compound and the slight increase its blood levels at 1.5 h in the 30 mpk treated LF-fed mice compared to obese HF-fed mice, it is possible that the MGL inhibitor partitions towards fat mass and may remain pharmacologically active for an unknown period of time. On the other hand, incorporation of the inhibitor into lipid droplets within adipocytes may also result in an inability for the inhibitor to access intracellular MGL, effectively rendering it inactive.

The lack of dose-dependent changes in acylethanolamide in the small intestine, brain, and liver is in accordance with published studies of other MGL inhibitors. The most widely used MGL inhibitor JZL184 does not alter acylethanolamide species in murine brain (110, 111). In another study, acute JZL184 administration did not change 2-AG or AEA levels in the ileum of mice (221). Nor does genetic MGL ablation significantly affect acylethanolamide levels, as shown in the previous study (Aim 2) and in work by others (102, 103).

We did not observe any significant differences in MG levels in the small intestine, brain, or livers of inhibitor treated mice taken at 16 h after final compound administration. This is in accordance with the relatively short half-life ($t_{1/2}$ = 3.6 h) of the compound that we observed. While these results do not allow us to directly assess the *in vivo* efficacy of the compound following administration, we can conclude that any, if at all, effects of MGL inhibition on elevating tissue MG levels were transient and were not present after 16 h. Therefore, future studies should assess the MG concentration at more immediate time points following administration of the inhibitor. Additionally, the route of administration (orogastric gavage) and the delivery vehicle may be adjusted to determine optimal absorption of the drug and prolong its bioactivity. Finally, generation of a reversible inhibitor with improved pharmacokinetic properties should be considered.

We used Rimonabant as a positive control for EC-mediated food intake reductions in the chronic study. Rimonabant (SR141716A) was the first discovered selective and potent orally active antagonist for brain CB1 receptors (222). In our results, mice treated with 10 mg/kg body weight Rimonabant had reductions in body weight and fat percentage, as well as sharply decreased food intake during the first 4 days of administration. This is similar to other studies that show that the antagonism of CB1 receptors by chronic Rimonabant causes transient reductions in food intake, yet sustained weight loss, and lower body fat (205, 207). While it has been demonstrated to decrease body weight and ameliorate aspects of metabolic syndrome in obese humans (159), Rimonabant is no longer being developed as a anti-obesity drug due to increased adverse psychiatric events in clinical trials (223).

Perhaps the most interesting result from our study is that neither acute nor chronic MGL inhibition affected food intake. We had predicted that acute increases in brain 2-AG levels by MGL inhibition would produce an orexigenic effect mediated by the CB1 activation.

Unpublished results using the JNJ-MGLi inhibitor have shown antihyperalgesic effects in rats with a blood EC_{50} = 2.9 uM. We observed levels in blood compound above that threshold (3.1 uM for 10 mg/kg, 7.2 and 8.7 uM for 30 mg/kg) at 1.5 h post-administration, suggesting that the other behavioral effects of CB1 activation such as hyperphagia should also be present. Moreover, it has already been demonstrated that infusion of 2-AG into the nucleus accumbens of rats directly before the dark cycle stimulates hyperphagia, which can be blocked by Rimonabant (134). This is also supported by the single dose studies of diacylglycerol lipase (DAGL) inhibition in mice, which results in decreased 2-AG biosynthesis and subsequently inhibits intake of HFD and reduces body mass (224). However, we did not observe either orexigenic or anorectic changes in our inhibitor-treated mice. Reasons for this are unclear, but there may be several contributing factors. It is possible that the level of MGL inhibition insufficiently induced 2-AG concentrations in the brain or elsewhere to produce effects on appetite. It is also possible that effects on food intake were subtle, and masked by the generally decreased food intake as a result of oral gavage. Repeated daily oral gavage over 30 days has been shown in other studies to decrease food intake and body weight in mice, even when only vehicle is administered (207).

In summary, we demonstrate here that daily pharmacological inhibition of MGL in mice up to 27 days with a novel short-term reversible inhibitor does not produce significant effects on food intake, body weight, or aspects of obesity. Nevertheless, evidence from other studies demonstrates that the extent and duration of MGL inhibition are critical variables that determine any physiological and behavioral effects. Thus, from these results, we cannot yet conclude whether MGL inhibition is a valid pharmacological target for the treatment of obesity and metabolic syndrome.

Chapter 5.

General Conclusions and Future Directions

Tissue accumulation of TG in obesity

The storage of excess calories as fat is a basic biological function. Millions of years of adaption have honed systems of energy efficiency in living organisms. These systems maximize the absorption of calories when they are plentiful, and store energy to overcome periods when external sources are limited. And so it seems rather tragic that, in our current age when the global food supply is at an all-time peak of stability and production, one of humankind's major health challenges is coping with the outgrowths of caloric abundance: obesity and the metabolic syndrome. Moreover, it appears that the ways in which obesity affects human physiology is more complicated and possibly more harmful than we currently know.

In some instances, ectopic TG deposition of has been likened to an overflowing cup. High circulating levels of dietary fat and sugar exceed the capacity of adipocytes to store as TG, and so it "spills over" into peripheral tissues such as muscle and the liver. However, this description is somewhat incomplete. Fat cells have an incredible ability to expand and store TG, and new adipocytes can be created from progenitor cells as needed (225, 226). Yet in a metabolic disease state, when the hypertrophy of adipocytes is rapid and there is persistent hyperlipidemia accompanied by systemic inflammation and insulin resistance, other tissues upregulate pathways to stimulate lipid synthesis, as well as reduce lipolysis and oxidation, resulting in ectopic fat accumulation (163). Perhaps a good accompanying analogy would be "keeping up with the Joneses", in which other tissues with TG storing capacity become more adipose-like under obese conditions, often to their own detriment.

We have studied TG accumulation in the intestine under conditions of both high fat feeding and obesity. Our results showed that, like muscle and liver, the intestinal mucosa in obese conditions has significant neutral lipid accumulation. A pertinent question is whether it is

"bad" that the intestine stores excess TG. In other words, do a fatty diet and/or obesity cause

intestinal dysfunction or merely aberrations? Evidence from other cell types suggests that TG

accumulation is a signifier of tissue dysfunction and may progress to more serious disease

states. Ectopic fat deposition in myocardium, vasculature, and the kidney due to high fat diets

may all contribute to cardiovascular disease (227). Initially, intracellular TG may act as a sink to

limit FA toxicity, but increasing neutral lipid accumulation and insulin resistance, coupled with

enhanced oxidation, can all lead to increased risk for thrombosis and cardiac dysfunction.

Accordingly, mice with global ATGL ablation accumulate TG in the heart, resulting in cardiac

myopathy and early death (58). The hepatic TG accumulation that occurs in fatty liver disease is

associated with cirrhosis and liver cancers in humans (178, 179). Thus, is it possible that

sustained intestinal TG accumulation is also pathophysiological.

Secretion of chylomicron particles is an important determinant of intestinal TG levels in

the postprandial state, which our research and others support. What then regulates this balance

between TG storage and export within enterocytes? Signaling through insulin is one potential

mode, supported by studies demonstrating jejunal steatosis in diabetic humans and rodents

(182, 184). PPARα may be another candidate, as binding by ligands such as LCFA and OEA

induces changes in the expression of target genes involved in lipid absorption and metabolism in

intestinal mucosa (228, 229). Interestingly, PPARα was also found to be downregulated in the

steatotic mucosa of iATGL-deficient mice (59).

Downstream of signaling, the expression and activities of enzymes involved in TG

synthesis and degradation are also likely involved in maintaining that storage-export balance.

The DGAT enzymes in particular are poised to drive TG towards storage or secretion. Evidence

from over-expressing and knockout mouse models supports a distinct role for intestinal DGAT1

in TG synthesis for chylomicron incorporation, while DGAT2-synthesized TG may be shunted

towards intracellular lipid droplets (46, 47, 230). Additionally, lipolytic enzymes that mobilize

enterocyte TG pools may also be subject to the same regulatory processes that control lipolysis

in adipocytes. We observed significantly blunted intestinal TG secretion in mice lacking MGL.

Considering these results with prior evidence that MGL activity in the mucosa may be subject to

post-transcriptional regulation (64), it appears that the regulation of lipid metabolism in the

intestinal epithelium is complex and the mechanisms have certainly not been fully elucidated.

Our findings demonstrate that as little as 3 weeks of high fat feeding is sufficient to

induce impaired postprandial TG secretion, which also occurs under obese conditions, impacting

intracellular lipid content. From this, it is apparent that consumption of a high fat diet and

obesity lead to changes in the components and regulation of the TG absorption system that

warrant further investigation. Future experiments might include examining insulin signal

transduction and its downstream pathways in relationship to lipid metabolism in the

enterocytes of diet-induced obese (DIO) mice. Additionally, enterocyte fatty acid oxidation,

which has been shown to impact mucosal TG storage pools (228), should also be assessed in

states of high fat feeding and obesity, both under fed and fasted conditions. Further analyzing

the assembly and secretion of chylomicron particles within "obese" enterocytes may be

informative, particularly the trafficking of CM from the ER to the Golgi apparatus, which is

considered the rate-limiting step in CM formation (231). Lastly, subjecting high fat fed and obese

mice to an oral fat challenge, and investigating the apolipoprotein and lipid composition of their

circulating chylomicron particles may also yield insight into the defective TG secretion we

observed.

Intestinal lipid metabolism and whole body energy homeostasis

There is increasing evidence that that the lipids in the small intestine have profound and global effects on whole body energy homeostasis in many different ways. First, dietary lipids themselves are "sensed" by enteroendocrine cells and influence whole body metabolism. This is demonstrated by the binding of GPR119 receptors on intestinal L-cells by 2-oleoylglycerol (2-OG), a major product of dietary lipid digestion, effecting the release of glucagon-like peptide 1 (GLP-1) and ultimately pancreatic insulin secretion (217, 218, 232). While mostly unexplored, MG hydrolyzing enzymes such as MGL are uniquely poised to regulate epithelial levels of 2-OG, and thus impact insulin release and its downstream effects. In fact, this may, in part, underlie the obese phenotype observed in the iMGL mice (65).

Other intestinal proteins that bind lipids or catalyze their metabolism have global effects on body weight and fat depots. Mice lacking IFABP or LFABP have distinctly different alterations in intestinal lipid metabolism (28), which correspond to divergent whole body lean or obese phenotypes, respectively (233). Deficiency of MGAT2, another important enzyme in mucosal lipid absorption, does not quantitatively alter dietary fat uptake. Yet lipid absorption rates are decreased in MGAT2-/- mice and thermogenesis is upregulated in BAT, resulting in increased energy expenditure and resistance to diet-induced obesity (41, 212). Re-introduction of intestinal MGAT2 expression in global MGAT2-/- mice (MGAT2IntONLY) restores the defect in the fat absorption rate and partially restores the energy phenotype, resulting in susceptibility to high fat diet-induced weight gain (234). Similarly to MGAT2, mice null for DGAT1 have a normal capacity for lipid uptake and chylomicron secretion, but accumulate pools of neutral lipids in the cytoplasm of their enterocytes, have increased energy expenditure, and are resistant to diet-induced obesity (47, 48). Mice null for DGAT1 in all its expressed tissues but intestine (DGAT1IntONLY) have normalized intestinal TG secretion and are susceptible to high fat diet-induced obesity and the development of hepatosteatosis (235).

Overall, the evidence suggests that even modestly altering intestinal lipid metabolism and secretion, without affecting overall bulk uptake, can result in global changes that affect energy homeostasis. Consequently, it is possible that a new generation of therapeutic methods for treating obesity may come from pharmacological compounds that target intestinal proteins involved in lipid trafficking or metabolism. Pharmacological inhibitors of MGL, MGAT2, DGAT1, and IFABP, may prove to be particularly beneficial towards treating metabolic disorders such as obesity, type 2 diabetes, and dyslipidemia.

Role of MGL in energy homeostasis

Is the catabolism of MG throughout the body linked to energy homeostasis? We present evidence that loss of MGL activity does indeed affect aspects of energy balance, although the specific pathways involved are not yet fully determined. The results suggest that reducing MGL hydrolysis is beneficial towards treating obesity. Certainly, the studies using MGL specific inhibitors do not indicate any adverse metabolic effects. And there is currently no evidence that knockout or inhibition of MGL produces cannabimimetic effects and drives the development of obesity and insulin resistance.

The loss of MGL profoundly impacts MG levels in many different bodily tissues. Given the diversity of MG fates and ways in which energy homeostasis may be affected – signaling through multiple G-protein coupled receptors, precursors for DG and TG synthesis, catabolism to yield fatty acids for substrates in oxidation, prostaglandin synthesis, and more – future research into MG metabolism may explore more tissue-specific functions and even particular MG isomeric forms. We focused on *sn*-2-MG species in our experiments, yet MGL also efficiently hydrolyzes *sn*-1-MG. Some saturated long chain 1-MG species, such as 1-stearoylglycerol (C18:0

MG) and 1-palmitoylglycerol (C16:0 MG), have been shown to potentiate glucose-stimulated insulin release in pancreatic β-cells (81). Whether MGL plays a role in regulating these particular 1-MGs and influencing pancreatic function is unknown.

The mechanism by which intestinal MGL activity influences energy balance is still unclear. We have found evidence for dysregulation of appetite signaling in the iMGL mice, and also changes in energy expenditure (65), suggesting that a broad homeostatic system may be involved. While there is currently no method for pharmacologically inhibiting MGL in the intestine only, the generation and investigation of an intestine-specific MGL knockout mouse may yield more valuable information. Based on the iMGL phenotype, it may be predicted that these mice would be lean and resistant to diet-induced obesity, as well as have the reduced intestinal TG secretion seen in the MGL-/- mice.

The short and long-term effects of global MGL inhibition on eating behaviors and energy homeostasis are also unresolved. Although we observed no effects of reversible MGL inhibition on food intake or adiposity, future studies may investigate this further. Different levels of MGL inhibition over time should be an integral component of future studies, considering evidence that the extent and duration of which MG are elevated is a large factor in determining EC-mediated effects (112). In particular, experiments should be performed utilizing established MGL inhibitors, such as the irreversible inhibitor JZL184, at varying concentrations and time courses of dosing, in conjunction with real-time food intake monitoring. Intraperitoneal administration of an MGL inhibitor may also allow for easier determination of effects on food intake, without interference from the gastric distension and handling stress from orogastric gavage.

The pharmacological blockade of MGL may prove to be useful in treating the systemic inflammation associated with obesity. Inhibiting MGL improves the outcome of other diseases

with an inflammatory component, such as Alzheimer's disease (113). The coupling of

inflammatory pathways through the catabolism of 2-AG by MGL is an important new concept in

the function of this enzyme (109). In future studies, treating mice with MGL inhibitors may

ameliorate the negative effects of DIO through decreasing arachidonic acid precursor pools for

pro-inflammatory eicosanoid synthesis, as well as enhanced anti-inflammatory signaling through

CB2 activation on immune cells. Thus, independent of any potential effects on fat mass or food

intake, MGL inhibitor therapy may beneficial towards a range of inflammation-linked metabolic

disease, including CVD and type 2 diabetes.

In conclusion, we have identified novel changes in tissue lipid metabolism that are related to the

intake of high fat diets and the developments of obesity. Further, we have investigated the role

of MGL in energy homeostasis and the development of obesity. Results from these studies will

be useful for understanding the physiology of obesity, and will also aid in the direction and

design of future experiments to explore new aspects of lipid metabolism and the many ways it

affects human health.

Appendix

Metabolism of apically and basolaterally delivered fatty acids in the intestinal mucosa of acyl coA synthetase 5-deficient mice

Collaboration with the laboratory of Andrew Greenberg, Jean Mayer USDA Human Nutrition Research Center, Tufts University, Boston, MA

ABSTRACT

Small intestinal mucosal cells have been shown to have distinct intracellular metabolic partitioning of fatty acids depending on their uptake through the apical or basolateral membranes. The mechanisms for this intestinal polarity are entirely unknown. A potential determinant in the fate of intestinal fatty acids may be the action of the acyl coA synthetase enzymes, which catalyze the energy-dependent condensation of fatty acids and coenzyme A to form a fatty acyl CoA. This is an essential step in the activation of fatty acids for a variety of anabolic and metabolic purposes. We tested the hypothesis that acyl coA synthetase 5 (ACSL5), which is highly expressed in the small intestine, plays a role in the partitioning of fatty acids towards specific metabolic fates in small intestinal mucosa. Female wild type (WT) and ACSL5-/- mice were given simultaneous injections of radiolabeled oleic acid (C18:1) both intraduodenally ([3H]-18:1) and intravenously ([14C]-18:1), mucosa was isolated after 2 minutes, and lipid metabolism was assessed. There were decreases in labeled fatty acid incorporation in triacylglycerols, and increased incorporation into phospholipids for both apically and basolaterally derived fatty acids, resulting in a decreased triacylglycerol/phospholipid ratio for ACSL5-/- mice. We also determined the extent of oxidation of basolaterally administered [14C]oleic acid, and found that the ACSL5-/- mice had reduced oxidation relative to WT. These results indicate that ACSL5 may be responsible, in part, for directing fatty acids taken up into the enterocyte towards specific metabolic pathways.

BACKGROUND

The acyl-coA synthetase (ACS) enzymes catalyze the ATP-dependent conversion of long chain fatty acids (FA) and coenzyme A into fatty acyl CoAs (Fa-CoAs). This is an obligatory first step for the metabolism of both intracellularly and extracellularly derived FA. Fa-CoAs are used within cells for a variety of reactions, including incorporation into diacylglycerol (DG), triacylglycerol (TG), phospholipids (PL), cholesterol esters (CE), or oxidation inside mitochondria and peroxisomes. There are 5 known isoforms of the major group of ACS proteins that activate long chain FA, known as ACSL1-5, each having distinct substrate preferences and subcellular localizations, suggesting different functions (31). Only ACSL5, and to a lesser extent ACSL3, are significantly expressed in the small intestine (31), indicating that that they likely participate in the uptake and metabolism of intestinal lipids.

The ACSL proteins have been proposed to activate and target FA towards specific metabolic purposes (236). Reduction of ACSL3 activity in hepatocytes resulted in decreased *de novo* FA synthesis through a mechanism likely involving the Fa-CoA activation of transcription factors (237). Hepatic ACSL5 knockdown reduced FA incorporation into TG, CE, and PL, and decreased hepatic TG secretion (238). Similarly, over-expression of ACSL5 in rat hepatoma cells increased FA synthesis into TG by 42% in both re-esterification and *de novo* pathways (239). These studies suggest that ACSL5 is involved in channeling FA towards anabolic pathways in the liver.

It is well established that FA can be taken up from both the apical and basolateral membranes of enterocytes. Early studies in rodents and humans demonstrated that radiolabeled oleate administered intraduodenally is primarily esterified to TG, while that administered intravenously is mostly oxidized (42%) and used for PL synthesis (28%) (240, 241).

This "metabolic compartmentation" of different lipid pools within enterocytes was later shown in Caco-2 cells, demonstrating that apical delivery of FA, and also MG, resulted in a higher incorporation TG than PL (18, 20). *In vivo* studies in rats and mice again demonstrated that FA and MG are metabolized differently depending on their uptake from the apical or basolateral sides of the mucosa (63). In general, apically absorbed fatty acids appear to be targeted towards TG synthesis, while systemically absorbed FA are shunted towards oxidation and PL synthesis. Since activation of FA is necessary for subsequent anabolic or catabolic metabolism, It is possible that ACSL5 activity is contributing to this intestinal polarity.

In the current study, we tested the hypothesis that intestinal ACSL5 participates in directing FA towards specific metabolic pathways by administering radiolabeled FA to the apical (3H-18:1) or basolateral (14C-18:1) membranes of control and ACSL5 deficient mice. We found reduced TG and increased PL incorporation in the mucosa of ACSL5-/- mice, regardless of the site of FA entry. Further, we measured oxidation of basolaterally delivered FA and found reduced oxidation in ACSL5 null mouse mucosa relative to WT. These findings implicate ACSL5 in the partitioning of FA towards specific metabolic fates in the small intestine.

MATERIALS AND METHODS

Animal Model

Mice null for ACSL5 (whole body knockout) were generated at Tufts University using a lox P insertion into the ACSL5 gene. The DNA genomic construct was inserted into C57BL6/J embryonic stem cells and injected into C57BL6/J mice. Homozygous ACSL5$^{loxP/loxP}$ mice were mated with hemizygous Cre-expressing C57BL6/J mice to generate the ACSL5$^{-/-}$ mice, which have

a premature stop codon in exon 20 of the ACSL5 gene. Loss of gene expression and protein was confirmed by RT-PCR and Western blot analysis.

Female 188 day old ACSL5$^{loxP/loxP}$ (WT) and ACSL5$^{-/-}$ mice were received from Andrew Greenberg at Tufts University and group housed upon arrival. All mice received *ad libitum* access to water and Teklad Global Protein Rodent Diet (22% protein (kcal), 12% fat, 66% carbohydrate; 2016S, Harlan Laboratories Inc., Madison, WI). Mice were acclimated to the new facility for 7 days prior to any experiments. All animal procedures were approved by the Rutgers University Animal Use Protocol Review Committee and conformed to the National Institutes of Health *Guide for the Care and Use of Laboratory Animals*.

Mucosal FA Metabolism

Simultaneous administration of intraduodenal and intravenous dual-labeled fatty acid administration was performed as previously described (28, 233). In short, lipids were prepared for bloodstream and intraduodenal administration as followed: For intravenous FA administration, 15 µCi [14C] oleate (275 nmols) was dried under a nitrogen stream and then 0.5% ethanol (final volume) and 150 µl of a solution containing 0.1M NaCl and mouse serum (1:1) were added sequentially. For duodenal FA administration, 1.5 µCi [3H] oleate (34 nmols) was dried under a nitrogen stream and then 150 of 10mM sodium taurocholate in 0.1M NaCl was added.

Mice were fasted 16 h prior to experiment. Mice were then deeply anaesthetized, and given a intraduodenal injection of 28 nmol [3H]oleic acid (18:1) and a intravenous injection of 300 nmol 1-[14C]oleic acid into the jugular vein. Two minutes following lipid injection, mice were sacrificed by exsanguination and the small intestine was excised. Mucosal samples were collected by scraping, the homogenized in 1X PBS pH 7.4 and protein concentration determined

by Bradford assay (174). Mucosal lipids were extracted according the Folch method (175). Lipids were separated by thin layer chromatography, and incorporation of FA into mucosal lipid metabolites was determined by phosphorimaging for [14C]-labeled oleate or scraping and scintillation counting for [3H]-labeled oleate.

Fatty acid oxidation

Fatty acid oxidation measurements on mucosa from mice administered [14C]-oleate (basolateral administration) were carried out according to the method of Ontko and Jackson (242) as described previously (28, 233). In brief, 1 ml of 1 mg/ml (cellular protein concentration) homogenate from intestinal mucosa was put in a 15 ml tube. A 500 ul microcentrifuge tube with 400 ul of ethanolamine (Sigma E0135) was suspended over the upper portion of the 15 ml tube, and 400 ul of 7% perchloric acid was added to the homogenate then the tube immediately sealed. After 24 h incubation with shaking at $37^{\circ}C$, the contents were centrifuged, and the supernatant holding the acid soluble lipid metabolites and ethanolamine containing $^{14}CO_2$ were subjected to scintillation counting. Total FA oxidation was calculated as the sum of the $^{14}CO_2$ and ^{14}C-acid soluble metabolites.

Statistical Analyses

Group data were expressed as average ± s.e.m. Statistical differences between genotypes were calculated two-sided *Student's* t-test and $p < 0.05$ considered significant.

RESULTS

Tissue parameters on day of dual labeling experiment

Female mice null for ACSL5 had trends for lower body weight and gonadal fat pad weight (Fig 1A-B). The liver weight of ASCL5-/- mice was significantly lower (p < 0.01) than their WT counterparts (Fig 1C). There were no differences in length of the small intestine after (Fig 1D).

Metabolism of FA in intestinal mucosa

To test whether intestinal ACSL5 is responsible for determining the metabolic fate of absorbed FA, we assessed the incorporation of radiolabeled FA into acylated lipid species in the intestinal mucosa. For fatty acids delivered across the apical membrane of enterocytes, there was a trend for decreased FA incorporation into TG, increased incorporation into PL and increased labeled FA levels in the ACSL5 mice relative to WT, however results did not reach statistical significance (Fig 2A). Similarly, basolaterally delivered FA had trends for decreased incorporation into TG and increased PL incorporation (Fig 2B). Accordingly, the TG/PL ratio, an indication of partitioning towards specific lipid species, for both apically and basolaterally absorbed FA was decreased (p = 0.02 for AP, p = 0.18 for BL) in the ACSL5-/- mice (Fig 2C).

Oxidation of basolateral incorporated FA in intestinal mucosa

Previous studies have indicated that FA taken up via the basolateral membrane in enterocytes are predominantly used for oxidation and PL synthesis (63). We measured the catabolism of basolaterally administered enterocytic FA, finding less radioactivity (p = 0.19) in the acid-soluble metabolites and CO_2 in the mucosa of ACSL5-/- mice (Fig 2D). This result

suggests that less basolaterally absorbed FA in ACL5-/- mice is oxidized in the intestinal mucosa.

The oxidation of apically administered FA was also decreased in ACSL5-/- mice relative to WT,

however, the sample size (n = 2) was insufficient for a reliable assessment (data not shown).

Figure 1
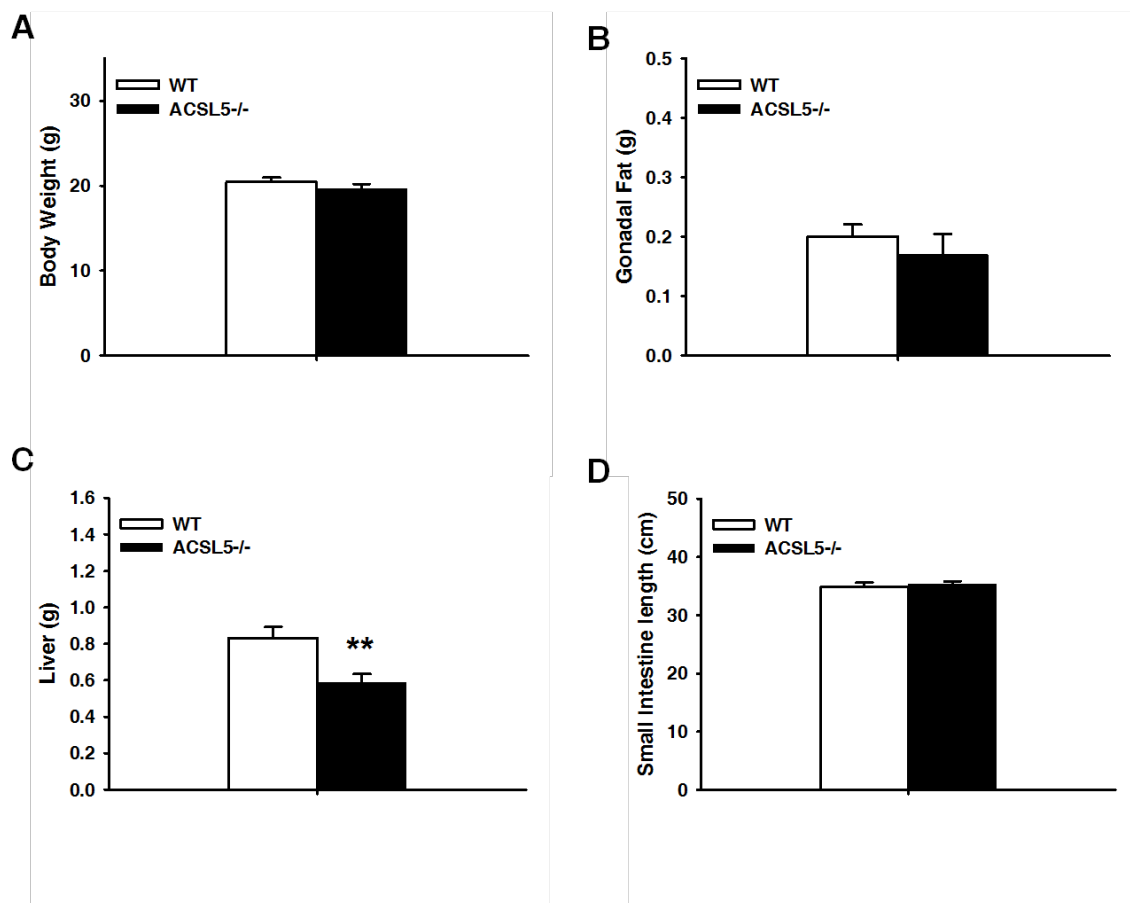
Figure 1. Tissue parameters of female WT and ACSL5-/- mice taken after immediately after the dual-labeling lipid experiments. (A) Body weight (B) Gonadal fat pad weight (C) Liver weight (D) Length of small intestine. Data are expressed as average ± SEM (n = 10), ** p < 0.01.

Figure 2
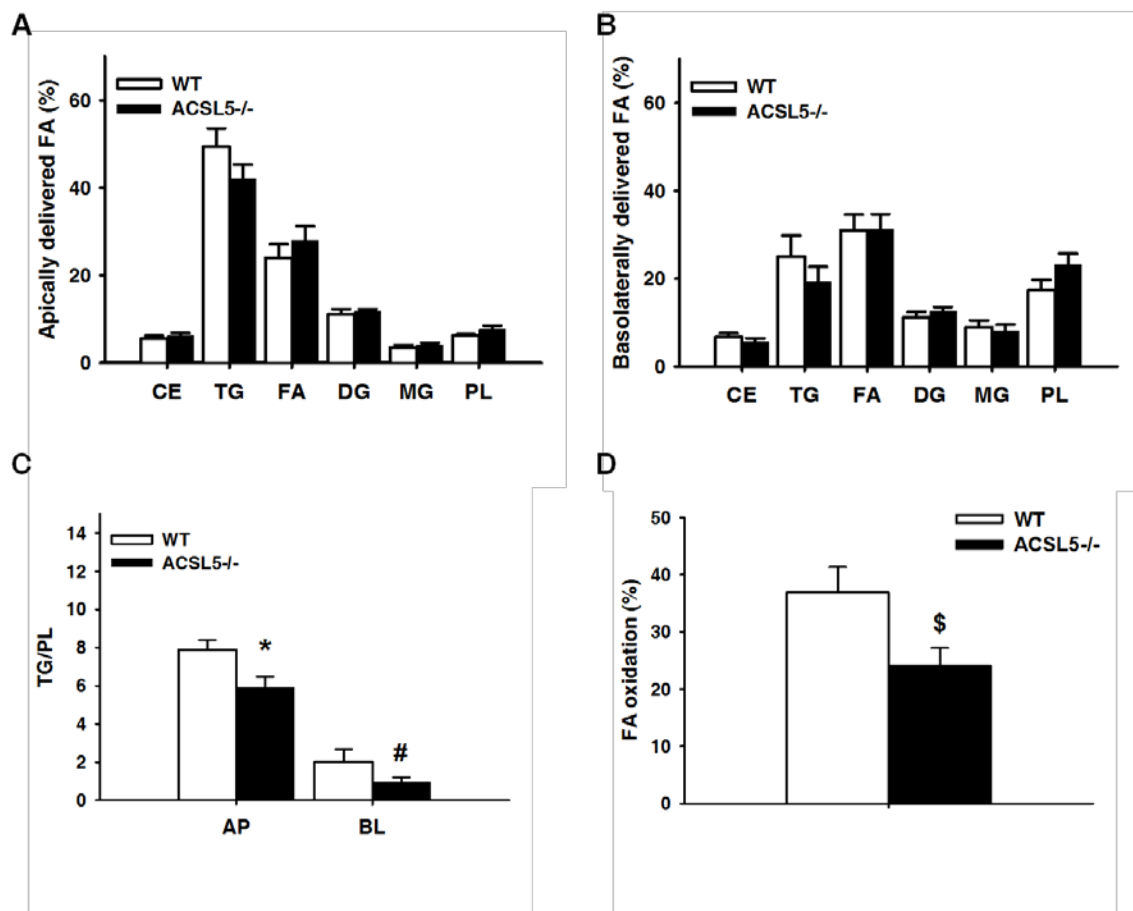
Figure 2. Metabolism of radiolabeled FA two minutes after administration in the small intestine mucosa of WT and ACSL5 mice. (A) Percentage of intraduodenally (apically, AP) delivered [3H]oleate incorporation into lipid species (B) Percentage of intravenously (basolaterally, BL) delivered [14C]oleate (C) TG/PL ratio of both apically and basolaterally absorbed FA (D) Percentage of basolaterally added [14C]oleate converted to CO_2 and acid-soluble metabolites. Data are expressed as average ± SEM (n = 10), * p < 0.05, # p = 0.18, $ p = 0.19.

DISCUSSION

The ability of ACSL5-/- mice to anabolize and catabolize FA in mucosa indicates that other intestinal enzymes having significant ACS activity are present. This was corroborated in a recent published study of ACSL5-/- mice, who displayed a 60% reduction in jejunal FA-CoA synthesis, yet had unchanged dietary fat absorption (243). Two potential candidates for maintaining the residual ACS activity in the small intestine are fatty acid transport protein 4 (FATP4) and ACSL3. FATP proteins share sequence homology with ASCL proteins, although they may have *in vivo* specificity towards very long chain FA (carbon chains longer than 22) as substrates for ACS reactions (236). Additionally, FATP4 is highly expressed on the apical side of enterocytes and is also considered an intracellular FA transporter (26). ACSL3 has also been shown to be expressed in the small intestine, albeit to a much lesser extent than ACSL5 (31). The role of ACSL3 in intestine has not been explored to our knowledge, but it is also expressed in liver and has been shown to generate Fa-CoA species that bind multiple transcription factors, including PPARγ and SREBP1c , involved in lipid metabolism to influence hepatic *de novo* lipogenesis (237).

While there were overall differences of FA metabolism, the loss of ACSL5 resulted in similar changes regardless of apical or basolateral delivery. This could mean that other yet undetermined proteins or pathways are responsible for the metabolic compartmentation observed in enterocytes. Fatty acid binding proteins (FABP) have been implicated in metabolic polarity, and a recent study of mice lacking the intestinal proteins LFABP and IFABP show different responses between genotypes between apically absorbed FA and the TG/PL ratio (233).

In summary, here we show that loss of ACSL5 in mice results in decreased FA incorporation into TG relative to PL in intestinal mucosa; similar alterations were found for the

metabolism of both apical and basolaterally derived FA. The ACSL5-/- mice also displayed

reduced oxidation of basolaterally absorbed FA. On the whole, our results indicate that ACSL5

may be participating in the partitioning of intestinal FA towards TG synthesis and away from PL

synthesis. Further research into the aspects of intestinal lipid metabolism in the absence of

ACSL5 will undoubtedly better determine the *in vivo* role of this protein. Future studies should

include a similar analyses of intestinal lipid metabolism using ACSL5-/- and WT mice fed a high

fat diet, as well as investigating the potential compensatory upregulation of other ACS enzymes

such as FATP4 and ACSL3.

Acknowledgement of Collaborative Efforts and Previous Publications

Scientific research is often jointly performed according to the knowledge and skills of many researchers. This dissertation contains studies that have been the collaborative efforts of multiple parties. The results of some of these studies have also been previously published. All other sources for reference and background information have been cited (as numbers) in the text and can be found accordingly in the bibliography. The author (John Douglass) is the sole writer of all dissertation sections.

Co-authors and collaborations

Chapters 3 and 4, regarding the monoacylglycerol lipase knockout and pharmacological inhibition of MGL, are joint collaborations between Janssen Research and Development, LLC (Spring House, PA), and Rutgers University (New Brunswick, NJ). The laboratory research work for these studies was conducted primarily by John Douglass. Contributions at Rutgers University were also made by Yin Xiu Zhou (technician), Amy Wu and Janek (John) Zadroga (undergraduate researchers), and Judith Storch (primary advisor). At Janssen, Kristen M. Chevalier, Steven Sutton, Sui-Po Zhang, and Christopher M Flores assisted in the development and characterization of the MGL-/- mouse line, with technical assistance from Sandy Wilson. Margery Connelly, formerly of Janssen (currently at LipoScience, Raleigh, NC) contributed to the design and development of these studies. All LC/MS lipid and pharmacological compound analyses for Chapter 3 and 4 were performed by Wensheng Lang at Janssen. The MGL inhibitor (JNJ-MGLi) and Rimonabant were generously provided under legal agreement from Janssen. For Chapter 3, the MGL-/- and wild type mice, as well as diagnostic reagents for measuring plasma lipids and peptides, were also generously provided by Janssen.

The study described in the Appendix chapter is part of a collaborative effort with the laboratory of Andrew Greenberg at the Tufts University School of Medicine. The mice used in the study were generated and sent by the Comparative Biology Unit at Tufts University under the direction of Andrew Greenberg, and with help from Kayleigh O'Keefe and Donald Smith. The experiments detailed were performed entirely at Rutgers University by John Douglass, with help from Yin Xiu Zhou and Judith Storch.

Previously published work

Chon, S.H., Douglass, J.D., Zhou, Y.X., Malik, N., Dixon, J.L., Brinker, A., Quadro, L., and Storch, J. Over-expression of monoacylglycerol lipase (iMGL) in small intestine alters endocannabinoid levels and whole body energy balance, resulting in obesity. <u>PLoS ONE</u>. 7(8):e43962 (2012)

All work referring to the over-expression of intestinal MGL was conducted primarily by Su-Hyoun Chon and published in the journal PLoS ONE in 2012. Su-Hyoun Chon was also the primary author of the publication. Co-authors who also contributed to this publication are: John Douglass, Yin Xiu Zhou, Nashmia Malik , Joseph L. Dixon, Anita Brinker Loredana Quadro, and Judith Storch. Reprinting of figures and content from this article is permitted under the Creative Commons Attributions license.

Douglass, J.D., Malik, N., Chon, S.H., Wells, K., Zhou, Y.X., Choi, A.S., Joseph, L.B., and Storch, J. Intestinal mucosal triacylglycerol accumulation secondary to decreased lipid secretion in obese and high fat fed mice. <u>Frontiers in Physiology</u>. 3:25 (2012)

The entire chapter 2 was published in 2012 in the journal Frontiers In Physiology. The scientific research and writing were performed primarily by John Douglass, with contributions from Su-Hyoun Chon (graduate student), Nashmia Malik, Kevin Wells, , Andrew Choi (undergraduate

students), Yin Xiu Zhou (technician), Laurie B. Joseph (collaborator for histology), and Judith

Storch. Reprinting of this article for the dissertation is permitted by the author (John Douglass),

who maintains ownership of the article content, and as allowed by the open access journal

Frontiers in Physiology.

Literature Cited

1.	Badman MK, Flier JS. The gut and energy balance: visceral allies in the obesity wars. *Science (80-)* 2005;307:1909–1914.

2.	Radtke F, Clevers H. Self-renewal and cancer of the gut: two sides of a coin. *Science (80-)* 2005;307:1904–1909.

3.	Guarner F, Malagelada JR. Gut flora in health and disease. *Lancet* 2003;361:512–519.

4.	Stipanuk MH. *Biochemical, Physiological & Molecular Aspects of Human Nutrition*. 2nd ed. W.B. Saunder Co.; 2006.

5.	Creamer B, Shorter RG, Bamforth J. The turnover and shedding of epithelial cells. I. The turnover in the gastro-intestinal tract. *Gut* 1961;2:110–118.

6.	Claude P, Goodenough DA. Fracture faces of zonulae occludentes from "tight" and "leaky" epithelia. *J Cell Biol* 1973;58:390–400.

7.	Phan CT, Tso P. Intestinal lipid absorption and transport. *Front Biosci a J virtual Libr* 2001;6:D299–D319.

8.	Tso P, Balint JA, Bishop MB, Rodgers JB. Acute inhibition of intestinal lipid transport by Pluronic L-81 in the rat. *Am J Physiol* 1981;241:G487–G497.

9.	Carrière F, Rogalska E, Cudrey C, Ferrato F, Laugier R, Verger R. In vivo and in vitro studies on the stereoselective hydrolysis of tri- and diglycerides by gastric and pancreatic lipases. *Bioorg Med Chem* 1997;5:429–435.

10.	Carrière F, Renou C, Ransac S, Lopez V, De Caro J, Ferrato F, De Caro A, Fleury A, Sanwald-Ducray P, Lengsfeld H, Beglinger C, Hadvary P, Verger R, Laugier R. Inhibition of gastrointestinal lipolysis by Orlistat during digestion of test meals in healthy volunteers. *Am J Physiol Gastrointest liver Physiol* 2001;281:G16–G28.

11.	Rogalska E, Ransac S, Verger R. Stereoselectivity of lipases. II. Stereoselective hydrolysis of triglycerides by gastric and pancreatic lipases. *J Biol Chem* 1990;265:20271–6.

12.	Niot I, Poirier H, Tran TTT, Besnard P. Intestinal absorption of long-chain fatty acids: Evidence and uncertainties. *Prog Lipid Res* 2009;48:101–115.

13.	Mansbach CM, Gorelick F. Development and physiological regulation of intestinal lipid absorption. II. Dietary lipid absorption, complex lipid synthesis, and the intracellular packaging and secretion of chylomicrons. *Am J Physiol Gastrointest liver Physiol* 2007;293:G645–G650.

14.	Milger K, Herrmann T, Becker C, Gotthardt D, Zickwolf J, Ehehalt R, Watkins PA, Stremmel W, Füllekrug J. Cellular uptake of fatty acids driven by the ER-localized acyl-CoA synthetase FATP4. *J Cell Sci* 2006;119:4678–4688.

15. Sallee VL, Dietschy JM. Determinants of intestinal mucosal uptake of short- and medium-chain fatty acids and alcohols. *J Lipid Res* 1973;14:475–84.

16. Murota K, Storch J. Uptake of micellar long-chain fatty acid and sn-2-monoacylglycerol into human intestinal Caco-2 cells exhibits characteristics of protein-mediated transport. *J Nutr* 2005;135:1626–1630.

17. Stremmel W. Uptake of fatty acids by jejunal mucosal cells is mediated by a fatty acid binding membrane protein. *J Clin Invest* 1988;82:2001–2010.

18. Trotter PJ, Ho SY, Storch J. Fatty acid uptake by Caco-2 human intestinal cells. *J Lipid Res* 1996;37:336–46.

19. Chaves CRM, Elias PRP, Cheng W, Zaltman C, Iglesias ACR, Braulio VB. Long chain fatty acid uptake by human intestinal mucosa in vitro: mechanisms of transport. *Digestion* 2003;67:32–36.

20. Ho SY, Storch J. Common mechanisms of monoacylglycerol and fatty acid uptake by human intestinal Caco-2 cells. *Am J Physiol Cell Physiol* 2001;281:C1106–C1117.

21. Abumrad NA, Sfeir Z, Connelly MA, Coburn C. Lipid transporters: membrane transport systems for cholesterol and fatty acids. *Curr Opin Clin Nutr Metab Care* 2000;3:255–262.

22. Stremmel W, Strohmeyer G, Borchard F, Kochwa S, Berk PD. Isolation and partial characterization of a fatty acid binding protein in rat liver plasma membranes. *Proc Natl Acad Sci U S A* 1985;82:4–8.

23. Poirier H, Degrace P, Niot I, Bernard A, Besnard P. Localization and regulation of the putative membrane fatty-acid transporter (FAT) in the small intestine. Comparison with fatty acid-binding proteins (FABP). *Fed Eur Biochem Soc J* 1996;238:368–373.

24. Nassir F, Wilson B, Han X, Gross RW, Abumrad NA. CD36 is important for fatty acid and cholesterol uptake by the proximal but not distal intestine. *J Biol Chem* 2007;282:19493–19501.

25. Drover VA, Ajmal M, Nassir F, Davidson NO, Nauli AM, Sahoo D, Tso P, Abumrad NA. CD36 deficiency impairs intestinal lipid secretion and clearance of chylomicrons from the blood. *J Clin Invest* 2005;115:1290–1297.

26. Stahl A, Hirsch DJ, Gimeno RE, Punreddy S, Ge P, Watson N, Patel S, Kotler M, Raimondi A, Tartaglia LA, Lodish HF. Identification of the major intestinal fatty acid transport protein. *Mol Cell* 1999;4:299–308.

27. Storch J. Diversity of fatty acid-binding protein structure and function: studies with fluorescent ligands. *Mol Cell Biochem* 1993;123:45–53.

28. Lagakos WS, Gajda AM, Agellon L, Binas B, Choi V, Mandap B, Russnak T, Zhou YX, Storch J. Different functions of intestinal and liver-type fatty acid-binding proteins in intestine and in whole body energy homeostasis. *Am J Physiol Gastrointest liver Physiol* 2011;300:G803–G814.

29. Thumser AE, Storch J. Liver and intestinal fatty acid-binding proteins obtain fatty acids from phospholipid membranes by different mechanisms. *J Lipid Res* 2000;41:647–656.

30. Lagakos, W.S, Storch J., Zhou Y., Mandap B. and BB. Intestinal lipid metabolism is altered in Liver Fatty Acid-Binding Protein-null mice (LFABP–/–). *FASEB J* 2007:21: lb167.

31. Mashek DG, Li LO, Coleman RA. Rat long-chain acyl-CoA synthetase mRNA, protein, and activity vary in tissue distribution and in response to diet. *J Lipid Res* 2006;47:2004–10.

32. Mansbach CM. , I, Nevin P. Intracellular movement of triacylglycerols in the intestine. *J Lipid Res* 1998;39:963–968.

33. Johnston J, Rao G, Lowe P. The separation of the α-glycerophosphate and monoglyceride pathways in the intestinal biosynthesis of triglycerides. *Biochim Biophys Acta - Lipids Lipid Metab* 1967;137:578–580.

34. Bugaut M, Myher JJ, Kuksis A, Hoffman AG. An examination of the stereochemical course of acylation of 2-monoacylglycerols by rat intestinal villus cells using [2H3]palmitic acid. *Biochim Biophys Acta* 1984;792:254–269.

35. Lockwood JF, Cao J, Burn P, Shi Y. Human intestinal monoacylglycerol acyltransferase: differential features in tissue expression and activity. *Am J Physiol - Endocrinol Metab* 2003;285:E927–E937.

36. Yen C-LE, Farese R V. MGAT2, a monoacylglycerol acyltransferase expressed in the small intestine. *J Biol Chem* 2003;278:18532–18537.

37. Cheng D, Nelson TC, Chen J, Walker SG, Wardwell-Swanson J, Meegalla R, Taub R, Billheimer JT, Ramaker M, Feder JN. Identification of acyl coenzyme A:monoacylglycerol acyltransferase 3, an intestinal specific enzyme implicated in dietary fat absorption. *J Biol Chem* 2003;278:13611–13614.

38. Cao J, Cheng L, Shi Y. Catalytic properties of MGAT3, a putative triacylgycerol synthase. *J Lipid Res* 2007;48:583–591.

39. Yen C-LE, Stone SJ, Cases S, Zhou P, Farese R V. Identification of a gene encoding MGAT1, a monoacylglycerol acyltransferase. *Proc Natl Acad Sci U S A* 2002;99:8512–8517.

40. Cao J, Lockwood J, Burn P, Shi Y. Cloning and functional characterization of a mouse intestinal acyl-CoA:monoacylglycerol acyltransferase, MGAT2. *J Biol Chem* 2003;278:13860–13866.

41. Yen C-LE, Cheong M-L, Grueter C, Zhou P, Moriwaki J, Wong JS, Hubbard B, Marmor S, Farese R V. Deficiency of the intestinal enzyme acyl CoA:monoacylglycerol acyltransferase-2 protects mice from metabolic disorders induced by high-fat feeding. *Nat Med* 2009;15:442–6.

42. Tsuchida T, Fukuda S, Aoyama H, Taniuchi N, Ishihara T, Ohashi N, Sato H, Wakimoto K, Shiotani M, Oku A. MGAT2 deficiency ameliorates high-fat diet-induced obesity and insulin resistance by inhibiting intestinal fat absorption in mice. *Lipids Health Dis* 2012;11:75.

43. Cases S, Smith SJ, Zheng Y-W, Myers HM, Lear SR, Sande E, Novak S, Collins C, Welch CB, Lusis AJ, Erickson SK, Farese R V. Identification of a gene encoding an acyl CoA:diacylglycerol acyltransferase, a key enzyme in triacylglycerol synthesis. *Proc Natl Acad Sci U S A* 1998;95:13018–13023.

44. Cases S, Stone SJ, Zhou P, Yen E, Tow B, Lardizabal KD, Voelker T, Farese R V. Cloning of DGAT2, a second mammalian diacylglycerol acyltransferase, and related family members. *J Biol Chem* 2001;276:38870–38876.

45. Yen C-LE, Monetti M, Burri BJ, Farese R V. The triacylglycerol synthesis enzyme DGAT1 also catalyzes the synthesis of diacylglycerols, waxes, and retinyl esters. *J Lipid Res* 2005;46:1502–1511.

46. Yamazaki T, Sasaki E, Kakinuma C, Yano T, Miura S, Ezaki O. Increased very low density lipoprotein secretion and gonadal fat mass in mice overexpressing liver DGAT1. *J Biol Chem* 2005;280:21506–21514.

47. Buhman KK, Smith SJ, Stone SJ, Repa JJ, Wong JS, Knapp FF, Burri BJ, Hamilton RL, Abumrad NA, Farese R V. DGAT1 is not essential for intestinal triacylglycerol absorption or chylomicron synthesis. *J Biol Chem* 2002;277:25474–25479.

48. Smith SJ, Cases S, Jensen DR, Chen HC, Sande E, Tow B, Sanan DA, Raber J, Eckel RH, Farese R V. Obesity resistance and multiple mechanisms of triglyceride synthesis in mice lacking Dgat. *Nat Genet* 2000;25:87–90.

49. Stone SJ, Myers HM, Watkins SM, Brown BE, Feingold KR, Elias PM, Farese R V. Lipopenia and skin barrier abnormalities in DGAT2-deficient mice. *J Biol Chem* 2004;279:11767–11776.

50. Owen MR, Corstorphine CC, Zammit VA. Overt and latent activities of diacylglycerol acytransferase in rat liver microsomes: possible roles in very-low-density lipoprotein triacylglycerol secretion. *Biochem J* 1997;323 (Pt 1:17–21.

51. Waterman IJ, Price NT, Zammit VA. Distinct ontogenic patterns of overt and latent DGAT activities of rat liver microsomes. *J Lipid Res* 2002;43:1555–1562.

52. McFie PJ, Banman SL, Kary S, Stone SJ. Murine diacylglycerol acyltransferase-2 (DGAT2) can catalyze triacylglycerol synthesis and promote lipid droplet formation independent of its localization to the endoplasmic reticulum. *J Biol Chem* 2011;286:28235–46.

53. Robertson MD, Parkes M, Warren BF, Ferguson DJP, Jackson KG, Jewell DP, Frayn KN. Mobilisation of enterocyte fat stores by oral glucose in humans. *Gut* 2003;52:834–839.

54. Zhu J, Lee B, Buhman KK, Cheng J-X. A dynamic, cytoplasmic triacylglycerol pool in enterocytes revealed by ex vivo and in vivo coherent anti-Stokes Raman scattering imagings. *J Lipid Res* 2009;50:1080–1089.

55. Lee B, Zhu J, Wolins NE, Cheng J-X, Buhman KK. Differential association of adipophilin and TIP47 proteins with cytoplasmic lipid droplets in mouse enterocytes during dietary fat absorption. *Biochim Biophys Acta* 2009;1791:1173–1180.

56. Grober J, Lucas S, Sörhede-Winzell M, Zaghini I, Mairal A, Contreras J-A, Besnard P, Holm C, Langin D. Hormone-sensitive lipase is a cholesterol esterase of the intestinal mucosa. *J Biol Chem* 2003;278:6510–6515.

57. Obrowsky S, Chandak PG, Patankar J V., Pfeifer T, Povoden S, Schreiber R, Haemmerle G, Levak-Frank S, Kratky D. Cholesteryl ester accumulation and accelerated cholesterol absorption in intestine-specific hormone sensitive lipase-null mice. *Biochim Biophys Acta* 2012;1821:1406–1414.

58. Haemmerle G, Lass A, Zimmermann R, Gorkiewicz G, Meyer C, Rozman J, Heldmaier G, Maier R, Theussl C, Eder S, Kratky D, Wagner EF, Klingenspor M, Hoefler G, Zechner R. Defective lipolysis and altered energy metabolism in mice lacking adipose triglyceride lipase. *Science (80-)* 2006;312:734–737.

59. Obrowsky S, Chandak PG, Patankar J V, Povoden S, Schlager S, Kershaw EE, Bogner-Strauss JG, Hoefler G, Levak-Frank S, Kratky D. Adipose triglyceride lipase is a TG hydrolase of the small intestine and regulates intestinal PPARalpha signaling. *J Lipid Res* 2013;54:425–435.

60. Pope J, McPherson J, Tidwell H. A study of a monoglyceride-hydrolyzing enzyme of intestinal mucosa. *J Biol Chem Print* 1966;241:2306–2310.

61. De Jong BJ, Kalkman C, Hülsmann WC. Partial purification and properties of monoacylglycerol lipase and two esterases from isolated rat small intestinal epithelial cells. *Biochim Biophys Acta* 1978;530:56–66.

62. Ho S-Y, Delgado L, Storch J. Monoacylglycerol metabolism in human intestinal Caco-2 cells: evidence for metabolic compartmentation and hydrolysis. *J Biol Chem* 2002;277:1816–23.

63. Storch J, Zhou YX, Lagakos WS. Metabolism of apical versus basolateral sn-2-monoacylglycerol and fatty acids in rodent small intestine. *J Lipid Res* 2008;49:1762–9.

64. Chon S-H, Zhou YX, Dixon JL, Storch J. Intestinal monoacylglycerol metabolism: developmental and nutritional regulation of monoacylglycerol lipase and monoacylglycerol acyltransferase. *J Biol Chem* 2007;282:33346–57.

65. Chon S-H, Douglass JD, Zhou YX, Malik N, Dixon JL, Brinker A, Quadro L, Storch J. Over-expression of monoacylglycerol lipase (MGL) in small intestine alters endocannabinoid levels and whole body energy balance, resulting in obesity. *PLoS One* 2012;7:e43962.

66. Porter CJH, Trevaskis NL, Charman WN. Lipids and lipid-based formulations: optimizing the oral delivery of lipophilic drugs. *Nat Rev Drug Discov* 2007;6:231–48.

67. Karlsson M, Contreras J a, Hellman U, Tornqvist H, Holm C. cDNA cloning, tissue distribution, and identification of the catalytic triad of monoglyceride lipase. Evolutionary relationship to esterases, lysophospholipases, and haloperoxidases. *J Biol Chem* 1997;272:27218–23.

68. Lyubachevskaya G, Boyle-Roden E. Kinetics of 2-monoacylglycerol acyl migration in model chylomicra. *Lipids* 2000;35:1353–1358.

69. Eichmann TO, Kumari M, Haas JT, Farese R V, Zimmermann R, Lass A, Zechner R. Studies on the substrate and stereo/regioselectivity of adipose triglyceride lipase, hormone-sensitive lipase, and diacylglycerol-O-acyltransferases. *J Biol Chem* 2012;287:41446–57.

70. Rodriguez JA, Ben Ali Y, Abdelkafi S, Mendoza LD, Leclaire J, Fotiadu F, Buono G, Carrière F, Abousalham A. In vitro stereoselective hydrolysis of diacylglycerols by hormone-sensitive lipase. *Biochim Biophys Acta* 2010;1801:77–83.

71. Stella N, Schweitzer P, Piomelli D. A second endogenous cannabinoid that modulates long-term potentiation. *Nature* 1997;388:773–778.

72. Gao Y, Vasilyev D V, Goncalves MB, Howell F V, Hobbs C, Reisenberg M, Shen R, Zhang M-Y, Strassle BW, Lu P, Mark L, Piesla MJ, Deng K, Kouranova E V, Ring RH, Whiteside GT, Bates B, Walsh FS, Williams G, Pangalos MN, Samad TA, Doherty P. Loss of retrograde endocannabinoid signaling and reduced adult neurogenesis in diacylglycerol lipase knock-out mice. *J Neurosci* 2010;30:2017–2024.

73. Sugiura T, Kondo S, Sukagawa A, Nakane S, Shinoda A, Itoh K, Yamashita A, Waku K. 2-Arachidonoylglycerol: a possible endogenous cannabinoid receptor ligand in brain. *Biochem Biophys Res Commun* 1995;215:89–97.

74. Schultz FM, Johnston JM. The synthesis of higher glycerides via the monoglyceride pathway in hamster adipose tissue. *J Lipid Res* 1971;12:132–138.

75. Jamdar SC, Cao WF. Adipose glycerolipid formation: effect of nutritional and hormonal states. *Lipids* 1993;28:607–612.

76. Ganong BR, Loomis CR, Hannun YA, Bell RM. Specificity and mechanism of protein kinase C activation by sn-1,2-diacylglycerols. *Proc Natl Acad Sci U S A* 1986;83:1184–8.

77. Labar G, Wouters J, Lambert DM. A review on the monoacylglycerol lipase: at the interface between fat and endocannabinoid signalling. *Curr Med Chem* 2010;17:2588–2607.

78. Taschler U, Radner FPW, Heier C, Schreiber R, Schweiger M, Schoiswohl G, Preiss-Landl K, Jaeger D, Reiter B, Koefeler HC, Wojciechowski J, Theussl C, Penninger JM, Lass a., Haemmerle G, Zechner R, Zimmermann R. Monoglyceride lipase-deficiency in mice impairs lipolysis and attenuates diet-induced insulin resistance. *J Biol Chem* 2011.

79. Blankman JL, Simon GM, Cravatt BF. A comprehensive profile of brain enzymes that hydrolyze the endocannabinoid 2-arachidonoylglycerol. *Chem Biol* 2007;14:1347–1356.

80. Savinainen JR, Saario SM, Laitinen JT. The serine hydrolases MAGL, ABHD6 and ABHD12 as guardians of 2-arachidonoylglycerol signalling through cannabinoid receptors. *Acta Physiol Oxford Engl* 2011:1–10.

81. Prentki M, Matschinsky FM, Madiraju SRM. Metabolic signaling in fuel-induced insulin secretion. *Cell Metab* 2013;18:162–85.

82. Thomas G, Betters JL, Lord CC, Brown AL, Marshall S, Ferguson D, Sawyer J, Davis MA, Melchior JT, Blume LC, Howlett AC, Ivanova PT, Milne SB, Myers DS, Mrak I, Leber V, Heier C, Taschler U, Blankman JL, Cravatt BF, Lee RG, Crooke RM, Graham MJ, Zimmermann R, Brown HA, Brown JM. The Serine Hydrolase ABHD6 Is a Critical Regulator of the Metabolic Syndrome. *Cell Rep* 2013.

83. Kupiecki FP. Partial purification of monoglyceride lipase from adipose tissue. *J Lipid Res* 1966;7:230–235.

84. Tornqvist H, Belfrage P. Purification and some properties of a monoacylglycerol-hydrolyzing enzyme of rat adipose tissue. *J Biol Chem* 1976;251:813–819.

85. Karlsson M, Reue K, Xia YR, Lusis AJ, Langin D, Tornqvist H, Holm C. Exon-intron organization and chromosomal localization of the mouse monoglyceride lipase gene. *Gene* 2001;272:11–18.

86. Labar G, Bauvois C, Borel F, Ferrer J-L, Wouters J, Lambert DM. Crystal structure of the human monoacylglycerol lipase, a key actor in endocannabinoid signaling. *Chembiochem* 2010;11:218–27.

87. Bertrand T, Augé F, Houtmann J, Rak A, Vallée F, Mikol V, Berne PF, Michot N, Cheuret D, Hoornaert C, Mathieu M. Structural basis for human monoglyceride lipase inhibition. *J Mol Biol* 2010;396:663–673.

88. Karlsson M, Tornqvist H, Holm C. Expression, purification, and characterization of histidine-tagged mouse monoglyceride lipase from baculovirus-infected insect cells. *Protein Expr Purif* 2000;18:286–292.

89. Vila A, Rosengarth A, Piomelli D, Cravatt B, Marnett LJ. Hydrolysis of prostaglandin glycerol esters by the endocannabinoid-hydrolyzing enzymes, monoacylglycerol lipase and fatty acid amide hydrolase. *Biochemistry* 2007;46:9578–9585.

90. Rindlisbacher B, Reist M, Zahler P. Diacylglycerol breakdown in plasma membranes of bovine chromaffin cells is a two-step mechanism mediated by a diacylglycerol lipase and a monoacylglycerol lipase. *Biochim Biophys Acta* 1987;905:349–357.

91. Vandevoorde S, Saha B, Mahadevan A, Razdan RK, Pertwee RG, Martin BR, Fowler CJ. Influence of the degree of unsaturation of the acyl side chain upon the interaction of analogues of 1-arachidonoylglycerol with monoacylglycerol lipase and fatty acid amide hydrolase. *Biochem Biophys Res Commun* 2005;337:104–109.

92. Ghafouri N, Tiger G, Razdan RK, Mahadevan A, Pertwee RG, Martin BR, Fowler CJ. Inhibition of monoacylglycerol lipase and fatty acid amide hydrolase by analogues of 2-arachidonoylglycerol. *Br J Pharmacol* 2004;143:774–784.

93. Duncan M, Thomas AD, Cluny NL, Patel A, Patel KD, Lutz B, Piomelli D, Alexander SPH, Sharkey KA. Distribution and function of monoacylglycerol lipase in the gastrointestinal tract. *Am J Physiol Gastrointest liver Physiol* 2008;295:G1255–G1265.

94. Dinh TP, Carpenter D, Leslie FM, Freund TF, Katona I, Sensi SL, Kathuria S, Piomelli D. Brain monoglyceride lipase participating in endocannabinoid inactivation. *Proc Natl Acad Sci U S A* 2002;99:10819–10824.

95. Dinh TP, Kathuria S, Piomelli D. RNA interference suggests a primary role for monoacylglycerol lipase in the degradation of the endocannabinoid 2-arachidonoylglycerol. *Mol Pharmacol* 2004;66:1260–1264.

96. Saario SM, Salo OMH, Nevalainen T, Poso A, Laitinen JT, Järvinen T, Niemi R. Characterization of the sulfhydryl-sensitive site in the enzyme responsible for hydrolysis of 2-arachidonoyl-glycerol in rat cerebellar membranes. *Chem Biol* 2005;12:649–656.

97. Rakhshandehroo M, Sanderson LM, Matilainen M, Stienstra R, Carlberg C, De Groot PJ, Müller M, Kersten S. Comprehensive Analysis of PPARα-Dependent Regulation of Hepatic Lipid Metabolism by Expression Profiling. *PPAR Res* 2007;2007:26839.

98. Nomura DK, Long JZ, Niessen S, Hoover HS, Ng S-W, Cravatt BF. Monoacylglycerol lipase regulates a fatty acid network that promotes cancer pathogenesis. *Cell* 2010;140:49–61.

99. Fredrikson G, Tornqvist H, Belfrage P. Hormone-sensitive lipase and monoacylglycerol lipase are both required for complete degradation of adipocyte triacylglycerol. *Biochim Biophys Acta* 1986;876:288–293.

100. Jaworski K, Sarkadi-Nagy E, Duncan RE, Ahmadian M, Sul HS. Regulation of triglyceride metabolism. IV. Hormonal regulation of lipolysis in adipose tissue. *Am J Physiol Gastrointest liver Physiol* 2007;293:G1–G4.

101. Schweiger M, Schreiber R, Haemmerle G, Lass A, Fledelius C, Jacobsen P, Tornqvist H, Zechner R, Zimmermann R. Adipose triglyceride lipase and hormone-sensitive lipase are the major enzymes in adipose tissue triacylglycerol catabolism. *J Biol Chem* 2006;281:40236–40241.

102. Schlosburg JE, Blankman JL, Long JZ, Nomura DK, Pan B, Kinsey SG, Nguyen PT, Ramesh D, Booker L, Burston JJ, Thomas EA, Selley DE, Sim-Selley LJ, Liu Q, Lichtman AH, Cravatt BF. Chronic monoacylglycerol lipase blockade causes functional antagonism of the endocannabinoid system. *Nat Neurosci* 2010;13:1113–1119.

103. Chanda P, Gao Y, Mark L, Btesh J, Strassle B, Lu P, Piesla M, Zhang M-Y, Bingham B, Uveges A, Kowal D, Garbe D, Kouranova E, Ring R, Bates B, Pangalos M, Kennedy J, Whiteside G, Samad T. Monoacylglycerol lipase activity is a critical modulator of the tone and integrity of the endocannabinoid system. *Mol Pharmacol* 2010.

104. Jung K-M, Clapper JR, Fu J, D'Agostino G, Guijarro A, Thongkham D, Avanesian A, Astarita G, DiPatrizio N V, Frontini A, Cinti S, Diano S, Piomelli D. 2-arachidonoylglycerol signaling in forebrain regulates systemic energy metabolism. *Cell Metab* 2012;15:299–310.

105. Lambert DM, Fowler CJ. The endocannabinoid system: drug targets, lead compounds, and potential therapeutic applications. *J Med Chem* 2005;48:5059–87.

106. Pan B, Wang W, Zhong P, Blankman JL, Cravatt BF, Liu QS. Alterations of Endocannabinoid Signaling, Synaptic Plasticity, Learning, and Memory in Monoacylglycerol Lipase Knock-out Mice. *J Neurosci* 2011;31:13420–13430.

107. Peng Zhong, Bin Pan, Xiu-ping Gao, Jacqueline L. Blankman, Benjamin F. Cravatt, and Qing-song Liu. Genetic deletion of monoacylglycerol lipase alters endocannabinoid-mediated retrograde synaptic depression in the cerebellum. *J Physiol* 2011;589:4847–4855.

108. Nomura DK, Morrison BE, Blankman JL, Long JZ, Kinsey SG, Marcondes MCG, Ward AM, Hahn YK, Lichtman AH, Conti B, Cravatt BF. Endocannabinoid Hydrolysis Generates Brain Prostaglandins That Promote Neuroinflammation. *Science (80-)* 2011;334:809–813.

109. Cao Z, Mulvihill MM, Mukhopadhyay P, Xu H, Erdélyi K, Hao E, Holovac E, Haskó G, Cravatt BF, Nomura DK, Pacher P. Monoacylglycerol Lipase Controls Endocannabinoid and Eicosanoid Signaling and Hepatic Injury in Mice. *Gastroenterology* 2013.

110. Long JZ, Li W, Booker L, Burston JJ, Kinsey SG, Schlosburg JE, Pavón FJ, Serrano AM, Selley DE, Parsons LH, Lichtman AH, Cravatt BF. Selective blockade of 2-arachidonoylglycerol hydrolysis produces cannabinoid behavioral effects. *Nat Chem Biol* 2009;5:37–44.

111. Kinsey SG, Long JZ, O'Neal ST, Abdullah RA, Poklis JL, Boger DL, Cravatt BF, Lichtman AH. Blockade of endocannabinoid-degrading enzymes attenuates neuropathic pain. *J Pharmacol Exp Ther* 2009;330:902–910.

112. Kinsey SG, Wise LE, Ramesh D, Abdullah R, Selley DE, Cravatt BF, Lichtman AH. Repeated Low Dose Administration of the Monoacylglycerol Lipase Inhibitor JZL184 Retains CB1 Receptor Mediated Antinociceptive and Gastroprotective Effects. *J Pharmacol Exp Ther* 2013;6040.

113. Chen R, Zhang J, Wu Y, Wang D, Feng G, Tang Y-P, Teng Z, Chen C. Monoacylglycerol lipase is a therapeutic target for Alzheimer's disease. *Cell Rep* 2012;2:1329–1339.

114. Ruby MA, Nomura DK, Hudak CSS, Mangravite LM, Chiu S, Casida JE, Krauss RM. Overactive endocannabinoid signaling impairs apolipoprotein E-mediated clearance of triglyceride-rich lipoproteins. *Proc Natl Acad Sci U S A* 2008;105:14561–14566.

115. Ruby MA, Nomura DK, Hudak CSS, Barber A, Casida JE, Krauss RM. Acute overactive endocannabinoid signaling induces glucose intolerance, hepatic steatosis, and novel cannabinoid receptor 1 responsive genes. *PLoSOne* 2011;6:e26415–.

116. Gulyas AI, Cravatt BF, Bracey MH, Dinh TP, Piomelli D, Boscia F, Freund TF. Segregation of two endocannabinoid-hydrolyzing enzymes into pre- and postsynaptic compartments in the rat hippocampus, cerebellum and amygdala. *Eur J Neurosci* 2004;20:441–458.

117. Gaoni Y, Mechoulam R. Isolation, Structure, and Partial Synthesis of an Active Constituent of Hashish. *J Am Chem Soc* 1964;86:1646–1647.

118. Di Marzo V. The endocannabinoid system: its general strategy of action, tools for its pharmacological manipulation and potential therapeutic exploitation. *Pharmacol Res Off J Ital Pharmacol Soc* 2009;60:77–84.

119. Pacher L, Ba N. The Endocannabinoid System as an Emerging Target of Pharmacotherapy. *Pharmacol Rev* 2006;58:389–462.

120. Fonseca BM, Costa MA, Almada M, Correia-da-Silva G, Teixeira NA. Endogenous cannabinoids revisited: A biochemistry perspective. *Prostaglandins other lipid Mediat* 2013.

121. Pacher P, Bátkai S, Kunos G. The endocannabinoid system as an emerging target of pharmacotherapy. *Pharmacol Rev* 2006;58:389–462.

122. Pagotto U, Marsicano G, Cota D, Lutz B, Pasquali R. The emerging role of the endocannabinoid system in endocrine regulation and energy balance. *Endocr Rev* 2006;27:73–100.

123. Matsuda LA, Lolait SJ, Brownstein MJ, Young AC, Bonner TI. Structure of a cannabinoid receptor and functional expression of the cloned cDNA. *Nature* 1990;346:561–4.

124. Munro S, Thomas KL, Abu-Shaar M. Molecular characterization of a peripheral receptor for cannabinoids. *Nature* 1993;365:61–5.

125. Sugiura T, Waku K. Cannabinoid receptors and their endogenous ligands. *J Biochem* 2002;132:7–12.

126. Spoto B, Fezza F, Parlongo G, Battista N, Sgro E, Gasperi V, Zoccali C, Maccarrone M. Human adipose tissue binds and metabolizes the endocannabinoids anandamide and 2-arachidonoylglycerol. *Biochimie* 2006;88:1889–1897.

127. Ho W-S V, Barrett DA, Randall MD. "Entourage" effects of N-palmitoylethanolamide and N-oleoylethanolamide on vasorelaxation to anandamide occur through TRPV1 receptors. *Br J Pharmacol* 2008;155:837–46.

128. Bellocchio L, Cervino C, Pasquali R, Pagotto U. The endocannabinoid system and energy metabolism. *J Neuroendocrinol* 2008;20:850–7.

129. Di Marzo V, Matias I. Endocannabinoid control of food intake and energy balance. *Nat Neurosci* 2005;8:585–9.

130. Hilairet S, Bouaboula M, Carrière D, Le Fur G, Casellas P. Hypersensitization of the Orexin 1 receptor by the CB1 receptor: evidence for cross-talk blocked by the specific CB1 antagonist, SR141716. *J Biol Chem* 2003;278:23731–23737.

131. Cota D, Marsicano G, Tschöp M, Grübler Y, Flachskamm C, Schubert M, Auer D, Yassouridis A, Thöne-Reineke C, Ortmann S, Tomassoni F, Cervino C, Nisoli E, Linthorst ACE, Pasquali R, Lutz B, Stalla GK, Pagotto U. The endogenous cannabinoid system affects energy balance via central orexigenic drive and peripheral lipogenesis. *J Clin Invest* 2003;112:423–431.

132. Horvath TL. Endocannabinoids and the regulation of body fat: the smoke is clearing. *J Clin Invest* 2003;112:323–326.

133. Jamshidi N, Taylor DA. Anandamide administration into the ventromedial hypothalamus stimulates appetite in rats. *Br J Pharmacol* 2001;134:1151–1154.

134. Kirkham TC, Williams CM, Fezza F, Di Marzo V. Endocannabinoid levels in rat limbic forebrain and hypothalamus in relation to fasting, feeding and satiation: stimulation of eating by 2-arachidonoyl glycerol. *Br J Pharmacol* 2002;136:550–557.

135. Tucci SA, Rogers EK, Korbonits M, Kirkham TC. The cannabinoid CB1 receptor antagonist SR141716 blocks the orexigenic effects of intrahypothalamic ghrelin. *Br J Pharmacol* 2004;143:520–523.

136. Kola B, Farkas I, Christ-Crain M, Wittmann G, Lolli F, Amin F, Harvey-White J, Liposits Z, Kunos G, Grossman AB, Fekete C, Korbonits M. The Orexigenic Effect of Ghrelin Is

Mediated through Central Activation of the Endogenous Cannabinoid System Bartolomucci A (ed.). *PLoS One* 2008;3:8.

137. Di Marzo V, Goparaju SK, Wang L, Liu J, Bátkai S, Járai Z, Fezza F, Miura GI, Palmiter RD, Sugiura T, Kunos G. Leptin-regulated endocannabinoids are involved in maintaining food intake. *Nature* 2001;410:822–825.

138. Hanus L, Avraham Y, Ben-Shushan D, Zolotarev O, Berry EM, Mechoulam R. Short-term fasting and prolonged semistarvation have opposite effects on 2-AG levels in mouse brain. *Brain Res* 2003;983:144–151.

139. Quarta C, Bellocchio L, Mancini G, Mazza R, Cervino C, Braulke LJ, Fekete C, Latorre R, Nanni C, Bucci M, Clemens LE, Heldmaier G, Watanabe M, Leste-Lassere T, Maitre M, Tedesco L, Fanelli F, Reuss S, Klaus S, Srivastava RK, Monory K, Valerio A, Grandis A, De Giorgio R, Pasquali R, Nisoli E, Cota D, Lutz B, Marsicano G, Pagotto U. CB(1) signaling in forebrain and sympathetic neurons is a key determinant of endocannabinoid actions on energy balance. *Cell Metab* 2010;11:273–285.

140. LoVerme J, Duranti A, Tontini A, Spadoni G, Mor M, Rivara S, Stella N, Xu C, Tarzia G, Piomelli D. Synthesis and characterization of a peripherally restricted CB1 cannabinoid antagonist, URB447, that reduces feeding and body-weight gain in mice. *Bioorg Med Chem Lett* 2009;19:639–643.

141. Tam J, Vemuri VK, Liu J, Bátkai S, Mukhopadhyay B, Godlewski G, Osei-Hyiaman D, Ohnuma S, Ambudkar S V, Pickel J, Makriyannis A, Kunos G. Peripheral CB1 cannabinoid receptor blockade improves cardiometabolic risk in mouse models of obesity. *J Clin Invest* 2010;120:2953–66.

142. Cluny NL, Vemuri VK, Chambers AP, Limebeer CL, Bedard H, Wood JT, Lutz B, Zimmer A, Parker LA, Makriyannis A, Sharkey KA. A novel peripherally restricted cannabinoid receptor antagonist, AM6545, reduces food intake and body weight, but does not cause malaise, in rodents. *Br J Pharmacol* 2010;161:629–642.

143. Herling AW, Kilp S, Juretschke H-P, Neumann-Haefelin C, Gerl M, Kramer W. Reversal of visceral adiposity in candy-diet fed female Wistar rats by the CB1 receptor antagonist rimonabant. *Int J Obes 2005* 2008;32:1363–1372.

144. Bensaid M, Gary-Bobo M, Esclangon A, Maffrand JP, Le Fur G, Oury-Donat F, Soubrie P. The cannabinoid CB1 receptor antagonist SR141716 increases Acrp30 mRNA expression in adipose tissue of obese fa/fa rats and in cultured adipocyte cells. *Mol Pharmacol* 2003;63:908–914.

145. Osei-Hyiaman D, DePetrillo M, Pacher P, Liu J, Radaeva S, Bátkai S, Harvey-White J, Mackie K, Offertáler L, Wang L, Kunos G. Endocannabinoid activation at hepatic CB1 receptors stimulates fatty acid synthesis and contributes to diet-induced obesity. *J Clin Invest* 2005;115:1298–1305.

146. Osei-Hyiaman D, Liu J, Zhou L, Godlewski G, Harvey-White J, Jeong W, Bátkai S, Marsicano G, Lutz B, Buettner C, Kunos G. Hepatic CB1 receptor is required for development of diet-induced steatosis, dyslipidemia, and insulin and leptin resistance in mice. *J Clin Invest* 2008;118:3160–3169.

147. Eckardt K, Sell H, Taube A, Koenen M, Platzbecker B, Cramer A, Horrighs A, Lehtonen M, Tennagels N, Eckel J. Cannabinoid type 1 receptors in human skeletal muscle cells participate in the negative crosstalk between fat and muscle. *Diabetologia* 2009;52:664–674.

148. Liu YL, Connoley IP, Wilson CA, Stock MJ. Effects of the cannabinoid CB1 receptor antagonist SR141716 on oxygen consumption and soleus muscle glucose uptake in Lep(ob)/Lep(ob) mice. *Int J Obes (Lond)* 2005;29:183–7.

149. Kola B, Hubina E, Tucci SA, Kirkham TC, Garcia EA, Mitchell SE, Williams LM, Hawley SA, Hardie DG, Grossman AB, Korbonits M. Cannabinoids and ghrelin have both central and peripheral metabolic and cardiac effects via AMP-activated protein kinase. *J Biol Chem* 2005;280:25196–25201.

150. Gomez R, Navarro M, Trigo M, Bilbao A, Arco I Del, Cippitelli A, Nava F, Piomelli D, Rodrı F. A Peripheral Mechanism for CB1 Cannabinoid Receptor-Dependent Modulation of Feeding. *Animals* 2002;22:9612–9617.

151. Fride E, Ginzburg Y, Breuer A, Bisogno T, Di Marzo V, Mechoulam R. Critical role of the endogenous cannabinoid system in mouse pup suckling and growth. *Eur J Pharmacol* 2001;419:207–214.

152. Wright KL, Duncan M, Sharkey KA. Cannabinoid CB2 receptors in the gastrointestinal tract: a regulatory system in states of inflammation. *Br J Pharmacol* 2008;153:263–270.

153. Croci T, Manara L, Aureggi G, Guagnini F, Rinaldi-Carmona M, Maffrand JP, Le Fur G, Mukenge S, Ferla G. In vitro functional evidence of neuronal cannabinoid CB1 receptors in human ileum. *Br J Pharmacol* 1998;125:1393–1395.

154. Burdyga G, Lal S, Varro A, Dimaline R, Thompson DG, Dockray GJ. Expression of cannabinoid CB1 receptors by vagal afferent neurons is inhibited by cholecystokinin. *J Neurosci* 2004;24:2708–2715.

155. Burdyga G, Varro A, Dimaline R, Thompson DG, Dockray GJ. Expression of cannabinoid CB1 receptors by vagal afferent neurons: kinetics and role in influencing neurochemical phenotype. *Am J Physiol Gastrointest Liver Physiol* 2010;299:G63–9.

156. Kunos G, Osei-Hyiaman D, Liu J, Godlewski G, Bátkai S. Endocannabinoids and the control of energy homeostasis. *J Biol Chem* 2008;283:33021–5.

157. Engeli S, Böhnke J, Feldpausch M, Gorzelniak K, Janke JJ, Bátkai S, Pacher PP, Harvey-White J, Luft FC, Sharma AM, Jordan J, Bohnke J, Batkai S, Bo J. Activation of the Peripheral Endocannabinoid System in. *Diabetes* 2005;54:2838–2843.

158. Matias I, Bisogno T, Di Marzo V. Endogenous cannabinoids in the brain and peripheral tissues: regulation of their levels and control of food intake. *Int J Obes (Lond)* 2006;30 Suppl 1:S7–S12.

159. Leite CE, Mocelin CA, Petersen GO, Leal MB, Thiesen F V. Rimonabant: an antagonist drug of the endocannabinoid system for the treatment of obesity. *Pharmacol reports PR* 2009;61:217–224.

160. Alvheim AR, Malde MK, Osei-Hyiaman D, Lin YH, Pawlosky RJ, Madsen L, Kristiansen K, Frøyland L, Hibbeln JR. Dietary linoleic acid elevates endogenous 2-AG and anandamide and induces obesity. *Obesity (Silver Spring)* 2012;20:1984–94.

161. Engeli S, Heusser K, Janke J, Gorzelniak K, Bátkai S, Pacher P, Harvey-White J, Luft FC, Jordan J. Peripheral endocannabinoid system activity in patients treated with sibutramine. *Obes Silver Spring Md* 2008;16:1135–1137.

162. Eckel RH, Grundy SM, Zimmet PZ. The metabolic syndrome. *Lancet* 2010;365:1415–1428.

163. Rasouli N, Molavi B, Elbein SC, Kern PA. Ectopic fat accumulation and metabolic syndrome. *Diabetes Obes Metab* 2007;9:1–10.

164. Cali AMG, Caprio S. Ectopic fat deposition and the metabolic syndrome in obese children and adolescents. *Horm Res* 2009;71 Suppl 1:2–7.

165. Li M, Paran C, Wolins NE, Horowitz JF. High muscle lipid content in obesity is not due to enhanced activation of key triglyceride esterification enzymes or to the suppression of lipolytic proteins. *Am J Physiol - Endocrinol Metab* 2011.

166. Fabbrini E, Magkos F, Mohammed BS, Pietka T, Abumrad NA, Patterson BW, Okunade A, Klein S. Intrahepatic fat, not visceral fat, is linked with metabolic complications of obesity. *Proc Natl Acad Sci U S A* 2009;106:15430–15435.

167. Pan DA, Lillioja S, Kriketos AD, Milner MR, Baur LA, Bogardus C, Jenkins AB, Storlien LH. Skeletal muscle triglyceride levels are inversely related to insulin action. *Diabetes* 1997;46:983–988.

168. Fielding BA, Callow J, Owen RM, Samra JS, Matthews DR, Frayn KN. Postprandial lipemia: the origin of an early peak studied by specific dietary fatty acid intake during sequential meals. *Am J Clin Nutr* 1996;63:36–41.

169. Mansbach CM, Dowell R. Effect of increasing lipid loads on the ability of the endoplasmic reticulum to transport lipid to the Golgi. *J Lipid Res* 2000;41:605–612.

170. Zhang Y, Proenca R, Maffei M, Barone M, Leopold L, Friedman JM. Positional cloning of the mouse obese gene and its human homologue. *Nature* 1994;372:425–432.

171. Drel VR, Mashtalir N, Ilnytska O, Shin J, Li F, Lyzogubov V V, Obrosova IG. The leptin-deficient (ob/ob) mouse: a new animal model of peripheral neuropathy of type 2 diabetes and obesity. *Diabetes* 2006;55:3335–43.

172. Friedman JM, Halaas JL. Leptin and the regulation of body weight in mammals. *Nature* 1998;395:763–770.

173. Unger RH, Zhou Y-T, Orci L. Regulation of fatty acid homeostasis in cells: novel role of leptin. *Proc Natl Acad Sci U S A* 1999;96:2327–2332.

174. Bradford MM. A rapid and sensitive method for the quantitation of microgram quantities of protein utilizing the principle of protein-dye binding. *Anal Biochem* 1976;72:248–54.

175. Folch J., Less M. and SS. A Simple Method For The Isolation and Purification of Total Lipids From Animal Tissues. *J Biol Chem* 1957:497–508.

176. Humason G. *Animal Tissue Techniques*. Third. San Francisco, CA: W.H. Freeman and Company; 1972.

177. Petro AE, Cotter J, Cooper DA, Peters JC, Surwit SJ, Surwit RS. Fat, carbohydrate, and calories in the development of diabetes and obesity in the C57BL/6J mouse. *Metab Clin Exp* 2004;53:454–457.

178. Festi D, Colecchia A, Sacco T, Bondi M, Roda E, Marchesini G. Hepatic steatosis in obese patients: clinical aspects and prognostic significance. *Obes Rev an Off J Int Assoc Study Obes* 2004;5:27–42.

179. Reddy JK, Rao MS. Lipid metabolism and liver inflammation. II. Fatty liver disease and fatty acid oxidation. *Am J Physiol Gastrointest liver Physiol* 2006;290:G852–G858.

180. De La Serre CB, Ellis CL, Lee J, Hartman AL, Rutledge JC, Raybould HE. Propensity to high-fat diet-induced obesity in rats is associated with changes in the gut microbiota and gut inflammation. *Am J Physiol Gastrointest Liver Physiol* 2010;299:G440–8.

181. Iqbal J, Li X, Chang BH-J, Chan L, Schwartz GJ, Chua SC, Hussain MM. An intrinsic gut leptin-melanocortin pathway modulates intestinal microsomal triglyceride transfer protein and lipid absorption. *J Lipid Res* 2010;51:1929–42.

182. Bobo RC, Partin JC, Schubert WK, Saalfeld K. Abnormal lipid accumulation within the small intestinal mucosa of children with juvenile-onset diabetes mellitus. *Am J Dis Child* 1977;131:962–9.

183. Loirdighi N, Ménard D, Levy E. Insulin decreases chylomicron production in human fetal small intestine. *Biochim Biophys Acta* 1992;1175:100–106.

184. Haidari M, Leung N, Mahbub F, Uffelman KD, Kohen-Avramoglu R, Lewis GF, Adeli K. Fasting and postprandial overproduction of intestinally derived lipoproteins in an animal model of insulin resistance. Evidence that chronic fructose feeding in the hamster is accompanied by enhanced intestinal de novo lipogenesis and ApoB48-containing li. *J Biol Chem* 2002;277:31646–31655.

185. Tobin V, Le Gall M, Fioramonti X, Stolarczyk E, Blazquez AG, Klein C, Prigent M, Serradas P, Cuif M-H, Magnan C, Leturque A, Brot-Laroche E. Insulin internalizes GLUT2 in the enterocytes of healthy but not insulin-resistant mice. *Diabetes* 2008;57:555–562.

186. Atzel A, Wetterau JR. Mechanism of microsomal triglyceride transfer protein catalyzed lipid transport. *Biochemistry* 1993;32:10444–10450.

187. Swift LL, Jovanovska A, Kakkad B, Ong DE. Microsomal triglyceride transfer protein expression in mouse intestine. *Histochem Cell Biol* 2005;123:475–482.

188. Nadler ST, Stoehr JP, Schueler KL, Tanimoto G, Yandell BS, Attie AD. The expression of adipogenic genes is decreased in obesity and diabetes mellitus. *Proc Natl Acad Sci U S A* 2000;97:11371–11376.

189. Memon RA, Grunfeld C, Moser AH, Feingold KR. Fatty acid synthesis in obese insulin resistant diabetic mice. *Horm Metab Res Horm und Stoffwechselforsch Horm Metab* 1994;26:85–87.

190. Cunningham KM, Daly J, Horowitz M, Read NW. Gastrointestinal adaptation to diets of differing fat composition in human volunteers. *Gut* 1991;32:483–486.

191. Castiglione KE, Read NW, French SJ. *Adaptation to high-fat diet accelerates emptying of fat but not carbohydrate test meals in humans.*; 2002:R366–R371.

192. Clegg ME, McKenna P, McClean C, Davison GW, Trinick T, Duly E, Shafat A. Gastrointestinal transit, post-prandial lipaemia and satiety following 3 days high-fat diet in men. *Eur J Clin Nutr* 2011;65:240–246.

193. Covasa M, Ritter RC. Adaptation to high-fat diet reduces inhibition of gastric emptying by CCK and intestinal oleate. *Am J Physiol Regul Integr Comp Physiol* 2000;278:R166–R170.

194. Windmueller HG, Spaeth AE. Identification of ketone bodies and glutamine as the major respiratory fuels in vivo for postabsorptive rat small intestine. *J Biol Chem* 1978;253:69–76.

195. Lewis GF, O'Meara NM, Soltys PA, Blackman JD, Iverius PH, Druetzler AF, Getz GS, Polonsky KS. Postprandial lipoprotein metabolism in normal and obese subjects: comparison after the vitamin A fat-loading test. *J Clin Endocrinol Metab* 1990;71:1041–1050.

196. Mekki N, Christofilis MA, Charbonnier M, Atlan-Gepner C, Defoort C, Juhel C, Borel P, Portugal H, Pauli a M, Vialettes B, Lairon D. Influence of obesity and body fat distribution on postprandial lipemia and triglyceride-rich lipoproteins in adult women. *J Clin Endocrinol Metab* 1999;84:184–191.

197. Ji H, Friedman MI. Reduced hepatocyte fatty acid oxidation in outbred rats prescreened for susceptibility to diet-induced obesity. *Int J Obes 2005* 2008;32:1331–1334.

198. Uchida A, Whitsitt MC, Eustaquio T, Slipchenko MN, Leary JF, Cheng J-X, Buhman KK. Reduced triglyceride secretion in response to an acute dietary fat challenge in obese compared to lean mice. *Front Physiol* 2012;3:26.

199. Cota D, Marsicano G, Lutz B, Vicennati V, Stalla GK, Pasquali R, Pagotto U. Endogenous cannabinoid system as a modulator of food intake. *Int J Obes Relat Metab Disord J Int Assoc Study Obes* 2003;27:289–301.

200. Kunos G, Osei-Hyiaman D. Endocannabinoids and liver disease. IV. Endocannabinoid involvement in obesity and hepatic steatosis. *Am J Physiol Gastrointest liver Physiol* 2008;294:G1101–G1104.

201. Zambrowicz BP, Friedrich GA. Comprehensive mammalian genetics: history and future prospects of gene trapping in the mouse. *Int J Dev Biol* 1998;42:1025–1036.

202. McLean JA, Tobin G. *Animal and Human Calorimetry*. Cambridge University Press; 1987.

203. Chomczynski P, Sacchi N. Single-step method of RNA isolation by acid guanidinium thiocyanate-phenol-chloroform extraction. *Anal Biochem* 1987;162:156–159.

204. Douglass JD, Malik N, Chon S-H, Wells K, Zhou YX, Choi AS, Joseph LB, Storch J. Intestinal mucosal triacylglycerol accumulation secondary to decreased lipid secretion in obese and high fat fed mice. *Front Physiol* 2012;3:25.

205. Hildebrandt AL, Kelly-Sullivan DM, Black SC. Antiobesity effects of chronic cannabinoid CB1 receptor antagonist treatment in diet-induced obese mice. *Eur J Pharmacol* 2003;462:125–132.

206. Ravinet Trillou C, Delgorge C, Menet C, Arnone M, Soubrié P. CB1 cannabinoid receptor knockout in mice leads to leanness, resistance to diet-induced obesity and enhanced leptin sensitivity. *Int J Obes Relat Metab Disord J Int Assoc Study Obes* 2004;28:640–648.

207. Zhang L-N, Gamo Y, Sinclair R, Mitchell SE, Morgan DG, Clapham JC, Speakman JR. Effects of chronic oral rimonabant administration on energy budgets of diet-induced obese C57BL/6 mice. *Obesity (Silver Spring)* 2012;20:954–62.

208. Di Marzo V. The endocannabinoid system in obesity and type 2 diabetes. *Diabetologia* 2008;51:1356–1367.

209. Kozak KR, Crews BC, Morrow JD, Wang L-H, Ma YH, Weinander R, Jakobsson P-J, Marnett LJ. Metabolism of the endocannabinoids, 2-arachidonylglycerol and anandamide, into prostaglandin, thromboxane, and prostacyclin glycerol esters and ethanolamides. *J Biol Chem* 2002;277:44877–44885.

210. Silvestri C, Di Marzo V. The Endocannabinoid System in Energy Homeostasis and the Etiopathology of Metabolic Disorders. *Cell Metab* 2013;17:475–490.

211. Polheim D, David JS, Schultz FM, Wylie MB, Johnston JM. Regulation of triglyceride biosynthesis in adipose and intestinal tissue. *J Lipid Res* 1973;14:415–421.

212. Nelson DW, Gao Y, Spencer NM, Banh T, Yen C-LE. Deficiency of MGAT2 increases energy expenditure without high-fat feeding and protects genetically obese mice from excessive weight gain. *J Lipid Res* 2011;52:1723–1732.

213. Steppan CM, Bailey ST, Bhat S, Brown EJ, Banerjee RR, Wright CM, Patel HR, Ahima RS, Lazar MA. The hormone resistin links obesity to diabetes. *Nature* 2001;409:307–312.

214. Li F-P, He J, Li Z-Z, Luo Z-F, Yan L, Li Y. Effects of resistin expression on glucose metabolism and hepatic insulin resistance. *Endocrine* 2009;35:243–251.

215. Rajala MW, Obici S, Scherer PE, Rossetti L. Adipose-derived resistin and molecule – β selectively impair. *J Clin Invest* 2003;111:225–230.

216. Qi Y, Nie Z, Lee Y-S, Singhal NS, Scherer PE, Lazar MA, Ahima RS. Loss of resistin improves glucose homeostasis in leptin deficiency. *Diabetes* 2006;55:3083–3090.

217. Lan H, Lin H V, Wang CF, Wright MJ, Xu S, Kang L, Juhl K, Hedrick JA, Kowalski TJ. Agonists at GPR119 mediate secretion of GLP-1 from mouse enteroendocrine cells through glucose-independent pathways. *Br J Pharmacol* 2012;165:2799–807.

218. Hansen KB, Rosenkilde MM, Knop FK, Wellner N, Diep TA, Rehfeld JF, Andersen UB, Holst JJ, Hansen HS. 2-Oleoyl glycerol is a GPR119 agonist and signals GLP-1 release in humans. *J Clin Endocrinol Metab* 2011;96:E1409–17.

219. Lombardi DP, Nomura DK, Cravatt BF. Blockade of monoacylglycerol lipase impairs prostate cancer cell pathogenicity. *Clin Transl Sci* 2010;3:S46.

220. Hotamisligil GS. Inflammation and metabolic disorders. *Nature* 2006;444:860–867.

221. Ramesh D, Ross GR, Schlosburg JE, Owens RA, Abdullah RA, Kinsey SG, Long JZ, Nomura DK, Sim-Selley LJ, Cravatt BF, Akbarali HI, Lichtman AH. Blockade of endocannabinoid hydrolytic enzymes attenuates precipitated opioid withdrawal symptoms in mice. *J Pharmacol Exp Ther* 2011;339:173–85.

222. Rinaldi-Carmona M, Barth F, Heaulme M, Shire D, Calandra B, Congy C, Martinez S, Maruani J, Neliat G, Caput D. SR141716A, a potent and selective antagonist of the brain cannabinoid receptor. *FEBS Lett* 1994;350:240–244.

223. Ioannides-Demos LL, Piccenna L, McNeil JJ. Pharmacotherapies for Obesity: Past, Current, and Future Therapies. *J Obes* 2011;2011:179674.

224. Bisogno T, Mahadevan A, Coccurello R, Chang JW, Allarà M, Chen Y, Giacovazzo G, Lichtman A, Cravatt B, Moles A, Di Marzo V. A novel fluorophosphonate inhibitor of the biosynthesis of the endocannabinoid 2-arachidonoylglycerol with potential anti-obesity effects. *Br J Pharmacol* 2013;169:784–93.

225. Faust IM, Johnson PR, Stern JS, Hirsch J. Diet-induced adipocyte number increase in adult rats: a new model of obesity. *Am J Physiol* 1978;235:E279–E286.

226. Jernås M, Palming J, Sjöholm K, Jennische E, Svensson P-A, Gabrielsson BG, Levin M, Sjögren A, Rudemo M, Lystig TC, Carlsson B, Carlsson LMS, Lönn M. Separation of human adipocytes by size: hypertrophic fat cells display distinct gene expression. *FASEB J* 2006;20:1540–1542.

227. Montani J-P, Carroll JF, Dwyer TM, Antic V, Yang Z, Dulloo AG. Ectopic fat storage in heart, blood vessels and kidneys in the pathogenesis of cardiovascular diseases. *Int J Obes Relat Metab Disord* 2004;28 Suppl 4:S58–S65.

228. Karimian Azari E, Leitner C, Jaggi T, Langhans W, Mansouri A. Possible Role of Intestinal Fatty Acid Oxidation in the Eating-Inhibitory Effect of the PPAR-α Agonist Wy-14643 in High-Fat Diet Fed Rats. Gaetani S (ed.). *PLoS One* 2013;8:e74869.

229. Rodríguez de Fonseca F, Navarro M, Gómez R, Escuredo L, Nava F, Fu J, Murillo-Rodríguez E, Giuffrida A, LoVerme J, Gaetani S, Kathuria S, Gall C, Piomelli D. An anorexic lipid mediator regulated by feeding. *Nature* 2001;414:209–12.

230. Wurie HR, Buckett L, Zammit VA. Diacylglycerol acyltransferase 2 acts upstream of diacylglycerol acyltransferase 1 and utilizes nascent diglycerides and de novo synthesized fatty acids in HepG2 cells. *FEBS J* 2012;279:3033–47.

231. Mansbach CM, Siddiqi SA. The biogenesis of chylomicrons. *Annu Rev Physiol* 2010;72:315–33.

232. Overton HA, Fyfe MCT, Reynet C. GPR119, a novel G protein-coupled receptor target for the treatment of type 2 diabetes and obesity. *Br J Pharmacol* 2008;153 Suppl :S76–81.

233. Gajda AM, Zhou YX, Agellon LB, Fried SK, Kodukula S, Fortson WM, Patel K, Storch J. Direct Comparison of Mice Null for Liver- or Intestinal Fatty Acid Binding Proteins Reveals Highly Divergent Phenotypic Responses to High-Fat Feeding. *J Biol Chem* 2013.

234. Gao Y, Nelson DW, Banh T, Yen M-I, Yen C-LE. Intestine-specific expression of MOGAT2 partially restores metabolic efficiency in Mogat2-deficient mice. *J Lipid Res* 2013;54:1644–52.

235. Lee B, Fast AM, Zhu J, Cheng J-X, Buhman KK. Intestine-specific expression of acyl CoA:diacylglycerol acyltransferase 1 reverses resistance to diet-induced hepatic steatosis and obesity in Dgat1-/- mice. *J Lipid Res* 2010;51:1770–1780.

236. Coleman RA, Mashek DG, Li LO. Long-chain acyl-CoA synthetases and fatty acid channeling. *Future Lipidol* 2007;2:465–476.

237. Bu SY, Mashek MT, Mashek DG. Suppression of long chain acyl-CoA synthetase 3 decreases hepatic de novo fatty acid synthesis through decreased transcriptional activity. *J Biol Chem* 2009;284:30474–83.

238. Bu SY, Mashek DG. Hepatic long-chain acyl-CoA synthetase 5 mediates fatty acid channeling between anabolic and catabolic pathways. *J Lipid Res* 2010;51:3270–3280.

239. Mashek DG, McKenzie MA, Van Horn CG, Coleman RA. Rat long chain acyl-CoA synthetase 5 increases fatty acid uptake and partitioning to cellular triacylglycerol in McArdle-RH7777 cells. *J Biol Chem* 2006;281:945–950.

240. Gangl A, Ockner RK. Intestinal metabolism of plasma free fatty acids. Intracellular compartmentation and mechanisms of control. *J Clin Invest* 1975;55:803–813.

241. Gangl A, Renner F. In vivo metabolism of plasma free fatty acids by intestinal mucosa of man. *Gastroenterology* 1978;74:847–50.

242. Ontko JA, Jackson D. Factors affecting the rate of oxidation of fatty acids in animal tissues: Effect of substrate concentration, ph, and coenzyme a in rat liver preparations. *J Biol Chem* 1964;239:3674–82.

243. Meller N, Morgan ME, Wong WP, Altemus JB, Sehayek E. Targeting of Acyl-CoA synthetase 5 decreases jejunal fatty acid activation with no effect on dietary long-chain fatty acid absorption. *Lipids Health Dis* 2013;12:88.